

論文 / 著書情報  
Article / Book Information

題目(和文)	
Title(English)	Studies on an Index of Operator ' s Haptic Sensation and System Parameters Design for a Master-Slave System
著者(和文)	周東博
Author(English)	Dongbo Zhou
出典(和文)	学位:博士(工学), 学位授与機関:東京工業大学, 報告番号:甲第11230号, 授与年月日:2019年6月30日, 学位の種別:課程博士, 審査員:只野 耕太郎,吉田 和弘,吉岡 勇人,金 俊完,松村 茂樹
Citation(English)	Degree:Doctor (Engineering), Conferring organization: Tokyo Institute of Technology, Report number:甲第11230号, Conferred date:2019/6/30, Degree Type:Course doctor, Examiner:,,,,
学位種別(和文)	博士論文
Type(English)	Doctoral Thesis

Tokyo Institute of Technology



Doctor Thesis

Studies on an Index of Operator's Haptic  
Sensation and System Parameters Design  
for a Master-Slave System

Department of Mechano-Micro Engineering  
Interdisciplinary Graduate School of Science and Engineering  
Tokyo Institute of Technology

Dongbo Zhou

Supervisor: Kotaro Tadano

Second supervisor: Kazuhiro Yoshida

2019

# Contents

Symbols and subscripts in this thesis.....	iii
Chapter 1 Introduction .....	1
1.1 Applications of the master-slave devices .....	2
1.1.1 Application in hostile environments.....	2
1.1.2 Application in inaccessible places.....	2
1.1.3 Application in the micro and medical cases.....	4
1.2 Haptic feedback in master-slave devices .....	6
1.2.1 Benefits of haptic feedback.....	6
1.2.2 Methods of providing haptic feedback .....	7
1.3 Parameters design in bilateral control.....	9
1.3.1 Objectives of parameters design.....	9
1.3.2 A review of works about parameter adjustment.....	11
1.4 Research objective .....	14
1.5 Thesis construction.....	15
Chapter 2 An index of operator's haptic sensation.....	18
2.1 Haptic mechanism during operation .....	19
2.2 Definition of the index .....	20
2.3 Characterization of the haptic sensation index.....	22
2.3.1 Experimental apparatus.....	22
2.3.1 Subjects and motions .....	24
2.3.2 Experiment for the index value stability to different operators .....	24
2.3.3 Experiment for reflecting a different haptic sensation in $C$ value.....	28
2.4 Validation of the haptic sensation index .....	34
2.4.1 Experiment for parameter settings with the same $C$ value .....	37
2.4.2 Experiment for parameter settings with $C$ values differing by $R_c$ .....	40
2.4.3 Experiment for parameter settings with $C$ values differing by 200% .....	42
2.4.4 Experiment for parameter settings with the same $C$ value and far different $K_{en}$ and $B_m$ values.....	44
2.5 Discussion of this chapter .....	46
2.5.1 Effect of each kind of parameter on the haptic sensation.....	46
2.5.2 Comparison of the other alternative motion factors .....	46
2.5.3 The relationship between $C$ value and the operator's sensation .....	49
2.6 Summarization of this chapter.....	50
Chapter 3 The relationship between the index value and the system parameters .....	52
3.1 Introduction of bilateral control architectures .....	52
3.2 Relationship between index value and system parameters in the ideal model... 54	
3.2.1 Control model introduction.....	54
3.2.2 Relationship function derivation .....	57
3.2.3 Effect analysis of different parameters .....	58
3.2.4 Validations of the $C$ calculation function from system parameters .....	60

3.3	Relationship between index value and system parameters in the real model ....	63
3.3.1	Control model introduction.....	63
3.3.2	Relationship function derivation .....	66
3.3.3	Validation of the $C$ calculation function from system parameters.....	73
3.4	Discussion of this chapter .....	75
3.4.1	The results in the experiment in Section 3.3.3. ....	75
3.4.1	Relationship between parameter values and solution of motion equations .	78
3.4.2	Influence of device inertia on haptic sensation .....	80
3.5	Summarization of this chapter.....	81
Chapter 4	Applications as a guideline for system parameter design .....	82
4.1	Assuring maximum and minimum values a parameter can be set.....	82
4.1.1	Assuring the maximum parameter setting to keep a haptic sensation .....	82
4.1.2	Assuring the minimum parameter setting to change a haptic sensation .....	85
4.2	Reasonable parameter design with consideration to both task requirement and haptic sensation.....	86
4.3	Summarization of this chapter.....	90
Chapter 5	Conclusions and future works .....	91
5.1	Conclusion of this study.....	91
5.2	Future works.....	92
Appendix	.....	94
References	.....	96
Acknowledgement	.....	102

## Symbols and subscripts in this thesis

### Symbol list

Symbol	Unit	Meaning
$B$	Ns/mm	Damping parameter
$C$	–	Haptic sensation index
$F$	N	Force
$F_{sc}$	–	Amplification scaling between the interaction and feedback forces
JND	–	Just noticeable difference to a reference haptic sensation
$K_p$	N/mm	Virtual stiffness parameter between the master and slave devices
$K_v$	Ns/mm	Virtual damper parameter between the master and slave devices
LT	–	Lower threshold to a reference haptic sensation
$M$	$\text{kg} \cdot 10^3$	Inertia
$P$	%	The predicted proportion of the indistinguishable answers
$P_{sc}$	–	Amplification scaling between the master and slave device positions
$R_c$	–	The necessary change ratio to a $C$ value to produce a just noticeable different haptic sensation
$s$	–	Laplace operator
$r$	mm	Position
UT	–	Upper threshold to a reference haptic sensation
$V$	mm/s	Velocity
$\alpha$	–	The ratio between $C$ values in the ideal and real control models
$\sigma$	–	Normal distribution variance

## Subscript list

Subscript	Meaning
a	After the slave device contacts with the environment
b	Before the slave device contacts with the environment
en	The operational environment
h	Operator's Limb (hand)
hm	Combination property of operator's hand and the master device
hen	Combination property of operator's hand and operational environment
ideal	The ideal position-force bilateral control architecture
JND	Just noticeable difference
LT	Lower threshold
m	The master device
ref	The reference
s	The slave device
UT	Upper threshold

# Chapter 1

## Introduction

In recent decades, the programmed robots can perform tasks more and more quickly and precisely because of the technical advances, and their automation and self-adaptation degree have become significant criterions of performances. Nonetheless, it is still difficult for them to handle sophisticated tasks that involve unpredictable situations. Hence, applications of programmed robot are mainly in repetitive tasks such as production processes, where the robots can run repetitive production cycles much faster than human.

On the contrary, it is difficult to establish models for the operation beforehand in cases where the tasks are non-repetitive. The artificial intelligence has been developed remarkably but it still cannot cope with most of the non-repetitive tasks, so a human operator is still needed to carry out the tasks.

However, these types of tasks are usually accompanied with inaccessible or hostile environment to the human operator, which precludes the operator to use his/her hands with tools directly. Thus, the operator has to stay in a friendly place and handle the object through a manipulator, in such cases a master-slave system will be particularly helpful, by which the human operator can stay in a friendly space, operating the master device; the slave device reproduces the human operator's motion in the hazardous environment. The masters-slave systems allow an operator to impose operation on the objects in an inaccessible environment.

## 1.1 Applications of the master-slave devices

### 1.1.1 Applications in hostile environment

The master-slave devices are first be invented and used in the nuclear industry. After knowing the dangers of radiation, the researchers realized that radioactive substance must be handled after a certain protection. For this requirement, a research team led by Ray Goertz at Argonne National Laboratory, USA, developed the first mater-slave system known today [1]. It was a mechanical master-slave manipulator, wherein cables and chains are used to transmit the motion between the master and the slave sides. The first master-slave manipulator was named “model M1” (Fig. 1.1), in which an original mechanical method was adopted to make the slave side reproduce the movement (elevation and rotation) at the master side.

Nowadays, the nuclear industry has become a large application field of the master-slave systems, many innovative master-slave systems have been developed. The state of art of master-slave systems used in the nuclear industry as the author knows is the model “TERMAN TAO” (Fig. 1.2) by GETINGE Co., which can reproduce dexterous and accurate motions input by an operator with a large motion scope (up to 4010 mm) and force output (Maximum load capacity 20kg).

### 1.1.2 Applications in inaccessible places

Master-slave systems allow the operator to complete a task in places where it is difficult to access, such as deep sea and the outer space. Nowadays, the underwater vehicles with a telemanipulator, manned or unmanned, are widely used in rescue, exploration, etc.

The outer space is a more difficult place for human to access comparing to the underwater. To replace the human astronauts for the extremely critical tasks that spacewalk is necessary, NASA’s Johnson Space Center developed the humanoid Robonaut that can reproduce the motion of human by tele-operating (Fig. 1.3). The Robonaut has been on board the ISS since 2012, but is still in the experimental stage.



Fig. 1.1 The first master-slave manipulator “model M1” [1].



Fig. 1.2 “TERMAN TAO”, a master-slave system widely used in nuclear industries around the world [2].

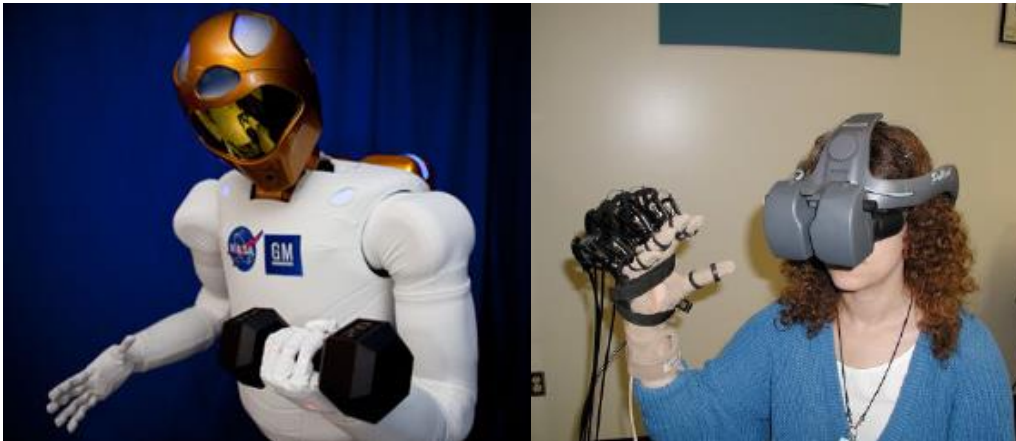


Fig. 1.3 Robonaut (left) and its remote control module (right) [3]

A predictable future application of the master-slave system in outer space will be the Mars exploration, some experts stand for that leaving the human astronaut stay in the Mars-orbit and tele-operating a robot is much more reasonable, simpler and safer than directly landing a human astronaut on the Mars surface. [4]

### 1.1.3 Application in the micro and medical cases

Another advantage of using the master-slave system is that the slave device can reproduce the motion of the operator in a space that much smaller than human finger's motion scale with an accuracy beyond human. Therefore, the applications of the master-slave system in the micrometer or sub micrometer process operation, such as MEMS, cell engineering, chromosome cutting, etc., are still noteworthy. For example, the Harbin Institute of Technology built a tele-nanomanipulation platform that can move a wire consist of single ZnO molecules (Fig. 1.4). In the field of nanotechnology, Ni et al. used the master-slave system to operate an optical tweezer on a Nano-stage [6].

Nowadays, the most profitable application field of master-slave systems is the medical field. As the fast development of minimally invasive surgery, laparoscopic surgery has become popular since 1990 because of its benefits including less pain, shorter recovery time, smaller trauma, etc. [7].

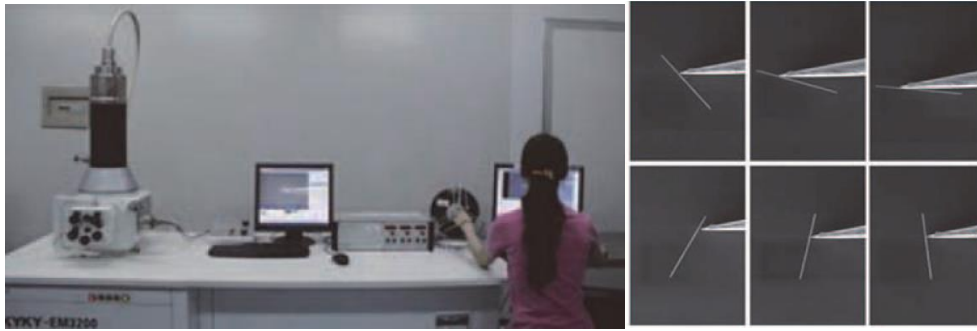


Fig. 1.4 The tele-nanomanipulation platform (left) and the appearance of moving a wire that consists of single ZnO molecules (right) [5].

As the development of computer and VR technology, scientists began to realize that the master-slave telemanipulator can be used in laparoscopic surgery, and many prototypes or products were developed. For example, Intuitive Surgical Co. released the master-slave surgery assistant robot Da Vinci in 1997 and got the FDA certification in 2001, now it has become the most widely-used surgery assistant robot in the world (Fig. 1.6 is the appearance of the latest version) [8]. Blake Hannaford et al. from University of Washington, developed the RAVEN surgical robot [9], it is an open-architecture surgical robot for laparoscopic surgery research now. Tadano and Kawashima group developed the IBIS series surgical manipulator, which is actuated by pneumatic cylinders, this innovative structure makes the end effector of the robot be able to measure the interaction force to environment without force sensor [10].



Fig. 1.6 The Da Vinci surgery assistant robot [11]

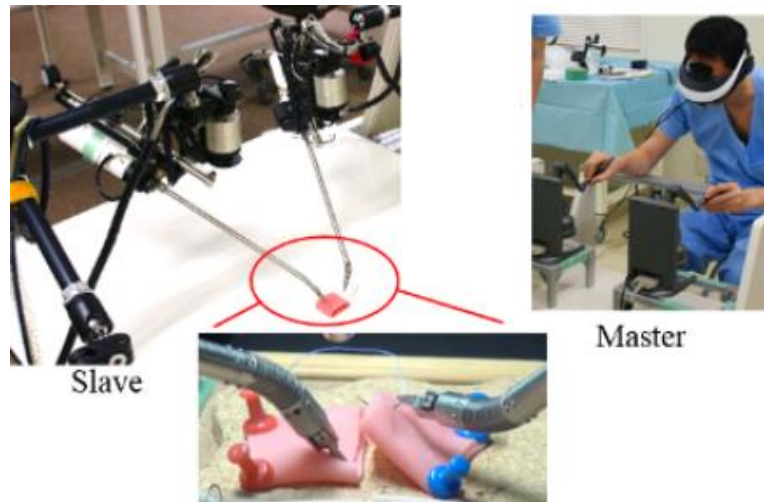


Fig. 1.5 The IBIS 4 surgical manipulator [12]

Using the robot-assisted surgery shows the following benefits: first, the surgeon's motion can be scaled down to enhance the operation accuracy, second, the robot provides much higher dexterity than traditional manually endoscopic instruments, third, master-slave formation enables surgeons to train students or assist other surgeons without traveling long distances.

## 1.2 Haptic feedback in master-slave systems

### 1.2.1 Benefits of haptic feedback

The operator's hand cannot touch the object directly when operating the master-slave system. Hence it is natural that the operator hopes the operational sensation to be the same as that of direct handling. Human's hands are dexterous due to the multi-DOF finger structure and sensitive haptic perceptions. During using the master-slave system, the fingers are used to hold the master device, so an effective way for providing the operator a real object handling sensation is to generate a haptic perceptions by haptic feedback.

The benefits of haptic feedback in master-slave system operation has been demonstrated in many studies [13] – [16]. From conclusions of these studies, the benefits of haptic feedback can be classified into the following three types: lessening operation miss, enhancing efficiency and reducing the cognitive workload [17], [18]. Especially, in robot-assisted surgery, providing haptic feedback would contribute significantly to the

performance; for example, the excessive suture breakage during knot tying can be reduced when performing suture manipulations with robot-assisted surgical systems with the help of haptic feedback [19]. Semere et al. confirmed that force feedback can lead to significant improvement on teleoperation compared to the cases without force feedback [20].

### 1.2.2 Methods of providing haptic feedback

Methods of haptic feedback in master-slave system can be classified into the following three types: sensory substitution, virtual fixture and direct force feedback. Sensory substitution aims to substitute haptic feedback with visual, auditory, or vibration cues. For example, Miyazaki et al. used the color change on the display to tell the operator the magnitude of contact force [21]. Meli et al. mounted the finger skin deformation devices on an operator's fingertips. The finger skin deformation device generates a haptic perception by changing the skin curve of operator fingertip when the slave side contacts the object [22]. Sensory substitution method can keep the system stable with the communication time delay; however, the performance promotion is inferior to direct force feedback.

Virtual fixture aims to providing auxiliary control instruction to the devices, such as guiding the end-effector along desired paths in the workspace (guidance virtual fixtures) or preventing the end-effector from entering undesired regions (forbidden-region virtual fixtures) [23]. Boessenkool et al. proposed a modified version of virtual fixture called "haptic shared control", by which the operator can resist the assistant forces if he does not agree with the system's guidance [23] [25]. However, extra sensors that can measure the real relative location between the slave robot and the environment is needed, making the device structure complicated. And this method doesn't focus on the sensation of interacting with environments.

Direct force feedback is the most widely-used method. By indicating the amount of interaction force, the operator can feel as if he/she was handling the object directly. This is the most intuitive method for the operators and can thus improve the performance better

than the other two methods [26]. This research only focuses on the direct force feedback method.

Fig. 1.7 is an exemplary method of realizing the direct force feedback. It works as the following mechanism.

The master and slave devices themselves are respectively controlled by their own controllers. But the control instructions are not independent, for the forward direction (from the master side to the slave side), a force input from the operator moves the master device, the movement information of the master device is transmitted to the slave device through a position scaling (for micro operation:  $P_{scale} < 1$ ; for augment operation:  $P_{scale} > 1$ ) and a virtual impedance coupling (often considering as a parallel connection of a virtual damper  $K_v$  and a virtual spring  $K_p$ ). The slave devices uses the transmitted information as a moving instruction to its controller, following the motion of the master device generated by the operator.

For the back direction (from the slave side to the master side), if no additional force is applied to the slave device, no force is fed back to the master side; the master device solely moves by the operator's input force. If an additional force such as the interaction force when contacting the object is applied to the slave device, the interaction force is transmitted back to the master side through a force scaling ( $F_{scale}$ ), generating a change in the master's original motion, which allows the operator to percept the interaction force. Meanwhile, the change in motion of the master device also affects the motion of the slave device through the forward direction.

The above analysis shows that inputting force at any side of the master-slave system can lead to a change in the motion situation at both of the two sides. Hence, this method is called "Bilateral Control" [27] (The word "Bilateral" is a compound word meaning "two directions").

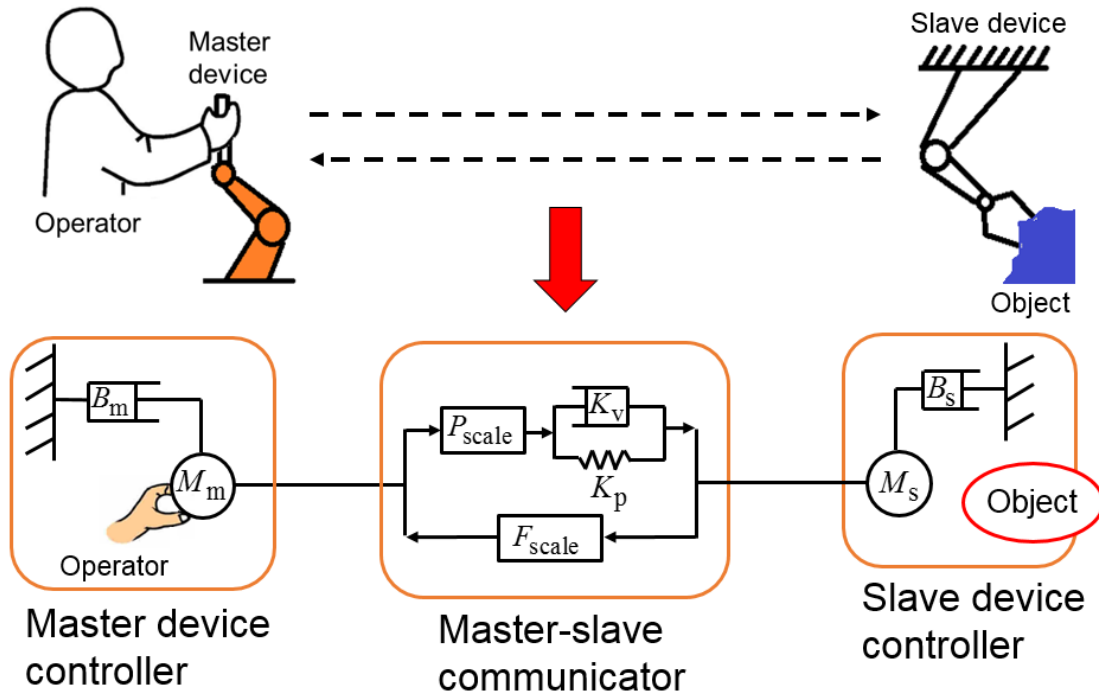


Fig. 1.7 An exemplary model of a master slave system with direct force feedback function

Moreover, from the operator standpoint, his/her force is the input source; the devices motion is the output. The effect of other factors in Fig. 1.7 can be considered as an impedance appeared to the operator relating his/her input and the output. Similarly, from the object standpoint, the interaction force is the input source; the devices motion is the output. The effect of other factors can be considered as an impedance appeared to the object.

Adjusting these “apparent impedance” generates various types of devices motion (output). Obviously the apparent impedance is determined by the parameters ( $K_v$ ,  $K_p$ ,  $P_{sc}$ ,  $F_{sc}$ , etc.) Hence the method of adjusting system parameters to generate a desirable “apparent impedance” is called “Impedance-adjusting bilateral control”, wherein the parameter adjustment is called “Parameter design”.

### 1.3 Parameters design in bilateral control

#### 1.3.1 Objectives of parameters design

Although the operator can actively change his/her input to generate a desirable device

motion according to the task requirements, it may result in some unwanted effects upon the operator. For example, the operator must be extremely cautious to prevent the force applied to a vulnerable object from exceeding a broken threshold, in such cases the operator is liable to be impatient, and having the operator restrain his/her hand vibration actively is easy to make him fatigue. An operator expects to input his/her motion within a routine range.

As mentioned above, the system parameter design can generate different impedance between the operator input and the system output, leading to a different device motion even the operator input is unchanged. So system parameter design is often used for satisfying the requirements of different tasks.

For example, if the operator input is unchanged, an impact into the environment with the system with low virtual impedance coupling  $K_v$  and  $K_p$  is obviously lower than that appeared with high  $K_v$  and  $K_p$  values. Thus reducing the  $K_v$  and  $K_p$  parameters between the master and slave devices is a common method to reduce the impact into the environment. Moreover, method of adding load is often used to stabilize something, thus increasing the damping parameter of the master device  $B_m$  is a common method to decrease hand vibration [28].

The objectives of system parameter design in the above examples are for the task requirements. Moreover, the human factors in operation should also be considered. From the standpoint of the operator, a direct benefit of providing the force feedback is allowing him to “feel” the interaction between the slave device and the environment. In many aspects of “feeling”, “how easily an operator can detect the contact occurrence” is important because an adequate perception of contact is crucial to determine spatial position and orientation of object [29]. This study concentrates on this human factor, which is called “Haptic Sensation” in this thesis.

When a human operator is performing a task via a bilateral controlled manipulator, the “feel” of the task is determined by the impedance appeared to him [30], which is affected by the system parameter design. So the “Haptic Sensation” is also affected by the system

parameter design.

Obviously, an inappropriate system parameter design results in an unexpected degrading in the operator's haptic sensation, weakening the benefits of force feedback function. Taking the two parameters design examples described above for instance, increasing the master damping parameter  $B_m$  generates a larger moving resistance. Thus an exceedingly larger moving resistance from a large  $B_m$  makes the operator feel as if groping in a sticky fluid, masking some delicate forces arising from the interaction with the object, making it difficult for the operator to sense a delicate contact [31], [21]. And setting the virtual impedance coupling  $K_v$  and  $K_p$  too low reduces the interaction force information fed back to the master side, such that it is also difficult for the operator to detect the contact.

From the above examples, designing one type of parameter results in trade-off effects on the task requirement and the operator's haptic sensation. The system parameter design requires considerations to both the task requirements and the operator's haptic sensation. Specifically, when designing parameters for the task requirements, the designer should check how it affects the haptic sensation after adjustment; if the haptic sensation decreases, the designer should recover it by additionally adjusting other parameters.

### 1.3.2 A review of works about parameters design for a bilateral control system

The conclusion in Section 1.3.1 indicates that the system parameters should be designed with considerations to both the task requirements and the operator's haptic sensation. Many related works have studied about the parameter design, these works can be classified by two topics: regarding to the system performance (task requirements) and regarding to the human factors. Here is a brief review on these works.

For the works regarding to the relationship between the parameters for the system performance, many works focused on the effect of parameter adjustment to the stability factor because the stability is the most critical factor of performance for a control system.

As to the effect of specific parameters to the system stability, [32] – [34] studied the

effect of time-delay; [35] studied the effect of velocity and feedback force scaling:  $P_{scale}$  and  $F_{scale}$ ; [36] studied the effect of virtual damping. Christiansson et al. studied the effect of slave device stiffness [37].

With regard to the concept of apparent impedance, because the motion of a bilateral control system is analogous to the voltage and current signals in an electrical network; the system parameters affects the system performance in the same manner as the circuit element parameters affects the voltage and current signals [38]. Therefore, many works used the methods with the 2-port electrical networks theory to analyze stability of the mechanical bilateral control system. In [38], Raju proposed a parameter design criterion that guarantees the positive realness of the apparent impedance matrix to keep the system stable. Similar to the impedance matrix. Hannaford used a hybrid matrix (a transformation of apparent impedance matrix) to check the system stability [39]. The authors in [30], [40] and [41] transferred the stability problem to keeping the passivity of scattering matrix of the system (another transformation of apparent impedance matrix) because the “System Passivity” is a useful tool to analyze the system stability and is affected by system parameters.

In addition to the stability, force and velocity at the input and output sides are also important factors of the system performance for a bilateral control system. Raju proposed a method that adjusts the system parameters that form the impedance matrix to generate a desirable output [42]. Hannaford proposed a guideline adjusting the system parameters to make the impedance of the slave side equals that of the master side [43]. Bobgan presented a method that guarantees the specific system behavior by designing the hybrid matrix elements [44]. Hansen et al. proposed a parameter estimation technique to reduce the unnecessary forces applied by the surgeon [45].

As to the control architecture optimization, Landi et al., studied how to adjust the inertia and damping to make the system stable [46]; Peer et al. used the parameter space approach to analyze the stability of different types of bilateral control algorithms [47]; Morimitsu et al. focused on designing the parameters in the position and force controllers to eliminate the unstable effects from the time-delay [48]; Ranatunga et al. developed a new inner-

loop/outer-loop robot controller formulation wherein the system parameters can be tuned automatically to keep the system stable [49].

The studies introduced above provided many effective methods for the system parameters design with consideration to the task requirements. However, they do not have a perspective of the human factors. As for the human factors, “Transparency” is an important indicator that correlates the system parameter design and the human factors. Fig.1.8 is the concept of a transparent system. Different from Fig. 1.7, no master and slave devices dynamics appears to the operator, indicating that the velocity input from the operator equals the velocity output of the slave device, and the force transmitted back to the operator equals the interaction force occurred between the slave device and the environment, such that the operator feel as if he/she is handling the environment directly by his/her hand.

The response of a transparent system is defined as an ideal system response in [27], since that, many works studied how to realize a transparent system by adjusting the system parameters [50] – [55]. These works are classified as transparency based method [56].

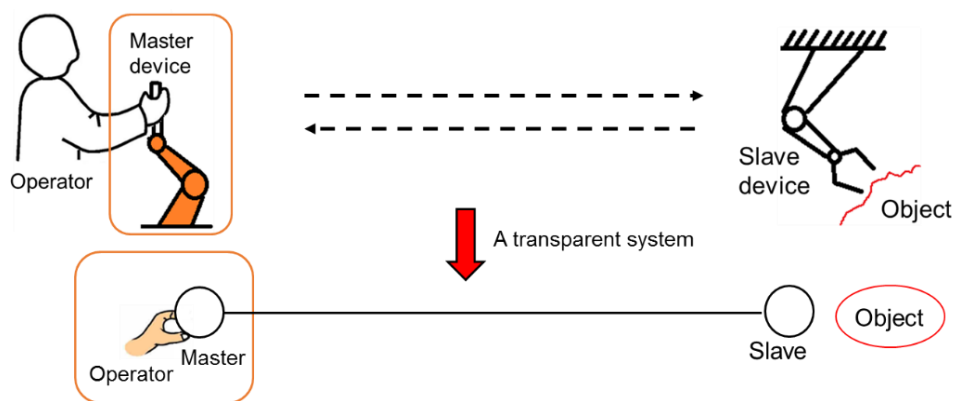


Fig. 1.8 The concept model of a transparent master slave system

However, the transparency based method has some limitations, first, a transparent system is not always ideal to the operator, for example, sometime an extreme large excitation signal from the environment is not expected [21], [57]; or the feeling that transmitted back to the operator by a transparent system is very weak when the

environment is very soft. Therefore, a certain level appeared impedance to the operator, rather than absolute transparency, can enhance the operational performance [58], [59]. In such cases the system transparency is often sacrificed for a desirable haptic sensation.

Moreover, the true magnitude of sensation felt by the operator is still unknown in any extent of system transparency (an absolute transparent system is unachievable) [50]. Hence other works focused on the relationship between system parameters and the operator's sensation. Rosenberg et al. measured the subjective hardness or crispness ranking felt by the subject by adjusting the environment stiffness and damper [60]; Christiansson et al. studied the operator's ability of discriminating the object size with different system stiffness and damper [61]; Gersem et al. studied how to enhance the operator's ability of discriminating a difference in environment stiffness by optimizing the controller [62]; Nisky et al, studied the operator's estimation of the object stiffness with time-delay [63]; Yamagawa et al. studied the difference threshold of a time-variant force with different feedback scaling gains [64]; Kouris et al. found that increasing the device damper and inertia increases the operational difficulty [65].

These works confirmed that the human factors are indeed affected by system parameters, but they did not clarify the quantitative relationships between the human factors and the system parameters; and none focused on the haptic sensation factor: how easily an operator can detect the contact occurred between the slave and the environment.

In a word, the existed works do not provide an effective guideline for the system parameters design with consideration to the operator's haptic sensation. This situation results that a system designer can only rely on an unfounded method: trial and error method when designing the system parameters to for the operator's haptic sensation in real applications of the master-slave systems.

#### 1.4 Research objective

Therefore, this study aims to build a new guideline for system parameter design with consideration to the operator's haptic sensation. In detail, the system designer expects to know the extent to which the operator's haptic sensation will change after the system

parameters are altered; or the limit value the system designer can set a parameter to if he/she wants to hold the haptic sensation unchanged; or the value to which another alternative parameter should be set to restore the haptic sensation when some parameters are inevitably set beyond the limit.

The parameter designer's expectation can be realized only if he/she knows the quantitative relationship between the parameters and the operator's haptic sensation. The most intuitive and convenient quantitative relationship is that represented as a mathematical function, from which the haptic sensation can be directly calculated from the parameters (parameters values are the independent variables and the haptic sensation is the dependent variable).

Just like calculating kinetic energy directly from velocity and calculating the electric power directly from current, the dependent variables at the left side are quantities with numerical values. Therefore, the dependent variable of the objective function in this study, namely, haptic sensation, should be quantified.

Therefore, an index that quantifies the operator's haptic sensation by its value is first proposed. Next, by clarifying the mathematical relationship between the index value and the system parameters, the following function is derived.

$$\text{Index value} = f(K_v, K_p, B_m, F_{sc}, P_{sc} \dots) \quad (1.1)$$

By using function (1.1), the index value can be directly calculated from the parameter values. If a parameter value at the right side is changed, the effect on operator's sensation can be directly known from the change in the index value. Moreover, by setting the desired haptic sensation as a fixed index value at the left, the reasonable system parameter values can be easily calculated back. In one word, the system parameter design will become well-founded and the trial and error method is no more needed. Findings of this research can be used as guidelines for system parameter design.

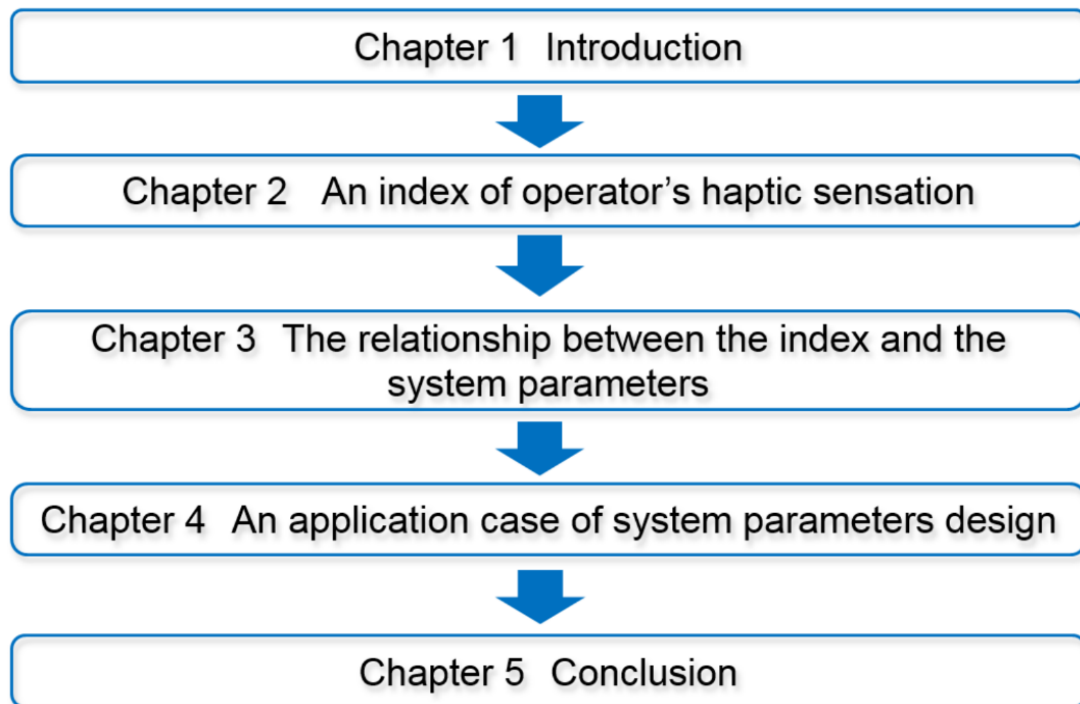


Fig. 1.9 Schematic configuration of this study

## 1.5 Thesis constitution

As Fig. 1.9 shows, this thesis is constituted from five parts. The current chapter is the introduction, where the research background and the objective are mentioned.

The operator's haptic sensation is an abstract concept which is difficult to correlate to the physics parameters. However, the haptic sensation is affected by the motion of the master device which is easily correlated to the parameters. So in Chapter 2, an index whose value is calculated from the device motion factors is proposed. Then correctness of the index to represent the haptic sensation by its value is also confirmed in Chapter 2. (See the orange part in Fig. 1.10.)

In Chapter 3, the mechanism that system parameters affect the device motion factors is clarified. Then implementing the mechanism into the index definition, the mathematical relationship between parameters and the proposed index is obtained. (See the pink part in Fig. 1.10.)

Chapter 4 introduces some application cases using the results obtained in the previous

two chapters to design system parameters for a desirable haptic sensation. The application cases in this chapter shows that the operator's haptic sensation and the parameters can be connected correctly through the proposed index. (See the blue part in Fig. 1.10.)

Chapter 5 summarizes the abovementioned contents; moreover, suggests some topics to be done in the future.

On the basis of the results in Chapters 2 and 3, the operator's haptic sensation and the system parameters are connected by the proposed index. Therefore, Chapter 4 introduces several exemplary application cases where the desirable operator's haptic sensation is obtained by just adjusting system parameters. (See the blue part in Fig. 1.10).

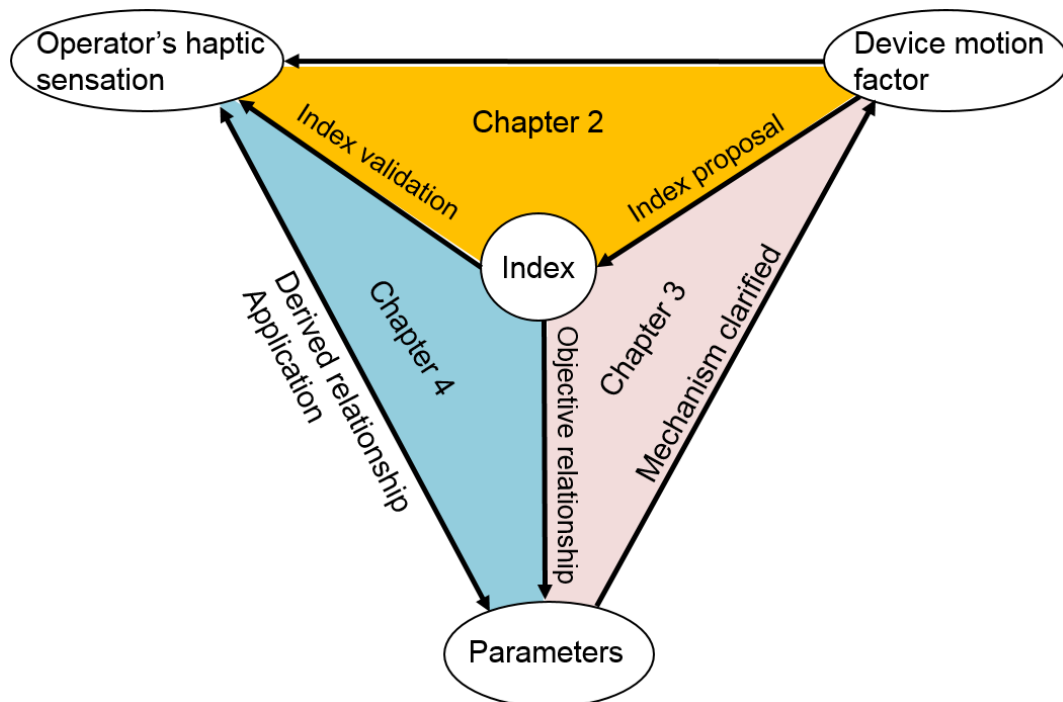


Fig. 1.10 Schematic configuration of this study

## Chapter 2

### An index of operator's haptic sensation

In this chapter, an index is proposed to quantify the haptic sensation felt by the operator when the slave device is in contact with the environment. As introduced in 1.3.1, haptic sensation means how easily an operator can sense the contact between slave device and the environment.

Regarding to human's perceptual capability sensation about the system properties or motion factors, Cholewiak et al. studied the operator's sensation of stiffness and force [66]; Klatzky et al. studied the perception discrimination of force and torque [67], but they didn't quantify the perceptual capabilities.

Song et al. quantified the sensation of resistance force generated from the device damping during moving the device [68], but the research object is not sensation for a contact. Lawrence et al. proposed the index known as "Rate-hardness" to quantify the operator's perception of the hardness of objects in using haptic interfaces, when the contact between the slave device and the environment happens [69], however, if objects in the target environment are fragile like soft tissue in surgical applications, how easily an operator can sense the contact between the slave device and the environment, is more important than the perception of environment property. These works cannot be used in system parameters design.

Son et al. proposed a perceptual index to quantify the detection and discrimination abilities [56], [70]; however, when applying this index in system parameter adjustment, a specialized knowledge of control theory is required, making the perceptual index impractical to use in parameter adjustment in the field, and the parameter optimization must be done before the system is deployed.

The limitation of the other works and the main objective of this study (clarify the relationship between the haptic sensation and the system parameters) show that, the new index is expected to easily related to the system parameters. As the system and the environment parameters directly affects the device's motion, which affects the operator's sensation, thus the new index proposal begins at the mechanism by which the operator detects the contact during operating a master-slave system.

## 2.1 Haptic mechanism during operation

When the slave device contacts the environment, the motion of both the master and slave devices will change due to the bilateral control. During operation of the master–slave system, the operator's fingers are always clinging to the master device, thus the dynamic factor of the master device will provide the stimuli that generate haptic sensation. Undoubtedly, the master device dynamic factor is easily correlated to the system parameters, thus the relationship between stimuli intensity (determines the haptic sensations) and the system parameters can be derived by first quantifying the stimuli intensity by the dynamic factors of the master device.

Based on the intensity of the feedback, different modalities of haptic sensations are used. If the feedback is weak, contact is sensed by cutaneous sensation. The cutaneous receptors under the finger pads work for such sensations. Tan et al. studied the detection and discrimination ability for finger-pad and claimed that the firing rate of these receptors is a function of the mechanical work exchange in a cutaneous interaction [71]. The firing rate of cutaneous receptors (FA and SA receptors) are functions of the skin curvature's changing speed [72].

If the feedback is intense, kinesthetic sensations from changes in the operator's wrist and arm positions will dominate the sensing of contact. From the review literature on kinesthetic sensation [73] and a study of the kinesthetic sensation in haptic feedback generated by a motor [74], [75], kinesthetic sensation are believed to be sensed by the primary spindle receptors in the arm muscles. The acceleration and velocity of the arm and wrist joints are coded by the primary spindle receptors to generate a sensation of

contact.

Unlike the visual and olfactory stimuli, for which people can easily distinguish a difference in modality, the border between cutaneous and kinesthetic sensations is unclear to a subject. Studies have testified that a combination of kinesthetic and cutaneous feedback improves teleoperator performance over the performance possible with cutaneous feedback alone [76]. Haptic-feedback devices are therefore usually designed to combine these two types of sensations [77].

As a dynamic factor of the master-slave system that tracks the operator's haptic sensation, that factor should be existed in both cutaneous and kinesthetic sensing. Based on the analysis above, the change extent on master device velocity before and after contact is hypothesized effectively match with the stimuli that provide the operator with a contact sensation.

Although the individual variance with different operator and time makes it impossible to indicate the accurate sensation level for a given operator or every contact, the stimuli intensity can indicate the degree of a haptic sensation at an average and general level.

## 2.2 Definition of the index

The index is defined from the stimuli intensity, which uses the dynamic factor of master device velocities before and after contact. So the index proposed here is call as Dynamic Contrast (abbreviation:  $C$  ).

Fig. 2.1 plots some examples of the master device's velocity profile before and after contact. If there is no velocity change in the master device after the contact with the environment, the operator will have no sensation about the contact; if the velocity of the master device drops smoothly after contact, the operator will be difficult to sense the contact; if the velocity of the master device reduces suddenly, it will be very easy for the operator to sense the contact.

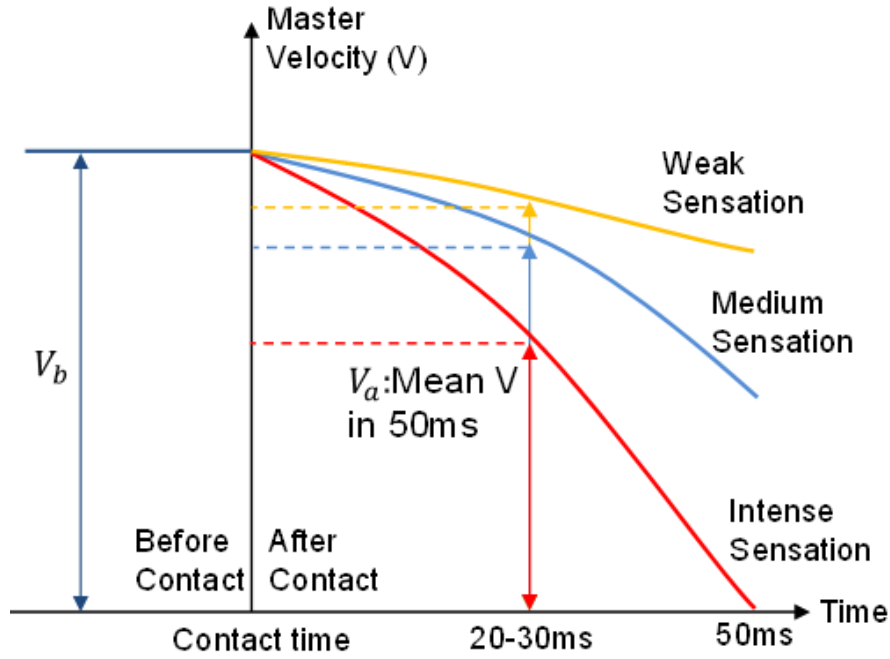


Fig. 2.1. Examples of master device velocity profiles. The sharpness in the change in velocity is hypothesized to be functionally related to the operator's haptic sensation

Therefore, the ratio of master-device velocity before and after contact is chosen as the dynamic factor that determines the stimuli of operator's haptic sensation. Thus the proposed index is defined as:

$$C = 1 - \frac{\bar{V}_a}{V_b} = \frac{V_b - \bar{V}_a}{V_b} \quad (2.1)$$

In function (2.1),  $V_a$  and  $V_b$  are the velocities of the master device before and after contact, respectively. In function (2.1), the average master velocities over the 50 ms after contact are used to calculate  $C$  value. This is supported by several considerations. First, the master velocity used in this calculation is not expected to be affected by the active muscle motion of the operator. According to [13], the time duration should be set to 30 ms to preclude volitional control; second, if the feedback is weak, the feedback can be looked upon as a vibration at low frequency. According to mechanism of a tactile sensation, the sensation of low-frequency vibration is generated by the FA1 receptor (Meissner corpuscles), temporal resolution of which ranges from 15 ms–50 ms [78]. If

the feedback is relatively intense, kinesthetic sensation dominates haptic sensation, of which the temporal resolution has been measured in the range 17 ms–35 ms [79].

Therefore, the first sensation magnitude of the contact by which the operator detects the contact is determined by the change level of the master device from the contact moment to 20 ms–30 ms after. The average velocity over 50 ms after contact is used to represent the change level from the contact moment to 20 ms–30 ms after.

According to function (2.1), the index value has no dimensions. If the master device's velocity does not change, no contact sensation is generated ( $C = 0$ ); if the master device after contact comes to a full stop within a temporal resolution time, the operator's will be very easy to detect it ( $C = 1$ ). The index value lies within the range  $[0, 1]$ .

### 2.3 Characterization of the haptic sensation index

In this section, characteristics of the proposed index are studied, including its stability to different operators and the necessary change ratio to an index  $C$  value to produce a just noticeable different haptic sensation.

#### 2.3.1 Experimental apparatus

We built a master–slave system with the bilateral control model diagrammed in Fig. 2.2. The master side is a Phantom Desktop haptic device (SensAble Technologies). To allow an ideal system without interference from mechanical factors, the slave side and the operational environment are modeled in a virtual world; the slave side is a virtual sphere and the operation environment is a virtual wall. The update rate of the system is fixed at 1 kHz.

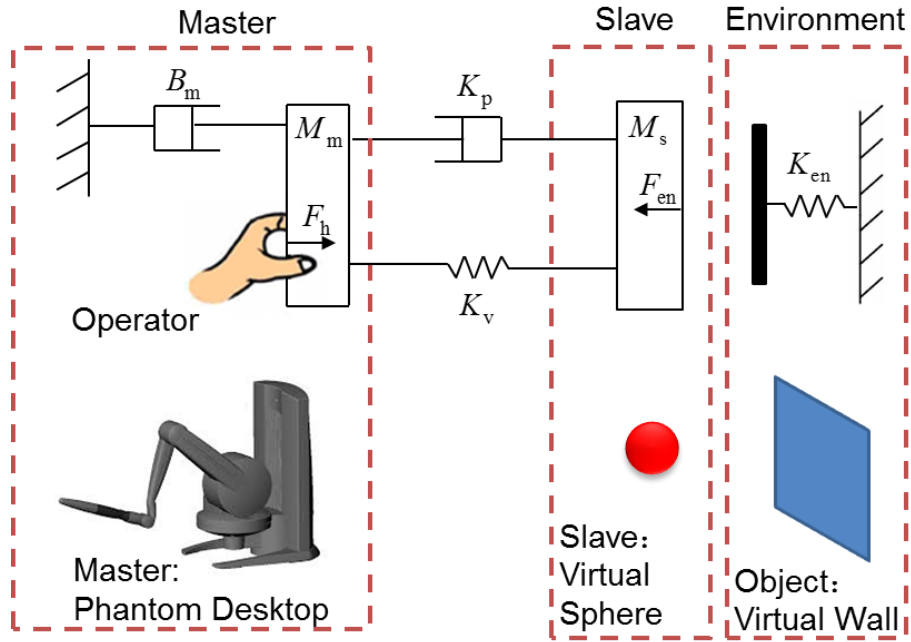


Fig.2.2. Control model and device of experiment system. The master side is a haptic device: Phantom Desktop, slave side is a virtual sphere and the operating environment is a virtual wall.

The definitions and units of each parameter in Fig. 2.2 are as follows:

$B_m$  : Damping of the master device, (Ns/mm);

$M_m$  : Inertia term in the controller of the master device, ( $\text{kg} \cdot 10^3$ );

$M_s$  : Inertia term in the controller of the slave device, ( $\text{kg} \cdot 10^3$ );

$K_p$  : Virtual stiffness between the master and the slave devices, (N/mm);

$K_v$  : Virtual damping between the master and the slave devices, (Ns/mm);

$K_{en}$  : Stiffness of the virtual wall, (N/mm);

$F_h$  : Force applied by the operator, (N);

$F_{en}$  : Force applied by the environment (virtual wall), (N).

The equations of motion for the system in Fig. 2.2 are as follows.

$$F_h = M_m \ddot{r}_m + B_m \dot{r}_m + F_{en} = M_m \ddot{r}_m + B_m \dot{r}_m + K_{en} (r_s - r_{wall}) \quad (2.2)$$

$$F_{en} = K_{en} (r_s - r_{wall}) = M_s \ddot{r}_s + K_p (r_s - r_m) + K_v (\dot{r}_s - \dot{r}_m) \quad (2.3)$$

In functions (2.2) and (2.3),  $r_m$  is the position of the master device,  $r_s$  is the position of the slave sphere, and  $r_{\text{wall}}$  is the position of the virtual wall, which is constant. For simplicity, only the stiffness of the wall is represented as the properties of the environment.

The damping of the master device  $B_m$  and the stiffness of the virtual wall  $K_{\text{en}}$  affected the operator's haptic sensation remarkably more than the other parameters when the experimental system is stable. Hence, in the following experiments,  $B_m$  and  $K_{\text{en}}$  parameters are adjusted to generate the different haptic sensations, the other system parameters are hold constant.

### 2.3.2 Subjects and motions

We enrolled 10 subjects, nine males and one female, all between 22 and 35 years old. All subjects were right-handed. The experiment was conducted in accordance with standard ethical practices and was approved by the ethics committee for human experiments of the Tokyo Institute of Technology.

Subjects performed the following motion in the experiments. As the master device moves forward, the slave sphere in the virtual world also moves forward and contacts with the virtual wall. The subject holds the stylus of the master device in their right hand and moved the stylus forward at an arbitrary speed (keep the velocity before contact constant is expected), and retract back after detecting the contact between the slave sphere and the virtual wall. The appearance of the experiment is shown in Fig. 2.3.

### 2.3.3 Experiment for the index value stability to different operators

The contact velocity will vary considerably for different operators of a master-slave system. Therefore, under the same parameter setting, the extent to which the index value is affected by different operators or contact velocities should be studied. To clarify this property, the statistical characteristics of the index value with different operators were studied.

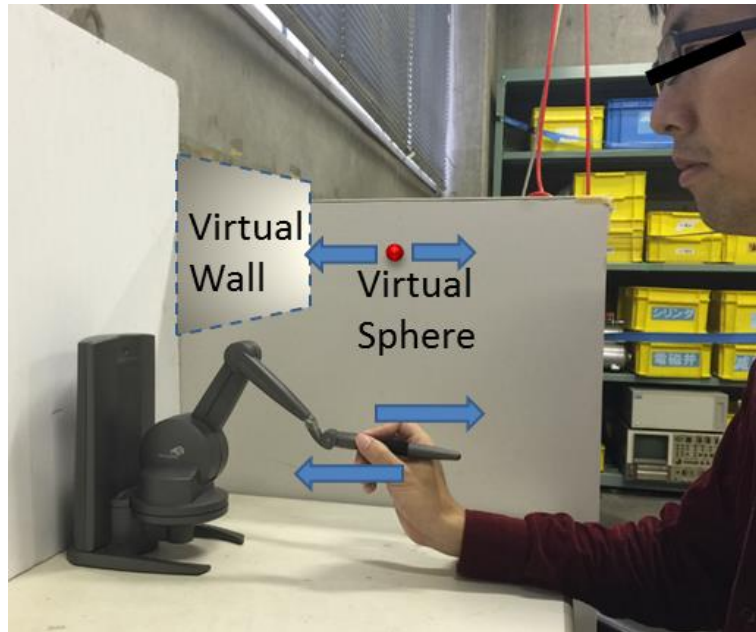


Fig. 2.3. Appearance of the experiment, subjects are instructed to hold the stylus, perform approach-retract movement, and remember the haptic sensation when the slave sphere contacts the virtual wall.

The ten subjects performed experiments with the master-slave system described in Section 2.3.1. For one parameter setting, the 10 subjects were instructed to repeat the approach-retract motion 10 times, consciously varying the speed with which they approached the target wall over the 10 motion. So the approach-retract motion is repeated 100 times from different subjects with various contact speed. The velocity profiles from every approach-retract motion are recorded, from which 100 index  $C$  values can be calculated.

In this experiment, ten parameter settings listed in column 2 of Table 2.1 were tested. For every parameter setting case, the calculated index values from different subjects with various contact speed are distributed normally according to the Kolmogorov-Smirnov normality test. As an example, histograms of the calculated  $C$  values from parameter setting case No.1 to No. 4 are shown in Fig. 2.4.

Table 2.1  
Statistical characteristics of  $C$  measurements

Case No.	Parameter setting	Sample size	Mean value of $C$	Standard deviation	Coefficient of variation
1	$B_m = 0.001, K_{en} = 0.1$	100	0.149	0.027	18.1 %
2	$B_m = 0.001, K_{en} = 0.2$	100	0.243	0.032	13.2 %
3	$B_m = 0.001, K_{en} = 0.3$	100	0.365	0.045	12.3 %
4	$B_m = 0.001, K_{en} = 0.4$	100	0.449	0.044	9.8 %
5	$B_m = 0.001, K_{en} = 0.5$	100	0.501	0.054	10.7 %
6	$B_m = 0.004, K_{en} = 0.1$	100	0.119	0.022	18.4 %
7	$B_m = 0.004, K_{en} = 0.2$	100	0.202	0.028	13.8 %
8	$B_m = 0.004, K_{en} = 0.3$	100	0.305	0.032	10.4 %
9	$B_m = 0.004, K_{en} = 0.4$	100	0.384	0.036	9.4 %
10	$B_m = 0.004, K_{en} = 0.5$	100	0.460	0.047	10.2 %

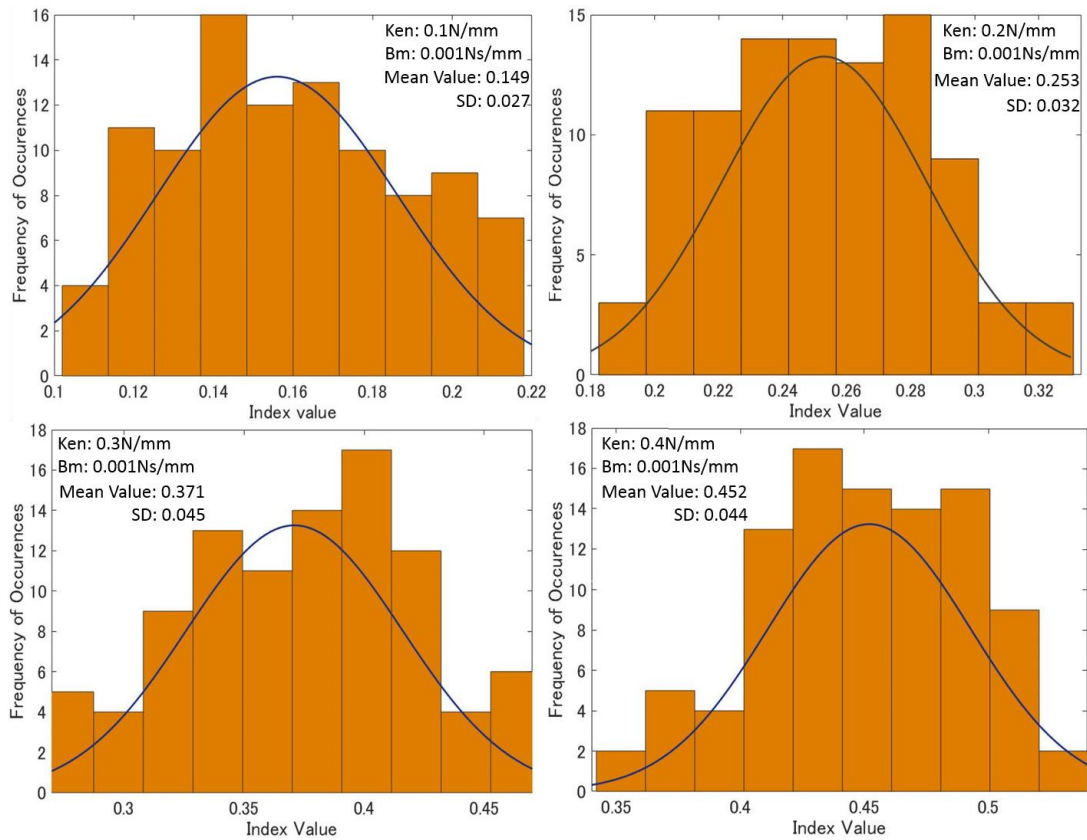


Fig. 2.4. Distribution of  $C$  value calculated from in 100 approach-retract motions for parameter setting No.1 to 4. All are normal distributions.

Although these 100 calculated index values are not under entirely independent conditions, the subjects were instructed to consciously change the approach velocity for each of the ten contacts they performed for each set of parameters, the 100 times approach-retract motions for each parameter setting are sufficiently independent for our purposes.

For all parameter settings No.1 to 10, the mean, standard deviation, and coefficient of variation of the 100 index values calculated from the recorded velocity profile are listed in Table 2.1. For all the parameter settings, the coefficients of variation are under 15 % except for cases No.1 and 6. According to [80], a coefficient of variation less than 15 % indicates that the index value will not diverge to an unacceptable level. Therefore, under different operators and different contact velocity, variation of the index value is within an acceptable range. Moreover, the 10 parameter settings can cover a wide range of operation conditions, meaning that the  $C$  value is stable to contact velocity in normal applications.

The value of  $C$  is independent of the approach velocity. Fig. 2.5 shows three velocity profile examples under the parameter setting case No.4. The approach velocities are far different (80 mm/s, 151 mm/s, 210mm/s); Fig. 2.5 shows that the index values calculated from the three velocity profiles by equation (2.1) are the nearly the same. For all the 100 velocity profiles under parameter setting case No.4, the approach velocities applied by the subjects varied from 50 to 350 mm/s, the correlation between the index values and the approach velocity was tested; the probability of the null hypothesis (that the  $C$  value is not correlated with approach velocity) was set to 0.05. The statistical significance  $P$  of the correlation between the approach velocity and  $C$  values is 0.37 and the correlation coefficient ranges from 0.18 to 0.43.

Except for parameter setting No. 4, the correlations between  $C$  values and the approach velocities under other parameter settings were tested; the statistical significance of the correlation between the approach velocity and  $C$  changes from 0.35 to 0.48 and the correlation coefficient ranges from 0.155 to 0.531, which means the  $C$  value is independent to the approach velocity except in extreme approach velocities.

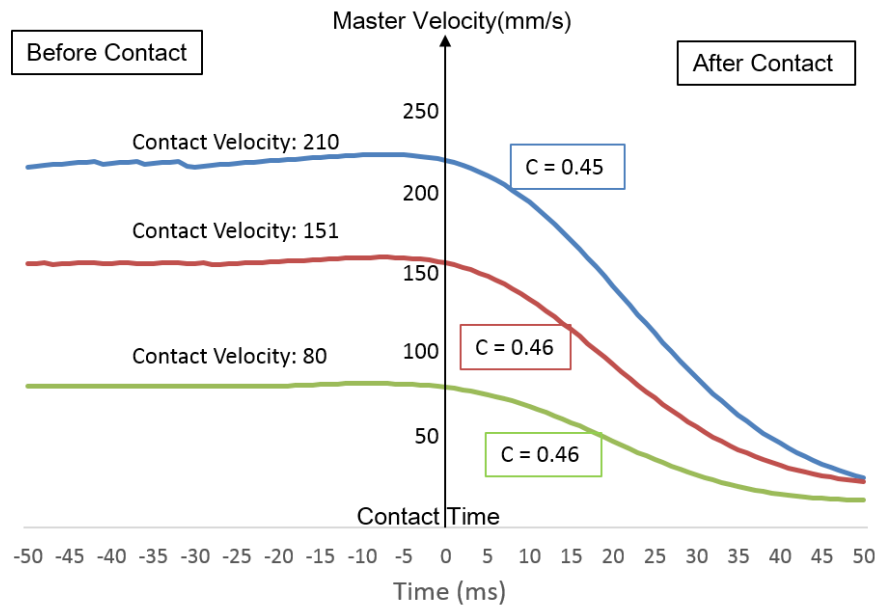


Fig. 2.5. Examples of velocity profiles with different approach velocities under the same parameter setting, using the velocity profiles to calculate the index value, the results are the nearly the same.

$C$  value being independent of the approach velocity means that the approach velocity doesn't affect operator's haptic sensation. This is true because of the following reasons: first, the experimental participants tended to report that their approach velocity did not affect how easily they can sense the contact. Secondly, as mentioned in Section 2.1, the haptic sensation for sensing contact is generated from a combination of cutaneous and kinesthetic sensations. Hirano et al. found that the approach velocity does not affect cutaneous sensation noticeably [81]. As for kinesthetic sensations, Jones claims that the ability to detect a change in the position of a limb is not affected by the angular velocity of the arm movement, which is correlated with the approach velocity [74]. Hence, the approach velocity is not likely to affect the sensibility for the operator to detect the contact between the slave device and the environment.

#### 2.3.4 Experiment for reflecting a different haptic sensation in $C$ value

While design system parameters for some requirements, the designer should check the effect to the operator's haptic sensation after adjusting the parameters. Among many kinds of changes, the simplest and most basic are strengthening and weakening effects,

whether the operator's sensation is strengthened or weakened is the first situation to be checked.

Human's haptic sensation is not continuous, the operator can feel a difference in haptic sensation only if it was altered to an extent. When using  $C$  values to estimate the operator's haptic sensation, the designer should know how much the index  $C$  value should be changed to produce a different haptic sensation.

Moreover, one objective of this study is calculating haptic sensation index directly from the system parameters; thus by knowing the necessary numerical change that makes the sensation different, the designer can calculate the setting limit for a parameter value; if a parameter value surpasses the limit is inevitable, the designer can know to which extent the other parameters should be set to restore the haptic sensation.

Therefore, in this chapter, a psychophysics experiment is implemented to study how to reflect a strengthening or weakening to operator's haptic sensation on the index value. The experiment first measures the just-noticeable difference (JND) against the reference haptic sensation; then calculates the numerical change in the index value between the JND and reference haptic sensation.

Each reference has two JNDs in directions of strengthening and weakening, i.e., the upper threshold (UT: the reference sensation is strengthened until the difference can be just noticed) and the lower threshold (LT: the reference sensation is weakened until the difference can be noticed) [82].

10 subjects performing the experiment in Section 2.3.3 were also used in this experiment, in every trial, the subject repeated this approach-retract motion for successively five times, just like knocking on a door. The experiment is designed based on the up-and-down method for testing JNDs. This method is used extensively in psychophysics studies [83].

A reference trial and a comparison trial were conducted as one set. Both the two trials were presented to the subject, and the subject was asked whether they noticed a difference in the easiness of detecting the contact with the environment in the two trials. The

presentations of reference and comparison trials are alternated in a random order to prevent time error.

To illustrate this experiment in detail, the process for obtaining the UT sensation to the reference sensation under parameter setting ( $K_{en} : 0.1 \text{ N/mm}$ ;  $B_m : 0.001 \text{ Ns/mm}$ ) is introduced; this process is also illustrated by Fig. 2.6. In the reference trials, the parameter setting was constant. In comparison trials,  $B_m$  was kept constant and  $K_{en}$  began at 0.3 N/mm, which is far higher than the reference trial of 0.1 N/mm, allowing the subjects to easily notice the difference between the reference and comparison trial and answer "Yes."

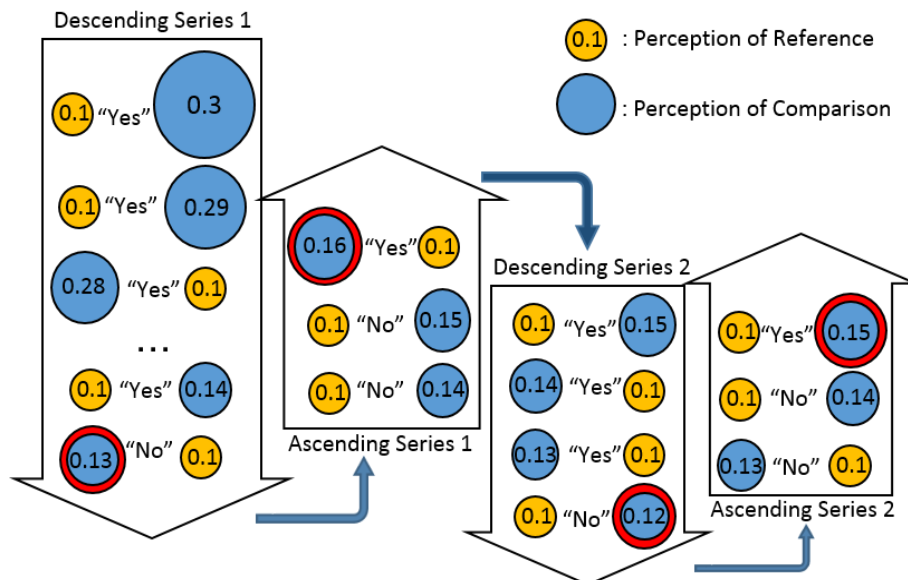


Fig. 2.6. Process for measuring the just-noticeable different haptic sensation with the reference sensation (environmental stiffness  $K_{en} = 0.1 \text{ N/mm}$ ). Descending and ascending series of trials are presented, and altered until a difference emerges or disappears. Haptic sensations are represented by the circle size. "Yes" or "No" between two circles are the subject's answer of whether a difference between the comparison and the reference sensation can be noticed. Circles with red rings are the recorded  $K_{en}$ , at which the subject's perception of a difference in the stimuli appeared or disappeared.

As long as the subjects noticed a difference in haptic sensation between the comparison and reference sensation,  $K_{en}$  in the comparison trials was reduced by increments of 0.01 N/mm to approach the  $K_{en}$  in the reference parameter setting (0.1) gradually until the subject could no longer detect a difference between the comparison and reference sensation. As shown in Fig. 2.6, the subject in this example could no longer detect the difference when  $K_{en}$  was reduced to 0.13 N/mm in the comparison trial, answering “No.”. The ring appears at left position means its sensation was represented first in comparison, and the ring appears at the right position means its sensation was represented second.

When the difference between reference and comparison sensations disappears, the experimenter increased the  $K_{en}$  in comparison trials with increments of 0.01 N/mm until the subject could again notice a difference in haptic sensation between the comparison and reference. As shown in Fig. 2.6, in this example, the answer “Yes” reappeared at  $K_{en} = 0.16$  N/mm.

The ascending and descending series were repeated twice each, during the experiment, subjects could not see the motion on the slave side; all motions were judged solely by their haptic sensation.

After representing the ascending and descending series, the  $K_{en}$  values at which the difference between reference and comparison emerges or disappears (subjects answer transition between “Yes” and “No” occurred, for example,  $K_{en} = 0.13$  N/mm, 0.16 N/mm, 0.12 N/mm, and 0.15 N/mm in Fig. 2.6) are recorded. The mean of the four recorded  $K_{en}$  values, 0.14 N/mm in this example, is the UT  $K_{en}$  parameter at which the upper difference in haptic sensation compared to the reference sensation is just noticeable.

Finally, the experimenter recorded the velocity profiles for the reference parameter settings ( $K_{en} : 0.1$  N/mm,  $B_m : 0.001$  Ns/mm) and its UT parameter settings ( $K_{en} : 0.14$  N/mm,  $B_m : 0.001$  Ns/mm), from which the  $C$  values that represent the reference haptic sensation ( $C_{UT}$ ) and the comparison sensation ( $C_{ref}$ ), and the change ratio between them ( $C_{UT} / C_{ref}$ ) can be calculated. 10 subjects performed this process, the

mean index change ratios between the reference and its UT ( $C_{UT} / C_{ref}$ ) from the 10 subjects is the necessary numerical change ratio ( $R_c$ ) for a reference index value to represent a just noticeably strengthened the haptic sensation, in this example, is 1.423.

The process of obtaining the necessary numerical change ratio ( $R_c$ ) for a reference index value ( $C_{ref}$ ) to represent a just noticeably weakened haptic sensation  $C_{LT}$  is the almost the same, the only difference is that  $R_c = C_{ref} / C_{LT}$ .

In this experiment, the JNDs to ten reference haptic sensations generated from the ten reference parameter settings listed in column 2 of Table 2.2 were measured. Index values for every reference parameter settings ( $C_{ref}$ ) are listed in column 3. To each reference cases, the index value for its upper threshold sensation ( $C_{UT}$ ) and lower threshold sensation ( $C_{LT}$ ) are listed in columns 4 and 6; the necessary numerical change ratios ( $R_c$ ) to represent a just noticeably different sensation are listed in columns 5 and 7.

As introduced above,  $R_c = C_{UT} / C_{ref}$  in trials of UT measurement; and  $R_c = C_{ref} / C_{LT}$  in trials of LT measurement, by plotting all the denominators in calculating  $R_c$  on the horizontal axis, and the  $R_c$  value on the vertical axis in Fig. 2.7, it can be observed that, as the reference index value ( $C_{ref}$ ) increases, the  $R_c$  becomes noticeable decreases. We consider this situation appears because of the difference in haptic modalities. When the feedback is weak, the contact sensation is the cutaneous sensation; as it increases, the kinesthetic sensation will be involved, which sensitizing the discrimination ability.

In extreme cases, when the reference haptic sensation is estimated to be minimal ( $C_{ref} \rightarrow 0$ ),  $R_c$  approaches infinity. When the reference haptic sensation is estimated to be very intense ( $C_{ref} \rightarrow 1$ ), the haptic sensation is close to perceiving the environment stiffness, which has been studied previously [59] and [70]. These studies revealed that the difference threshold will be about 10 ~ 20 % higher than the reference stimulus. Therefore, in this research, an intermediate value of  $R_c = 1.15$  was chosen as the appropriate index change ratio when the reference is very intense.

Table 2.2  
The experimental conditions and results for measuring  $R_c$

Case No.	Reference parameter setting	Reference C value: $C_{ref}$	Mean of UT C value: $C_{UT}$	$R_c = C_{UT} / C_{ref}$	Mean of LT C value: $C_{LT}$	$R_c = C_{ref} / C_{LT}$
1	$B_m = 0.001$ $K_{en} = 0.1$	0.149	0.212	1.423	0.087	1.712
2	$B_m = 0.001$ $K_{en} = 0.2$	0.243	0.340	1.399	0.165	1.447
3	$B_m = 0.001$ $K_{en} = 0.3$	0.365	0.456	1.249	0.253	1.445
4	$B_m = 0.001$ $K_{en} = 0.4$	0.449	0.530	1.180	0.300	1.496
5	$B_m = 0.001$ $K_{en} = 0.5$	0.501	0.610	1.220	0.361	1.385
6	$B_m = 0.004$ $K_{en} = 0.1$	0.119	0.185	1.554	0.073	1.630
7	$B_m = 0.004$ $K_{en} = 0.2$	0.202	0.314	1.554	0.138	1.463
8	$B_m = 0.004$ $K_{en} = 0.3$	0.305	0.445	1.459	0.203	1.525
9	$B_m = 0.004$ $K_{en} = 0.4$	0.384	0.480	1.250	0.263	1.460
10	$B_m = 0.004$ $K_{en} = 0.5$	0.460	0.552	1.196	0.341	1.353

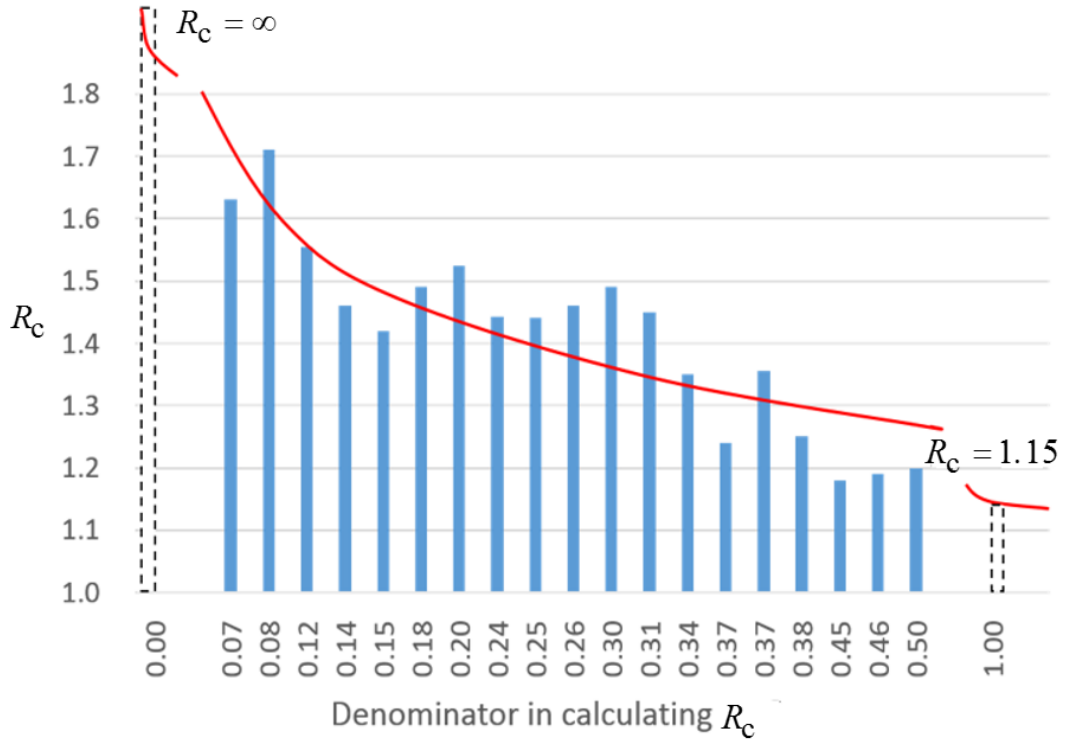


Fig. 2.7. Reference  $C$  values and  $R_c$ , the necessary change ratio  $R_c$  to a reference  $C$  value to make the difference between two haptic sensations noticeable, including extreme cases.

According to Fig. 2.7, the  $R_c$  and reference  $C$  ( $C_{\text{ref}}$ ) values can be fit to the following logarithmic function:

$$R_c = \log_{0.001} C_{\text{ref}} + 1.15 \quad C_{\text{ref}} \in [0, 1] \quad (2.4)$$

If  $C_{\text{ref}}$  is close to 1.0, to make a different sensation,  $C = C_{\text{ref}} \cdot R_c$  is larger than 1.0; this situation only arises when the master device bounces unstably faster than the temporal resolution of haptic sensation.

## 2.4 Validation of the haptic sensation index

This section validates the proposed haptic sensation that  $C$  value can represent the operator's haptic sensation correctly. Specifically, regardless of how the system parameters are set, haptic sensations they provide to the operator can be estimated as long as their  $C$  values is determined.

Therefore, despite the difference in parameters setting of trials, as well as the relationship of their corresponding values is known, the operator's performance in haptic sensation should be in accordance with prediction based on the index values. In this section, another psychophysics experiment was conducted. The experimenter tested pairs of parameter settings with designated relationships of  $C$  value with the pair elements, presented the sensations under the parameter setting pairs to the subjects and checked if their sensation performances were in accordance with the prediction.

As introduced in Section 2.3.1, the environment stiffness  $K_{en}$  and the master device damping  $B_m$  are adjusted to generate the different haptic sensations. To best adjust parameters settings to the desired  $C$  values, how the index  $C$  values changed as  $K_{en}$  increases was studied first, for two  $B_m$  levels. Fig. 2.8 plots all the reference, UT, and LT index  $C$  values against the corresponding parameter settings that were discussed in Section 2.3.4. Then, the functions of  $C = f(K_{en})$  for the two  $B_m$  levels were fit as the following equations:

$$C_{B_m=0.001} = 1 - e^{-1.355 \cdot K_{en}} \quad (2.5)$$

$$C_{B_m=0.004} = 1 - e^{-1.211 \cdot K_{en}} \quad (2.6)$$

The coefficients of determination for the two fitted curves are 0.987 and 0.990 respectively.

The experimental apparatus was the same as that used in the previous experiment. We enrolled 15 subjects, all males from 22 to 35 years old. The subjects performed the same motion described in Section 2.3.2.

The experiment was based on the method of constant stimuli. Sensations from 2 system parameter settings were presented in a pair with a time interval less than 0.5 s. After presenting one pair, the subject was asked to identify the trial in which they could more easily to sense the contact between the slave and the environment. Subjects could answer "Former", "Latter", or "Same".

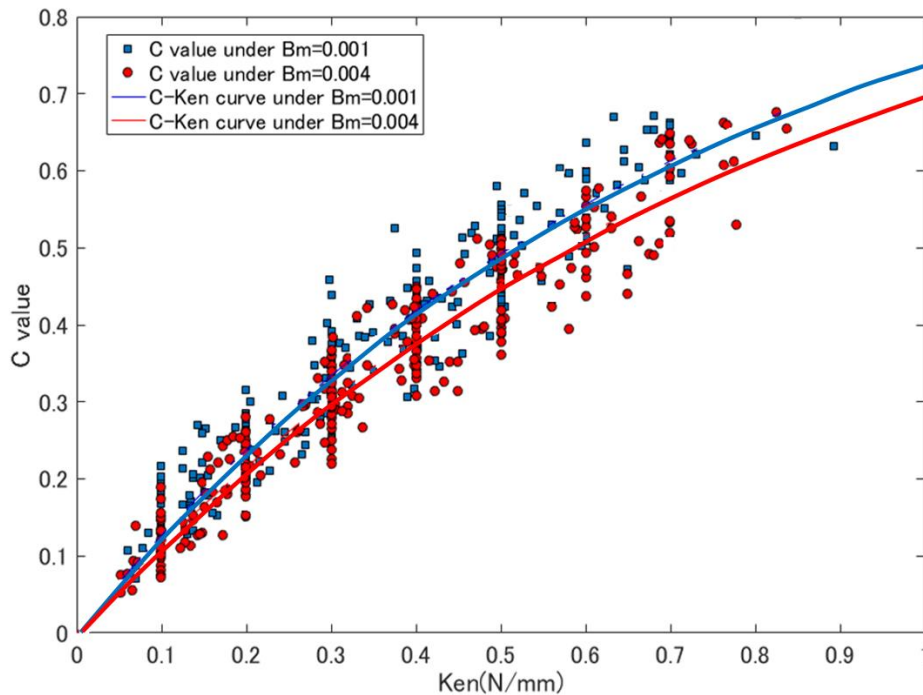


Fig. 2.8. Parameter settings and their corresponding  $C$  values as listed in Table 2.2. The curves are fitted functions for  $K_{en}$  and the index value.

The designated relationships between index values for pairs of parameter settings were divided into three types: 1. parameter settings with the same  $C$  value, 2. parameter settings with just-noticeably-different  $C$  values, and 3. parameter settings with  $C$  values differing by 200 %. We tested five pairs of parameter settings for the first two types and four parameter pairs for the third type, in which the pair elements are labeled A1–A5 and B1–B5.

For each subject, the experimenter repeated the presentation of sensations for the parameter setting pair elements 20 times. Therefore, for each pair, 300 trials were tested in total. To eliminate constancy errors, the sequence of presenting pair elements was random. To prevent the subject from deducing answers from the ongoing statistics, parameter setting pairs with the three kind of relationships were presented in a random sequence. Moreover, after every time a parameter pair was shown, if the subject answered that it was easier to detect the contact in element A, the trial was scored with “-1”; if the subject answered “Same”, the trial was scored with “+1” and if the subject pointed to element B, the trial was scored with “0”. For each parameter pair with one subject, total

points of the 20 trials for one subject were calculated. Therefore, a point array with 15 elements from subject No. 1 to No. 15 can be obtained. This array would be used in statistical tests for the experiment results.

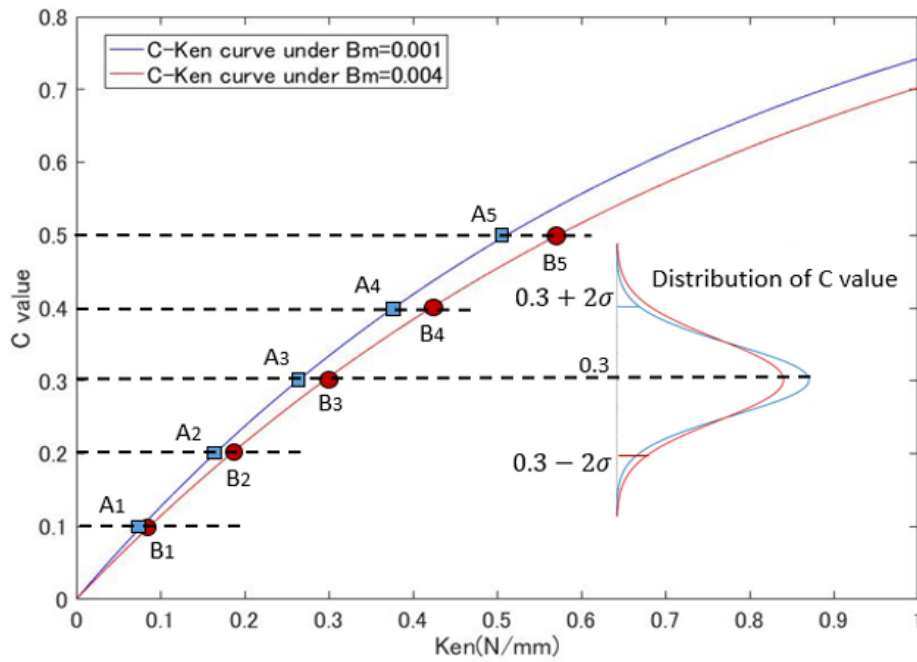
For each pair of parameter settings, the proportion of indistinguishable answer out of the 300 trials was counted, which includes the proportion of “Same” answer and the proportion of opposite responses that canceled out with each other.

If the  $C$  values under the two pair elements were the same, the operator would be difficult to tell the difference on the haptic sensation, which will lead to a high proportion of indistinguishable answers. If the change rate of index values between pair elements reaches  $R_c$ , according to psychophysics theory, the proportion of indistinguishable answers should be around 50 %; If the index values between pair elements differs by 200 %, proportion of the indistinguishable answers should be very low.

#### 2.4.1 Experiment for parameter settings with the same $C$ value

Fig. 2.9 shows the parameter pairs of which the  $C$  values of the pair elements are designated as the same; the five appointed  $C$  levels are shown in column 3 and 5 of the table in Fig. 2.9. Substituting the appointed  $C$  values into functions (2.5) and (2.6) for different  $B_m$  levels, the  $K_{en}$  parameter in each pair element is back-calculated respectively. Here, the  $K_{en}$  parameters in A1–B1 ~ A5–B5 are listed in column 2 and 4 of the table in Fig. 2.9.

The combinations of system parameters with the same index  $C$  value are expected to present the same haptic sensation to the subjects. In this experiment, for each pair of parameter settings, the proportion of indistinguishable answers after 300 trials is shown in Table 2.3, which shows that the proportion of indistinguishable answers is high and nearly more than 80%, which is a high proportion that the subject cannot tell the difference between pair elements. In addition, the t-test result shows that there are no significant differences between the point arrays of the five parameter-pairs, which means the five proportions of indistinguishable answers are at the same high level.



No.	<i>Ken</i> (N/mm) in parameter set A	<i>C</i> value of A	<i>Ken</i> (N/mm) in parameter set B	<i>C</i> value of B
1	0.078	0.10	0.087	0.10
2	0.165	0.20	0.184	0.20
3	0.263	0.30	0.295	0.30
4	0.377	0.40	0.422	0.40
5	0.512	0.50	0.572	0.50

Fig. 2.9. Five parameter setting pairs used in the experiment, for which the haptic sensation is expected to be same.

Table 2.3

Proportion of indistinguishable answers under the same *C* value, sample size of every pair is 300.

Parameter pair No.	Proportion of indistinguishable answers	Predicted proportion of indistinguishable answers
A <sub>1</sub> , B <sub>1</sub>	78 %	71.1 %
A <sub>2</sub> , B <sub>2</sub>	82 %	81.3 %
A <sub>3</sub> , B <sub>3</sub>	80 %	86.9 %
A <sub>4</sub> , B <sub>4</sub>	83 %	87.2 %
A <sub>5</sub> , B <sub>5</sub>	84 %	87.5 %

However, “high proportion” or “more than 80 %” are only independent results without any reference, they should be compared to a predicted proportion to check if the proportion is high enough to reflect the “same haptic sensation”. To check whether haptic sensation performances were in accordance with the prediction. The third column of Table 2.3 is the predicted proportion of indistinguishable answers, which is not 100 % even the  $C$  value between the pair elements are the same. Its algorithm is introduced as follows:

As mentioned in Section 2.3.2, the index values under a certain parameter setting are normally distributed, in Fig. 2.9, points on the curves are the mean values of the normal distributions, and true index value in each trial may be different from the point values on the curves. For example, if the true index value when presenting A3 in one trial was  $0.3 - 2\sigma$  of the red distribution, whereas the true index value when presenting B3 in another trial was  $0.3 + 2\sigma$  of the blue distribution (see the example of normal distributions in Fig. 2.9), in this pairwise comparison, the difference between the true haptic sensation provided by A3 and B3 may be more than the just-noticeable threshold, which makes the subject to notice the difference, Hence, the predicted proportion that the subject cannot notice the difference between two parameter settings is not 100 % even their  $C$  values are the same.

In the pairwise comparison, pair element A is presented firstly, the true index value  $C_A$  under pair element A from all subjects are within the range  $[\bar{C}_A - 2\sigma, \bar{C}_A + 2\sigma]$ , Then, pair element B is presented, the true index value  $C_B$  from all subjects are within the range  $[\bar{C}_B - 2\sigma, \bar{C}_B + 2\sigma]$ . Here,  $\bar{C}_A$  and  $\bar{C}_B$  are the mean index value under pair element A and B respectively. If  $C_B$  is within the range  $[C_A / R_c, C_A \cdot R_c]$ , the true haptic sensations difference between the pair elements A and B is within the JND, the subject should not notice the difference. Therefore, proportion of the indistinguishable answers is “The chance for the true index value of element B ( $C_B$ ) being within the difference unnoticeable range of element A's true index value:  $[C_A / R_c, C_A \cdot R_c]$ ”, which can be calculated by the following multiple integration.

$$P = \int_{\bar{C}_A - 2\sigma}^{\bar{C}_A + 2\sigma} \left( f_A(C_A) \cdot \int_{C_A/R_c}^{C_A \cdot R_c} f_B(C_B) dC_B \right) \cdot dC_A \quad (2.7)$$

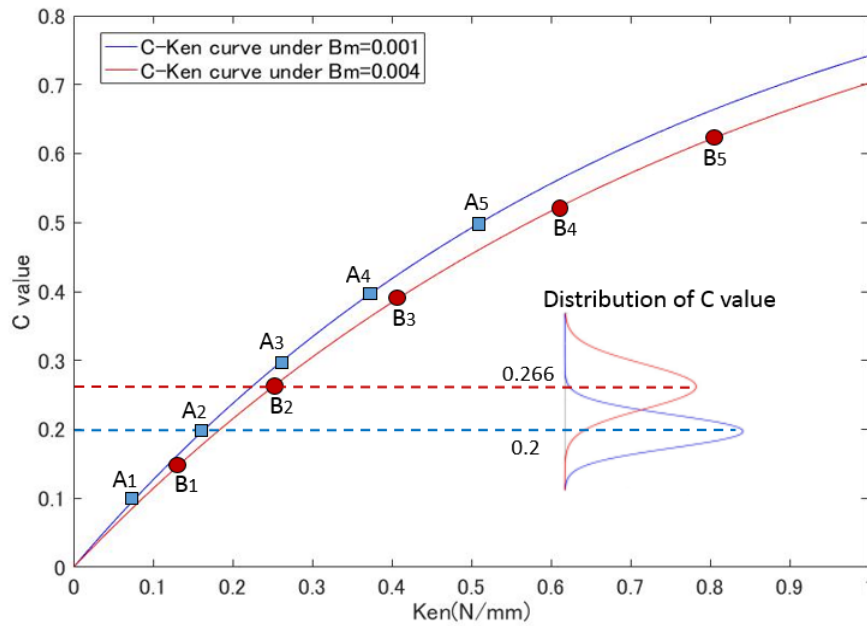
In function (2.7),  $P$  is the predicted proportion of the indistinguishable answers,  $C$  represents the true index value of the current pair element,  $f_A(C)$  and  $f_B(C)$  are the probability-density functions of the normal distributions of pair elements A and B.  $R_c$  can be calculated by substituting  $\bar{C}_A$  into function (2.4). For example, when calculating the expected proportion between A2 and B2, substitute the  $\bar{C}_A$  value of A2 (0.2) into function (2.4),  $R_c = 1.33$ .

Comparing the experimental proportion of indistinguishable answer to the prediction proportion, it can be seen that the haptic sensation performances were also in accordance with the prediction based on index relationship.

#### 2.4.2 Experiment for parameter settings with the same $C$ value differing by $R_c$

Fig. 2.10 shows the parameter setting pairs of which the  $C$  value difference between pair elements differed by  $R_c$ , which means difference between the haptic sensations generated by the pair elements is just noticeable. The five appointed  $C$  levels are shown in columns 3 and 5 of the table in Fig. 2.10. The  $K_{en}$  parameter in A1–B1 to A5–B5 are listed in columns 2 and 4 of the same table.

According to psychophysics theory, if two sensations are differed by the just noticeable difference, the proportion that the subjects cannot notice the difference (indistinguishable answers) should be 50 %. Considering the variance of true index value, the predicted proportions of indistinguishable answers calculated by function (2.7) are about 47 %. The experimental result is shown in Table 2.4. From Table 2.4, when the difference ratio between the  $C$  values of the two parameter settings reaches  $R_c$ , the proportion of indistinguishable answers is near the prediction.



No.	<i>Ken</i> (N/mm) in parameter set A	<i>C</i> value of A	<i>Ken</i> (N/mm) in parameter set B	<i>C</i> value of B
1	0.078	0.1	0.132	0.148
2	0.165	0.2	0.266	0.276
3	0.263	0.3	0.416	0.396
4	0.377	0.4	0.592	0.512
5	0.512	0.5	0.801	0.625

Fig. 2.10. Five parameter setting pairs used in the experiment, for which the haptic sensation is expected to be just noticeable.

Table 2.4 Proportion of Indistinguishable Answers under the parameter settings with the just noticeable different *C* values, Sample Size of every pair is 300

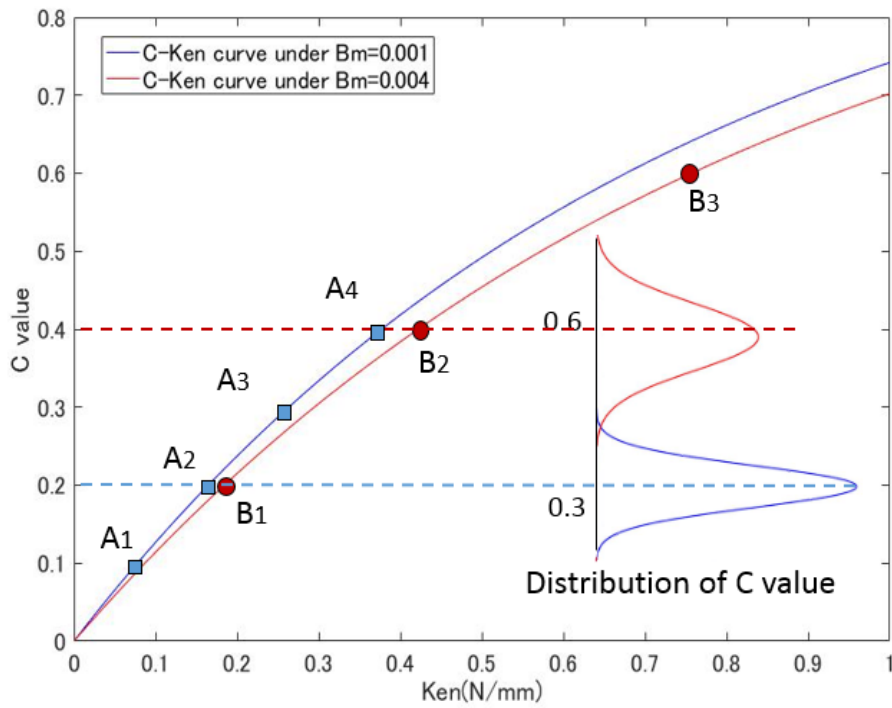
Parameter pair No.	proportion of indistinguishable answers	Predicted proportion of indistinguishable answers
A <sub>1</sub> , B <sub>1</sub>	44 %	46.3 %
A <sub>2</sub> , B <sub>2</sub>	40 %	47.6 %
A <sub>3</sub> , B <sub>3</sub>	41 %	47.6 %
A <sub>4</sub> , B <sub>4</sub>	46 %	47.6 %
A <sub>5</sub> , B <sub>5</sub>	45 %	47.5 %

In addition, the t-test result shows that there are no significant differences between the point arrays of the five parameter-pairs, which means the five proportions of indistinguishable answers are at the same level. Therefore, the difference in perceptual capability for detecting the virtual wall between pair elements is just noticeable, haptic sensation performances were in accordance with the prediction based on index relationship.

#### 2.4.3 Experiment for parameter settings with the $C$ value differing by 200%

Fig. 2.11 shows the parameter setting pairs of which the index values of pair elements differing by 200 %. The four appointed  $C$  levels are shown in columns 3 and 5 of the table in Fig. 2.11. The  $K_{en}$  parameter in A1–B1 to A5–B5 are listed in columns 2 and 4 of the same table.

The proportion of indistinguishable answers for each pair out of 300 trials, as well as the predicted proportion calculated by function (2.7), are shown in Table 2.5. From Table 2.5, when the change rate between pair element's index  $C$  values reaches 200 %, proportion of indistinguishable answers becomes less than 5 % of 300 trails. Haptic sensation performances were in accordance with the prediction based on index relationship. Moreover, the t-test result shows that there are no significant differences between the point arrays of the four parameter-pairs, which means the four proportions of indistinguishable answers are at the same low level.



No.	KEN(N/MM) IN PARAMETER SET A	C VALUE OF A	KEN(N/MM) IN PARAMETER SET B	C VALUE OF B
1	0.078	0.10	0.184	0.20
2	0.165	0.20	0.421	0.40
3	0.263	0.30	0.756	0.60
4	0.377	0.40	1.32	0.80

Fig. 2.11. Four parameter setting pairs used in the experiment, for which the haptic sensation is expected to be distinctly different.

Table 2.5

Proportion of Indistinguishable Answers with Distinctly Different  $C$  Values with Sample Size of Every Pair is 300

Parameter pair No.	proportion of indistinguishable answers	Predicted proportion of indistinguishable answers
$A_1, B_1$	12 %	11 %
$A_2, B_2$	3 %	2 %
$A_3, B_3$	6 %	0 %
$A_4, B_4$	3 %	0 %

#### 2.4.4 Experiment for parameter settings with the same $C$ value and far different $K_{en}$ and $B_m$ values

In section 2.4.1, change on operator's haptic sensation are generated by altering the  $K_{en}$  parameter, but  $K_{en}$  values in A1–A5 are not differed much to that in B1–B5. Someone will doubt that the high proportion of indistinguishable answers are just because of the similar  $K_{en}$  level. In this section, another type of parameter setting pairs was designated as follows: the difference between the  $K_{en}$  parameters of pair element A and B reaches the upper threshold, and the difference between the  $B_m$  parameter values are also enlarged to make the index value  $C$  of pair elements equal. The parameter setting pairs and their index  $C$  values are shown in the table included with Fig. 2.12. The subjects are expected to be unable to distinguish the difference even the both the  $K_{en}$  and  $B_m$  are differed distinctly.

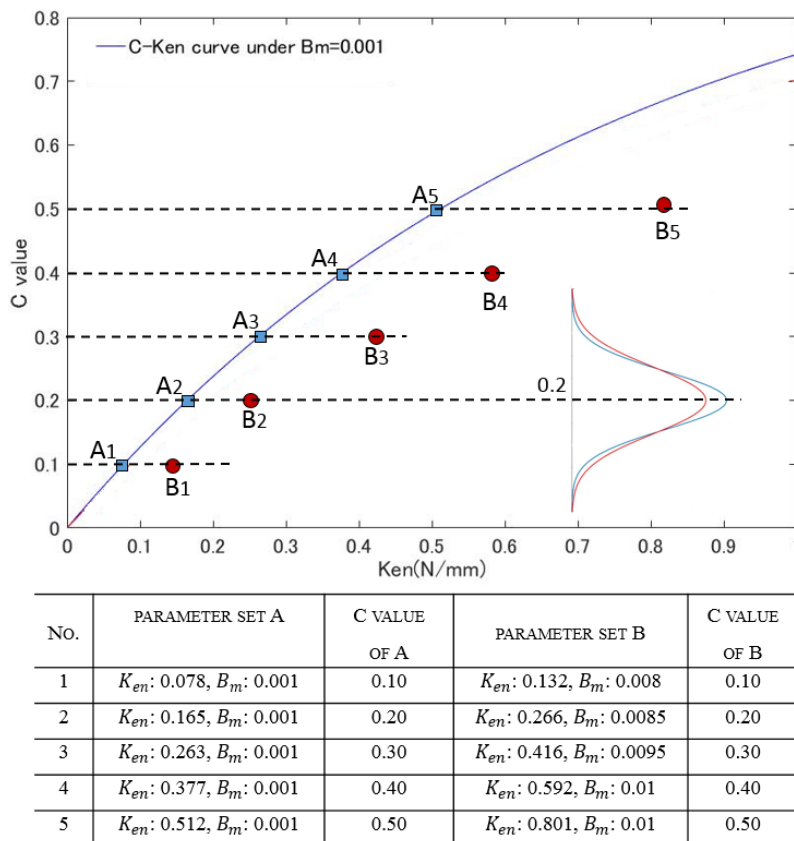


Fig. 2.12. Five parameter setting pairs used in the experiment, for which the haptic sensation is expected to be the same while the difference on the  $K_{en}$  parameters between the pair elements reaches the upper threshold.

Table 2.6

Proportion of indistinguishable answers with distinctly different  $K_{en}$  and the same  $C$  value; sample size of every pair is 300

Parameter pair No.	proportion of indistinguishable answers	Predicted proportion of indistinguishable answers
$A_1, B_1$	76.3 %	71.1 %
$A_2, B_2$	91.3 %	81.3 %
$A_3, B_3$	82.1 %	86.9 %
$A_4, B_4$	80.0 %	87.2 %
$A_5, B_5$	82.4 %	87.5 %

The proportion of indistinguishable answers for each pair out of 300 trials as well as the prediction are listed in Table 2.6. Results in Table 2.6 shows that haptic sensation performances were also in accordance with the prediction based on index relationship. Even the sensations are generated from far different parameter settings, the subjects cannot tell the difference between pair elements as long as the  $C$  values with the parameter settings are the same.

Moreover, the t-test result shows that no significant differences occur between the point arrays of this parameter setting pair type and that of the parameter pair setting pairs in Section 2.4.1, meaning that proportions of indistinguishable answers in this section are at the same high level with that of Section 2.4.1.

In addition, this experiment also confirmed the masking effect of master device damping  $B_m$  to the haptic sensation, when  $K_{en}$  parameters between pair elements A and B differs to the upper threshold to generate a different sensation, increase the  $B_m$  parameter can make the subject be unable to notice the difference. In other word, the master device damping obscures the sensibility of an operator to detect the contact.

According to the experimental results of Section 2.4, the proposed index value can represent operator's haptic sensation correctly. Validity of the proposed index is testified.

## 2.5 Discussion of this chapter

### 2.5.1 Effect of each kind of parameter on the haptic sensation

It can be observed from Fig. 2.8 that when  $K_{en}$  is zero, the index  $C$  values under both  $B_m$  levels are zero, meaning that there is no virtual wall to contact. As  $K_{en}$  increases, the sensation for the contact will become stronger until the  $C$  values finally approaches to 1, the results of the supplemental experiment show that the index value will reach 0.97 when  $K_{en}$  is larger than 3.0 N/mm (Under the  $B_m = 0.001$  Ns/mm).

Verbal reports from our subjects indicate that when the index  $C$  value is less than 0.07, the operator's sensation is very low and the existence of the virtual wall is difficult to detect. When the index  $C$  value is near 1.0, the sensation is very strong, and the virtual wall is very easy to detect. As Fig. 2.8 shows, when the damping parameter  $B_m$  is amplified from 0.001 to 0.004 Ns/mm, the index value decreases and the masking effect of damping is also represented by the index value. When the  $K_{en}$  parameter is low around 0.1 N/mm, and if  $B_m$  value is quadrupled, the  $C$  value will decrease by 25.2 %. When the  $K_{en}$  parameter is high at 0.5 N/mm, if  $B_m$  value is quadrupled, the  $C$  value decreases by only 8.9 %. This tendency shows that the masking effect of viscosity weakens as the stiffness increases. No matter how high the master viscosity is set, if the environment is sufficiently hard, the operator will perceive it easily.

### 2.5.2 Comparison of the other alternative motion factors

In this chapter, the master velocity is used to quantify the stimuli intensity and then the operator's haptic sensation. The force and velocity factor applied by the master device are interrelated, and it is natural to consider the force applied on the operator's hand before and after contact as the factor that determines the contact sensation stimuli, but an additional experimental result shows that force factor has less of an effect on the operator's haptic sensation than velocity factor.

The following three hypothesized dynamic factors is testified to represent the operator's haptic sensation: first, the difference in feedback force before and after contact; second, the ratio of feedback force before and after contact; third, the ratio of velocity

before and after contact.

In this additional experiment, the parameter setting for the reference trials was ( $K_{en} = 0.3$  N/mm,  $B_m = 0.001$  Ns/mm). The just noticeable lower threshold (LT) to the sensation under this reference parameter setting is obtained by adjusting two types of parameter. For one type, the LT haptic sensation is obtained by reducing the  $K_{en}$  parameter; for the other type, the LT haptic sensation is obtained by reducing the  $B_m$  parameter.

10 subjects were enrolled; the experimental process was the same as the JND measurement in Section 2.3.4. The experimental results are listed in Table 2.7, column 1 shows reference parameter setting and the parameter settings that an LT haptic sensation appeared. For the cases of reducing the  $K_{en}$  parameter, the LT haptic sensation appeared when  $K_{en}$  is reduced to 0.22 N/mm; for the cases of increasing the  $B_m$  parameter, the LT haptic sensation appeared when  $B_m$  is increased to 0.006 Ns/mm.

The index defined is expected to represent the operator's haptic sensation just by its value regardless how the system parameters are set as introduced in Section 2.4, as the dynamic factor that defines the index, no matter how the system parameters are adjusted to one reference parameter setting, if the haptic sensation after adjustment is just noticeable different from that for the reference parameter setting, the change magnitude of the dynamic factor should be the same.

When using the difference in feedback force before and after contact ( $F_a - F_b$ ) as the dynamic factor to define a haptic sensations, as shown in columns 3 and 4 of Table 2.8, the force difference in the reference trial is 0.974 N; if the experimenter reduced  $K_{en}$  to generate a just noticeable lower sensation (objective sensation appeared at  $K_{en} = 0.22$  N/mm),  $F_a - F_b$  at the objective sensation is 0.672 N, change extent to the force difference factor of the reference is 45 %; if the experimenter increased the  $B_m$  to generate a just noticeable lower sensation (objective sensation appeared at  $B_m = 0.006$  Ns/mm),  $F_a - F_b$  at the objective sensation is 0.788 N, change extent to the force difference factor of the reference is 23 %. When adjusting different types of system

parameters to generate a same change in haptic sensation, the dynamic factor ( $F_a - F_b$ ) is not the same, it cannot be used to define the index.

Table 2.7

In tasks of obtaining a LT sensation to a reference by adjusting two types of system parameters, the change magnitude of the hypothesized dynamic factors compared to that in the reference

Parameter Combination	Sample size	Factor 1 $F_a - F_b$	Change extent	Factor 2 $F_a / F_b$	Change extent	Factor 3 $V_a / V_b$	Change extent
Reference $K_{en} : 0.30\text{N/mm}$ $B_m : 0.001\text{Ns/mm}$	20	0.974	—	7.306	—	1.563	—
LT Type 1: $K_{en} : 0.22\text{N/mm}$ $B_m : 0.001\text{Ns/mm}$	10	0.672	45%	5.754	27%	1.201	30%
LT Type 2: $K_{en} : 0.30\text{N/mm}$ $B_m : 0.006\text{Ns/mm}$	10	0.788	23%	2.287	320%	1.185	32%

When use the ratio of feedback force before and after contact ( $F_a / F_b$ ) as the dynamic factor to define a haptic sensations, as shown in columns 5 and 6 of Table 2.8,  $F_a / F_b$  in the reference trial is 7.306; if the experimenter reduced  $K_{en}$  to generate a just noticeable lower sensation,  $F_a / F_b$  at the objective sensation is 5.754, change extent to the force difference factor of the reference is 27%; if the experimenter increased the  $B_m$  to generate a just noticeable lower sensation,  $F_a / F_b$  at the objective sensation is 2.287, change extent to the force difference factor of the reference is 320 %. When adjusting different types of system parameters to generate a same change in haptic sensation, the dynamic factor  $F_a / F_b$  is not totally different, it also cannot be used to define the index.

When using the ratio of velocity before and after contact ( $V_a / V_b$ ) as the dynamic factor to define a haptic sensations, as shown in columns 7 and 8 of Table 2.8,  $V_a / V_b$  in the reference trial is 1.563; if the experimenter reduced  $K_{en}$  to generate a just noticeable lower sensation,  $V_a / V_b$  at the objective sensation is 1.201, change extent to the force difference factor of the reference is 30 %; if the experimenter increased the  $B_m$  to

generate a just noticeable lower sensation,  $V_a / V_b$  at the objective sensation is 1.185, change extent to the force difference factor of the reference is 32 %. When adjusting different types of system parameters to generate a same change in haptic sensation, the dynamic factor  $V_a / V_b$  is almost the same, it can be used to define the index.

The experimental results also confirmed that that operators are likely to rely on velocity factor rather than the force factor to sense the contact between slave device and the environment. This choice of velocity factor is also in accord with the literature discussed in Section 2.1. Furthermore, for convenience of using, the index value should be normalized to a range of [0, 1], then, function (2.1) is proposed as its definition.

### 2.5.3 The relationship between $C$ value and the operator's sensation

As the author emphasized before, the  $C$  value is used to represent the easiness by which the operator can detect the occurrence of the contact.

For example, when letting a person with closed eyes explore an iron block just in front of him, when his hand is in contact with the iron block, it is very easy to detect the contact; the  $C$  value in such case will be near 1.0.

When letting a person with closed eyes explore an iron block covered by a blanket, when his hand arrives the right place where the iron block is, it will cost some time for him to make sure that the iron block is here exactly; the  $C$  value in such case will be less than 0.5.

When letting a person with closed eyes explore an iron block covered by a thick quilt, he may cannot detect the existence of the object if his hand arrives the right place where the iron block is; the  $C$  value in such case will be near 0.

However, the index  $C$  values cannot represent specific perceptions experienced by the operator.

For example, when letting a person with closed eyes explore a soft tissue just in front of him, there will be a little difficulty for him to detect the soft tissue; assuming the  $C$  value in such case to be 0.4.

Additionally, assuming the  $C$  value in cases that a person with closed eyes explore an iron block covered by a blanket to be also 0.4. The identical  $C$  values means that the “difficulty” for the person to detect the object in these two cases are same.

Nevertheless, if the person has known the exact position of the object in these two cases, because of the absolute difference between the stiffness of the objects, the perception when the person grasps the objects will be totally different.

## 2.6 Summarization of this chapter

In this chapter, the author proposes a new index to estimate the haptic sensation for operators to sense the contact between slave devices and the environment when operating a master-slave system.

First, the magnitude of the contrast in the velocity of master device before and after the slave device contact with the environment is hypothesized as the dynamic factor that determines the haptic sensation stimuli, which is then used to define the index called: Dynamic Contrast ( $C$ ).

Second, the statistical characteristic of the proposed index is checked by experiment. The result shows that the index value remains constant for different operators and is independent of the approach velocity applied by the operator. Then, by measuring the JND in the reference haptic sensations and comparing the calculated index value corresponding to the JNDs and references, the necessary change ratio to a reference index  $C$  value to produce a just noticeable different haptic sensation is calculated.

Third, validity of the index is confirmed by psychophysics experiments. Results show that regardless of how the parameters settings are combined to produce the haptic sensations to the operator. If the parameter settings are with the same  $C$  value, the haptic sensations they provided to the operator is the same; if the  $C$  values with parameter settings are just differed by the necessary extent to produce a just noticeably different haptic sensation, the haptic sensations they provided to the operator are just noticeably different; if the parameter settings are with far different  $C$  values, the haptic sensations they provided to the operator is totally different.

This correspondence between index values and subject's haptic performance implies that the value of  $C$  can represent the operator's haptic sensation correctly.

## Chapter 3

# The relationship between the index value and the system parameters

The proposed index is validated being able to represent the operator's haptic sensation, so if its relationship to the system parameters can be clarified, the objective of this study can be realized. This chapter summarized the process of clarifying the relationship between the system parameters and the proposed index: dynamic contrast ( $C$ ), and expressed the relationship as a mathematical function with the following objective formation.

$$C = f(K_v, K_p, B_m, F_{sc}, P_{sc} \dots) \quad (3.1)$$

The target function (3.1) is expected to be used as a guideline for the system parameter design by directly calculating the quantified haptic index ( $C$  value) from the parameters.

As introduced in Section 1.3.2, the related works [60] – [65] did not build a guideline for the system parameter design with considering the operator's sensibility for a contact; Motoji et al. built a method for optimizing the parameter for presenting the touch feelings [84], but this method is only for the parameters of a haptic device, which is usually used as a master device.

### 3.1 Introduction of bilateral control architectures

An exemplary concept of a bilateral controlled master-slave system is shown in Fig. 3.1. The master-slave communicator transmits the control and dynamic information between controllers of the master and slave devices in two directions, which makes the system called “bi-lateral”.

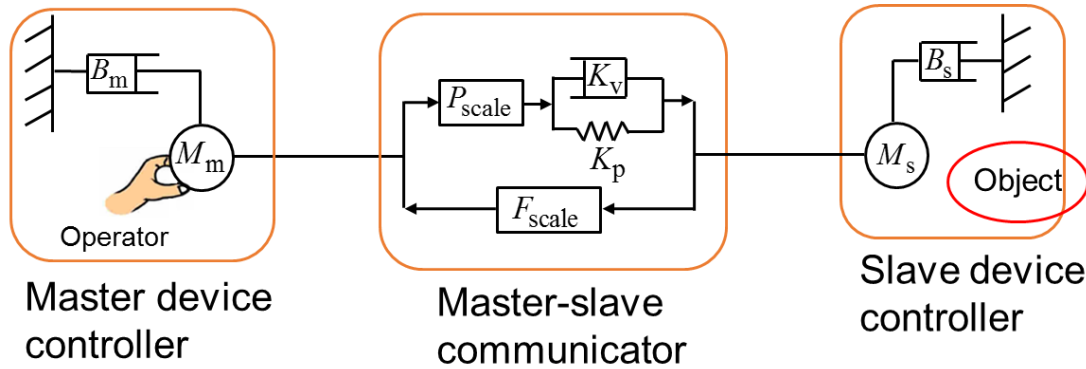


Fig 3.1. Concept of a bilateral control architecture.

According to the different feedback factors, the bilateral control architectures can be categorized into the position-force architecture and position-position architecture [50].

In the position-force architecture, the moving distance or velocity of the master device is the position instruction transmitted to the slave device, the slave device reproduces the instruction (amplifying or narrowing scaling gains is occasionally required). When the slave device contacts the environment, the contact force measured at the slave side is fed back to the master controller. (Amplifying or narrowing scaling gains of feedback force is occasionally required). The operator perceives the interaction between the slave device and the environment by the change of motion in the master device, which is generated by the feedback force information.

If the slave device is constrained by the size or cost, a force sensor at the slave side is not expected, and position-position architecture can be implemented in such cases. When the slave device contacts the environment, the interaction force changes the motion of the slave device and the change in the slave device's motion is fed back to the master controller. This allows the operator to perceive the interaction between the slave device and the environment by reproducing the slave motion at the master side (information regarding the feedback position is occasionally amplified or narrowed by a scaling gain).

This study mainly focuses on the position-force architecture.

## 3.2 Relationship between index value and system parameters in the ideal Position-Force model

### 3.2.1 Control model introduction

Regardless of the control architectures, an ideal device motion response is often expected, [46] described an ideal motion as that the slave device moves in accordance with the master device without any time delay. In this case, the control model of Fig. 3.1 appears as that shown in Fig. 3.2, and the master and slave devices are connected by a virtual rigid body.

During the operation, the operator holds the master device at all times. Hence, the affection of the operator's limb dynamics to the motion of the master device should also be considered. In Fig. 3.2, the operator's limb is modelled as a mass-damper-spring model. According to [86] – [88], the dynamic parameters of the operator's limb in this study are as follows: limb stiffness  $K_h = 0.08$  N/mm, limb damping  $B_h = 0.002$  Ns/mm, and limb inertia  $M_h = 2 \times 10^{-4}$  kg  $\cdot$  10<sup>3</sup>. As described in Section 2.2, this study focused on the master device motion within 50 ms after contact, and considered that a human operator cannot actively change their muscle motion in such a short amount of time. Therefore, we considered the operator's limb model as time invariant. The control model of Fig. 3.2 was adopted in works where the master and slave devices are rigidly connected [85], [88] or the distance between the devices are short [90].

This section aimed to express the relationship between the haptic sensation index  $C$  values and the system parameters as a mathematical function for this control model.

In function (2.1), the haptic sensation index  $C$  value is calculated from the master velocity information, which is affected by the system parameters. Hence, the target function can be obtained if the mathematical relationship between the master velocity and the system parameters can be derived.

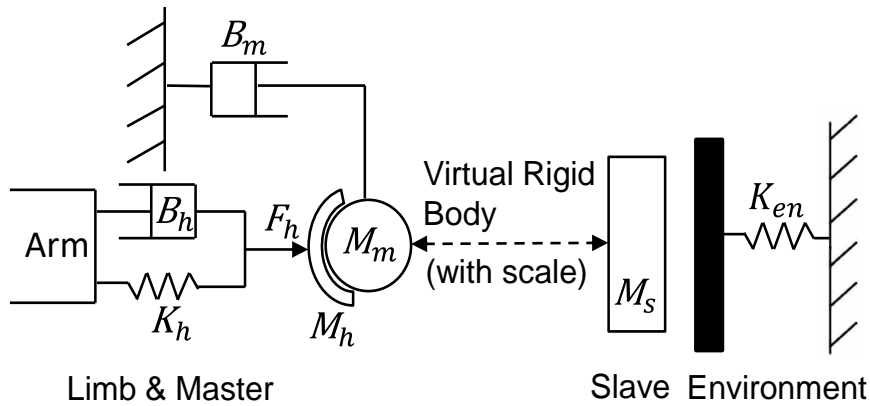


Fig. 3.2. Concept of position-force architecture for ideal system response, the master and slave devices are always moving in accordance with each other.

According to the control model shown in Fig. 3.2, within a very short amount of time after the slave device contacts the environment, the motion equation of the master device can be expressed as follows:

$$F_h + K_h (V_b \cdot t - r_m) + B_h (V_b - \dot{r}_m) = (M_m + M_h) \cdot \ddot{r}_m + B_m \cdot \dot{r}_m + F_{sc} \cdot K_{en} (P_{sc} r_m - r_{en}) \quad (3.2)$$

In (3.2),  $F_h$  is the force input from the operator's limb;  $B_m$  is the damping ratio of the master device;  $r_m$  is the position of the master device, and  $\dot{r}_m$  is its velocity;  $V_b$  is the velocity of the master device before contact;  $M_m$  and  $M_h$  are the inertia of the master device and the operator's hand, respectively;  $F_{sc}$  is the force feedback scaling gain;  $K_{en}$  is the stiffness of the environment;  $P_{sc}$  is the position scaling gain between the master and slave.

Because the motion of the master and slave in the ideal model are always in accordance, the position of the slave device can be substituted by  $P_{sc} \cdot r_m$ . Additionally,  $r_{en}$  denotes the initial position of the environment. Thus, the interaction force occurring between the slave device and the environment is  $K_{en} (P_{sc} \cdot r_m - r_{en})$ , and the feedback force is  $F_{sc} \cdot K_{en} (P_{sc} \cdot r_m - r_{en})$ . In this control model, both the position and force scaling gain operate as the amplification or reduction gain of  $K_{en}$ . Hence, their combination in the form of  $F_{sc} \cdot P_{sc} \cdot K_{en}$  is termed as the feedback stiffness for convenience.

Moreover,  $t=0$  is the time point when the contact between the slave device and the environment occurs. When  $t=0$ , the initial conditions are as follows: the master position  $r_m(0^+) = 0$ , and its velocity (the approaching velocity)  $\dot{r}_m(0^+) = V_b$ . The initial position of the environment  $r_{en}$  is set to zero, and the direction of invading into the environment, in other words, compress the spring representing the environment property, is defined as positive.

Before the slave device contact the environment, the equation of motion for the master device is expressed as follows:

$$F_h = B_m \cdot \dot{r}_m + (M_m + M_h) \cdot \ddot{r}_m \quad (3.3)$$

At a certain time after the operator begins to move the master device forward (before contact occurs),  $\ddot{r}_m$  will become zero, and  $F_h = B_m \cdot \dot{r}_m$ , the velocity of the master and operator's limb before contact will finally become constant as  $\frac{F_h}{B_m}$ , which is the approaching velocity  $V_b$ .

Within a short amount of time after contact,  $F_h$  is considered to be constant and the same as that before contact because the muscle reaction of the operator's limb is not involved. Moreover, because the operator's finger pad is soft, the operator's limb velocity will not change immediately and is considered identical to  $V_b$ . Hence, the displacement of the operator's limb is  $V_b \cdot t$ .

While the fed back force information immediately changes the velocity of the master device after contact, a discrepancy occurs with regard to the position and velocity between the master device and the operator's limb. Owing to the limb's dynamic property represented by the stiffness parameter  $K_h$  and damper parameter  $B_h$ , two additional forces  $K_h(V_b \cdot t - r_m)$  and  $B_h(V_b - \dot{r}_m)$  are passively generated from this discrepancy. By coupling these two forces with  $F_h$ , the total input force from operator's limb after contact is  $F_h + K_h \left( \frac{F_h}{B_m} \cdot t - r_m \right) + B_h \left( \frac{F_h}{B_m} - \dot{r}_m \right)$ , which is the left-hand side of (3.2).

### 3.2.2 Relationship function derivation

The  $\dot{r}_m$  term in (3.2) is equivalent to the  $V_a$  term of function (2.1), which can be solved from the differential equations (3.2) by using the Laplace transform and inverse Laplace transform. The result is shown in function (3.4), the details of derivation is presented in Appendix.

$$\dot{r}_m = V_a = \frac{F_h}{B_m} \cdot \frac{e^{-\frac{B_{hm}}{2M_{hm}}t} \left[ K_h \cdot e^{\frac{B_{hm}}{2M_{hm}}t} \cdot A + F_{sc} P_{sc} K_{en} \left( B_{hm} \cdot \sinh\left(\frac{A}{2M_{hm}}t\right) + A \cdot \cosh\left(\frac{A}{2M_{hm}}t\right) \right) \right]}{(K_h + K_{en} \cdot F_{sc} P_{sc}) \cdot A} \quad (3.4)$$

In function (3.4),  $M_{hm} = M_m + M_h$ ,  $B_{hm} = B_m + B_h$ ,  $K_{hen} = K_h + F_{sc} P_{sc} K_{en}$ , and  $A = \sqrt{B_{hm}^2 - 4(F_{sc} P_{sc} K_{en} + K_h)M_{hm}}$ .

The master velocity before contact  $V_b \equiv \frac{F_h}{B_m}$  is constant. By knowing the functions of  $V_a$  and  $V_b$ , the function that calculates the index value just from system parameters can be obtained by substitute them into the index definition, function (2.1).

In function (2.1), the mean  $V_a$  in 50 ms are used,  $\bar{V}_a$  is expressed as follows:

$$\frac{1}{50} \int_{t=0}^{t=50\text{ms}} \frac{F_h}{B_m} \cdot \frac{e^{-\frac{B_{hm}}{2M_{hm}}t} \left[ K_h \cdot e^{\frac{B_{hm}}{2M_{hm}}t} \cdot A + F_{sc} P_{sc} K_{en} \left( B_{hm} \cdot \sinh\left(\frac{A}{2M_{hm}}t\right) + A \cdot \cosh\left(\frac{A}{2M_{hm}}t\right) \right) \right]}{(K_h + K_{en} \cdot F_{sc} P_{sc}) \cdot A} dt.$$

Subsequently, this formula is substituted into (2.1). The  $V_b$  term ( $\frac{F_h}{B_m}$ ) is canceled.

For the ideal bilateral control model, the objective function that calculates the index  $C$

( $C_{ideal}$ ) from the system parameters can be obtained as follows:

$$C = 1 - \frac{1}{50} \int_{t=0}^{t=50\text{ms}} \frac{e^{-\frac{B_{hm}}{2M_{hm}}t} \left[ K_h \cdot e^{\frac{B_{hm}}{2M_{hm}}t} \cdot A + F_{sc} P_{sc} K_{en} \left( B_{hm} \cdot \sinh\left(\frac{A}{2M_{hm}}t\right) + A \cdot \cosh\left(\frac{A}{2M_{hm}}t\right) \right) \right]}{(K_h + K_{en} \cdot F_{sc} P_{sc}) \cdot A} dt \quad (3.5)$$

### 3.2.3 Effect analysis of different parameters

In function (3.5), the inertia term of the slave parameter is not contained, which means that adjusting the inertia of the slave device will have no effect on the operator's haptic sensation under the ideal conditions of the ideal position-force architecture. Under this ideal condition without time delay, the transient response speed of the devices is very fast. When the slave device contacts the environment, the contact force is transmitted to the master device and changes its motion immediately. Moreover, the motion of the slave device is in accordance with the master side without exhibiting transient characteristics, hence, the dynamics of the slave device have no effect on the system motion.

The changeable parameters in function (3.5) are master damping,  $B_m$ ; feedback stiffness,  $F_{sc} \cdot P_{sc} \cdot K_{en}$ ; inertia parameter in the master device controller,  $M_m$ .

Fig. 3.3 shows the change trend of the index  $C$  value as the feedback stiffness  $F_{sc} \cdot P_{sc} \cdot K_{en}$  changed from 0 N/mm to 1.5 N/mm, and the master device damping  $B_m$  changed from 0.001 Ns/mm to 0.009 Ns/mm. When the feedback stiffness was low, for example = 0.2 N/mm, As can be seen, when the feedback stiffness was low, for example when  $F_{sc} \cdot P_{sc} \cdot K_{en} = 0.2$  N/mm, the value of index  $C$  decreased by 33.5% (0.219 to 0.164) as the  $B_m$  parameter increased from 0.001 to 0.009 Ns/mm. While the decreasing effect on the value of index  $C$  exerted by the master damping became less remarkable as the feedback stiffness increased, for example, when  $F_{sc} \cdot P_{sc} \cdot K_{en} = 1.5$  N/mm, and as the  $B_m$  parameter changed by the same degree, the value of index  $C$  only decreased by 19.7% (0.858 to 0.717). When increasing the master damping parameter  $B_m$  to restrain the hand vibration, if the feedback intensity is low, caution must be exercised because the operator's haptic sensation can be easily weakened. If the feedback intensity is high, the  $B_m$  parameter can be increased more generously.

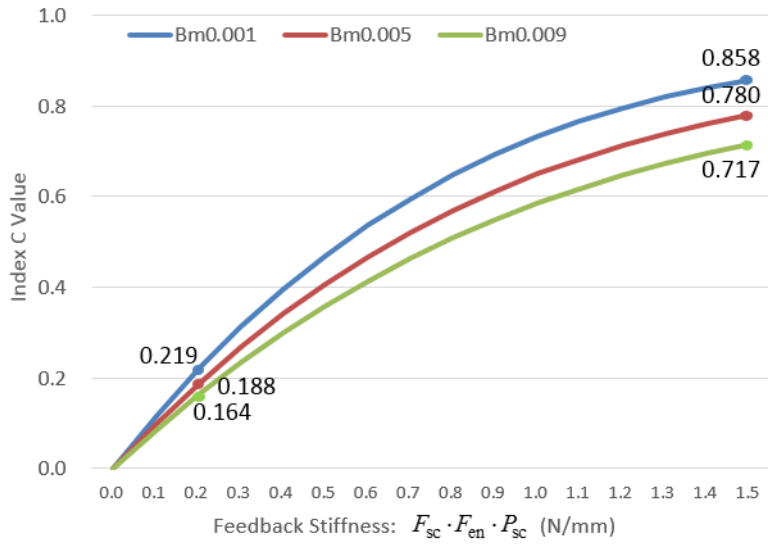


Fig. 3.3. Change situation of index  $C$  value when  $B_m$  parameter changes in the ideal force-position control architecture.

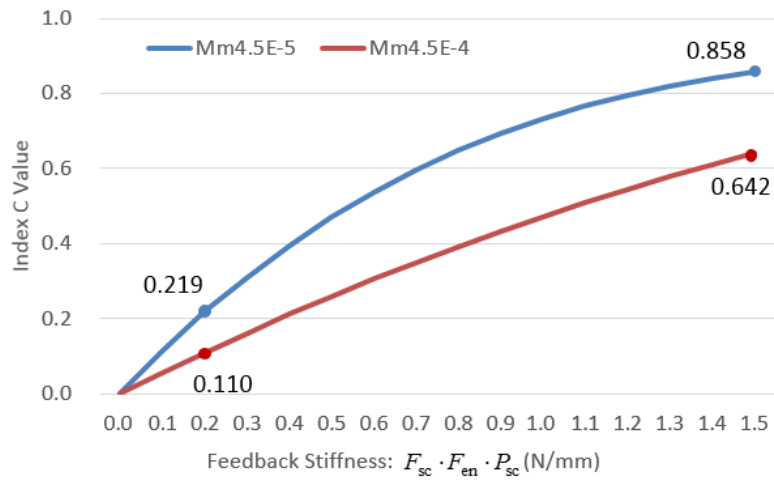


Fig. 3.4. Change situation of index  $C$  value when  $M_m$  parameter changes in the ideal force-position control architecture.

Fig. 3.4 shows the change trend of the index  $C$  value as  $F_{sc} \cdot P_{sc} \cdot K_{en}$  changed from 0 to 1.5 N/mm, and the inertia parameter  $M_m$  in the controller of the master device increased 10 times. As can be seen, when  $F_{sc} \cdot P_{sc} \cdot K_{en}$  was low, for example 0.2 N/mm, if the inertia parameter in the master controller  $M_m$  increased 10 times, the index  $C$  value decreased by 50% (0.219 to 0.110). When  $F_{sc} \cdot P_{sc} \cdot K_{en}$  was high, for example 1.5 N/mm, as the  $M_m$  parameter changed by the same degree, the value of index  $C$  only decreased by 33.5% (0.858 to 0.642).

When designing the controller of the master device, if the original feedback intensity is low, the inertia term should be set cautiously because the operator's haptic sensation can be easily weakened by a larger master inertia. If the original feedback intensity is high, the master inertia can be increased more generously.

#### 3.2.4 Validations of the $C$ calculation function from system parameters

After the deriving the function calculating index  $C$  value directly from the system parameters, its validation is confirmed in this section.

Chapter 2 have confirmed that the value of index  $C$  calculated from the recorded device velocity profiles using (2.1), can correctly represent the operator's haptic sensation. However, in the derivation process of the function expressed by (3.5), the master velocities  $V_a$  was estimated by (3.4), not the actual velocities. Therefore, if the estimated  $V_a$  approximates the actual values, the  $C$  value calculated from the function expressed by (3.5) can also reliably represent the haptic sensation. An experiment was conducted to confirm the difference between the estimated and the actual master velocities.

A master-slave system by implementing the ideal position-force bilateral control model is built as shown in Fig. 3.5. The master side was the haptic display Phantom Desktop and the slave side and the operational environment are a virtual sphere and a virtual wall developed in the virtual world. Hence, the ideal control condition of the position-force bilateral control architectures could be realized.

In the experimental model, the force feedback scaling gain  $F_{sc}$  and position scaling gain  $P_{sc}$  were set to 1.0; the inertia of the master device  $M_m$  is  $4.5 \times 10^{-5} \text{ kg} \cdot 10^3$ , which cannot be changed; the dynamic parameters of operator's limb is constant as the same value introduced in section 3.2; adjusting the inertia of the slave device  $M_s$  won't affect the system's motion. The adjustable parameters were the damping of the master ( $B_m$ ) and the stiffness of the virtual wall ( $K_{en}$ ).

The experimental motion was conducted as follows: the operator held the stylus of the master device in their right hand and moved forward with casual speed. The speed of the forward movement was expected to be constant. Owing to the bilateral control, the slave

sphere also moved forward and made contact with the virtual wall. After the operator detected the contact, the forward motion stopped naturally and retracted back to the starting position. Then, the approaching-retracting motion was repeated. The velocity profile of every contact was recorded, and compared to the velocities estimated by the function expressed in (3.4).

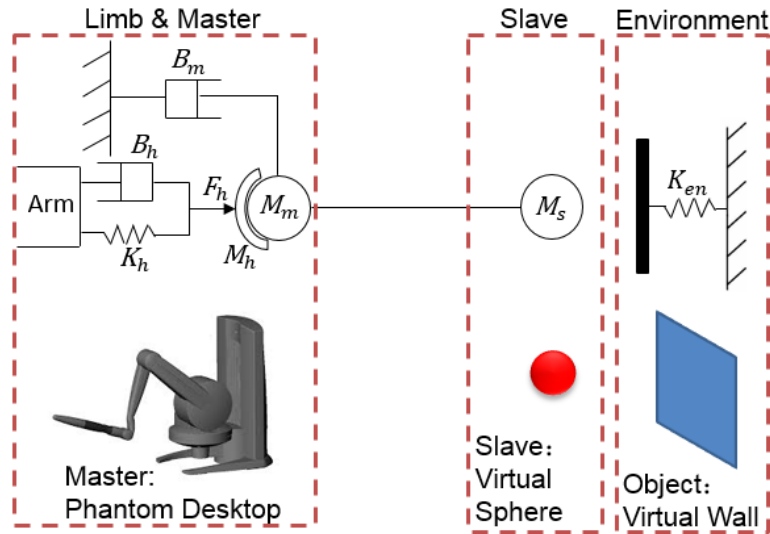


Fig. 3.5 Control model and apparatus in the confirmation experiment

Fig. 3.6 shows a comparison of the master velocity profile within 50 ms after contact. This comparison was made between an experimental case and  $V_a$  calculated from (3.4), under the operating conditions:  $B_m = 0.001$  Ns/mm,  $K_{en} = 0.1$  N/mm. As can be seen, the master device velocity calculated by the functions can reflect the actual situation with high fidelity. Moreover, the difference between the  $C$  value calculated from the real velocity profiles and the calculated  $V_a$  was as small as 8%.

Another reason to consider the dynamic parameters of the operator's limb unchanged is that it is difficult to measure the specific dynamic parameter value of every operator. However, it is natural to argue that when  $B_m$  parameter is high, the operator has to apply more forces to move the master device, resulting a high muscular tension in his/her limb, which may change the dynamic parameters of the limb and make the assumption of constant dynamic parameters improper. Moreover, a high feedback stiffness will produce a large shock at the master side, can the operator's limb dynamic parameters still be

considered as constant under a large shock?

Therefore, we conducted another experiment comparing the real master's velocity profile over 50 ms after the contact with the estimated one. The parameter settings condition is:  $B_m = 0.01$  Ns/mm,  $K_{en} = 1.0$  N/mm. Both the  $B_m$  and  $K_{en}$  parameters are high. The comparison result is shown in Fig. 3.7.

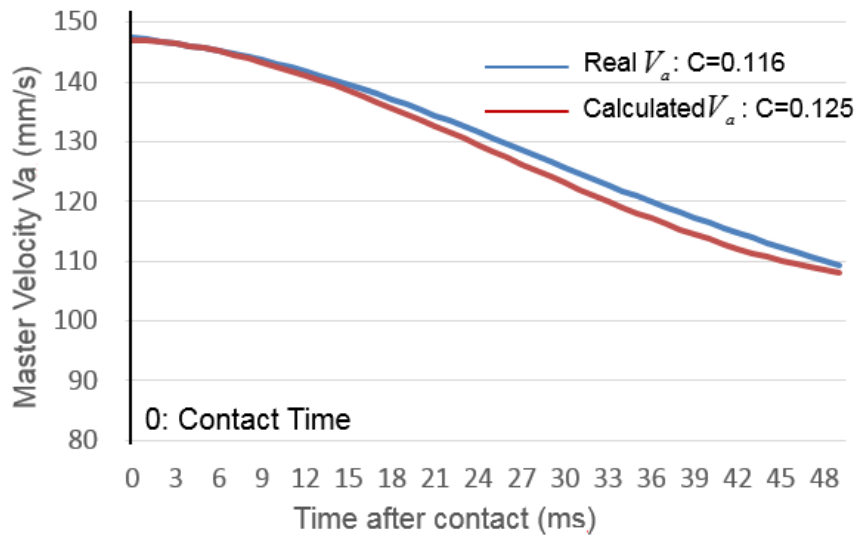


Fig. 3.6 Comparison of master device velocity obtained by experiment and the calculated result, operational condition was  $B_m = 0.001$  Ns/mm and  $K_{en} = 0.1$  N/mm.

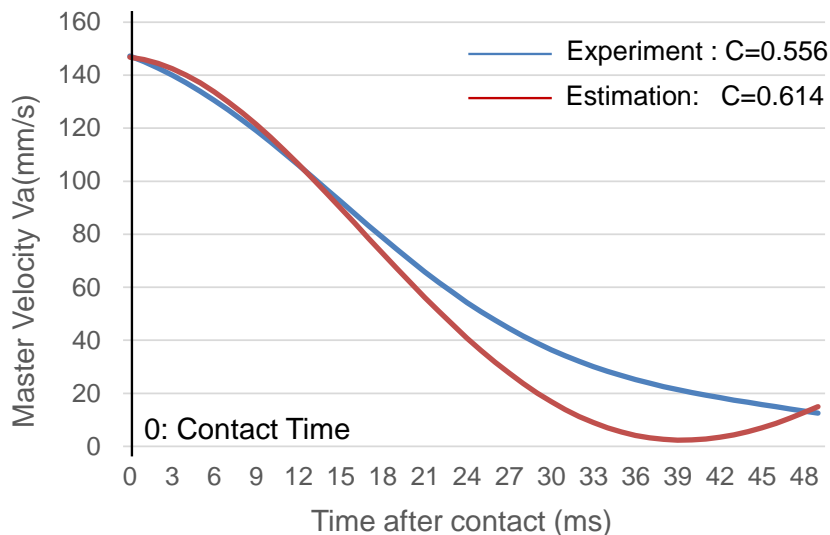


Fig. 3.7 Comparison of master device velocity obtained by experiment and the calculated result, operational condition was  $B_m = 0.01$  Ns/mm and  $K_{en} = 1.0$  N/mm.

Fig. 3.7 shows that if the damping of the master device is high, the experimental master velocity will decrease slower than the estimated velocity. This is attributed to the fact that the operator must input more force to move the master device with a high  $B_m$ , if the operational velocity is expected to be the same as that with a low  $B_m$  parameter. Hence, the operator's limb muscle became tense and the actual impedance of the limb was higher than the designated values, which prevented the deceleration of the master device by the feedback force.

However, difference between the two  $C$  values calculated from the true velocity profile and the estimated one was tiny as 10 %. The master device velocity calculated by the functions can still reflect the actual situation with high fidelity. Moreover, in this experiment, the  $B_m$  as high as 0.01 Ns/mm has made the operator feel difficult to move the device freely, A higher master damping is not likely to appear in actual operation. Hence, it was reasonable to consider the dynamic parameter of operator's limb dynamics as constant in normal application cases.

The experimental results indicate that the master velocity information estimated from function (3.4) is near the real situation. Hence, the  $C$  value calculated directly from the system parameters by function (3.5) is reliable.

### 3.3 Relationship between index value and system parameters in the real Position-Force model

#### 3.3.1 Control model introduction

In most actual master-slave system applications, the virtual rigid body connection cannot be realized. The connection between the devices is often considered as virtual spring with a  $K_p$  gain and virtual damping with a  $K_v$  gain. For example, in nanoscale operation, the  $K_p$  and  $K_v$  gains are added as a coupling factor in the system.

This type of control model is termed real bilateral control model in this study, and its configuration is shown Fig. 3.8.

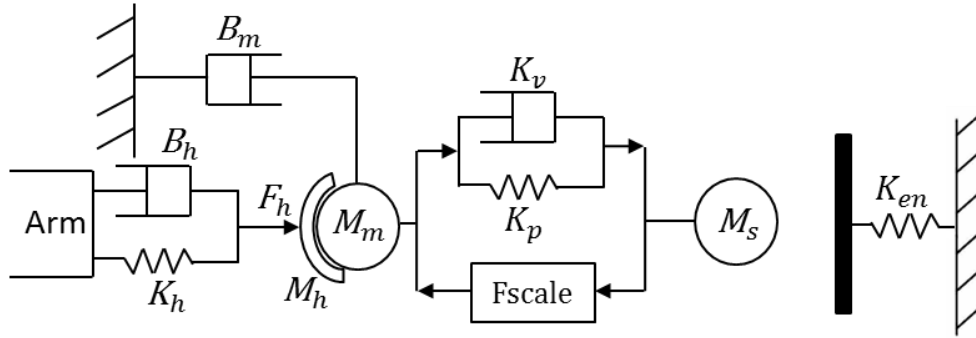


Fig. 3.8. Real bilateral control model: master and slave devices are connected by virtual spring and virtual damper.

As the motion of the master and slave devices is also affected by the virtual gains between them,  $K_p$  and  $K_v$  parameters are often adjusted actively by the system designer for some task requirements. Increasing the  $K_p$  and  $K_v$  values can make the device motion approach to the ideal ones; on the contrary, reducing them can reduce the impulse applied on the environment [90].

With this control model, the motions of the master and slave devices do not accord with each other. Therefore, the two devices have different motion equations, as follows:

Master device:

$$F_h + K_h (V_b \cdot t - r_m) + B_h (V_b - \dot{r}_m) = (M_m + M_h) \cdot \ddot{r}_m + B_m \cdot \dot{r}_m + F_{sc} \cdot K_{en} (r_s - r_{en}) \quad (3.6)$$

Slave device:

$$K_p (r_m - r_s \cdot P_{sc}) + K_v (\dot{r}_m - \dot{r}_s \cdot P_{sc}) = M_s \cdot \ddot{r}_s + K_{en} (r_s - r_{en}) \quad (3.7)$$

In (3.7),  $r_s$  is the position of the slave device and  $\dot{r}_s$  is its velocity;  $t=0$  is the time point when the contact between the slave device and the environment occurs. The initial conditions for the master side are as follows: position of master device  $r_m(0^+) = 0$ ;

velocity of master device and operator's limb  $\dot{r}_m(0^+) = V_b = \frac{F_h}{B_m}$ .

The initial conditions for the slave side are as follows: the initial position of the environment  $r_{en}$  is set to zero; thus, the position where the slave device contacts the

environment  $r_s(0^+)$  is also zero. The direction of invading into the environment, in other words, compress the spring representing the environment property, is defined as positive. The velocity of the slave device  $\dot{r}_s(0^+) = \frac{V_b}{P_{sc}}$ , which is the approaching velocity of the master device scaled by the  $P_{sc}$  parameter. The reason for setting the initial slave velocity as such is described below.

According to Fig. 3.8, after the operator begins to move forward, before the contact between the slave device and the environment occurs, the motion equation for the master device is the same as (3.3). Finally, the master device velocity will be  $\frac{F_h}{B_m}$  after a sufficiently long period of time, until contact occurs.

After the master device begins to move, position and velocity errors are introduced between the devices, which pushes the slave device to move forward. Thus, the motion equation for the slave device before it contacts the environment can be expressed as follows:

$$K_p(r_m - r_s \cdot P_{sc}) + K_v(\dot{r}_m - \dot{r}_s \cdot P_{sc}) = M_s \ddot{r}_s \quad (3.8)$$

In functions (3.7) and (3.8),  $r_s$  is the position of the slave device,  $(r_m - r_s \cdot P_{sc})$  and  $(\dot{r}_m - \dot{r}_s \cdot P_{sc})$  is position and velocity error between the master and slave devices,  $K_p$  and  $K_v$  are the virtual spring and virtual spring between devices.

After a sufficiently long amount of time, the slave device velocity  $\dot{r}_s$  will finally oscillate at the level of  $\frac{V_b}{P_{sc}}$ . If the slave device is adequately controlled, the oscillation will be very small. Thus both the position error  $(r_m - r_s \cdot P_{sc})$  and the velocity error  $(\dot{r}_m - \dot{r}_s \cdot P_{sc})$  will also be very small, and the left side of the function expressed in (3.8) will be approximately equal to zero. The slave device can be considered to move forward with stable velocity  $\dot{r}_s = \frac{V_b}{P_{sc}} = \frac{F_h}{B_m \cdot P_{sc}}$  until it makes contact with the environment.

This paper only discusses the case wherein the slave device contacts the environment at this stable velocity level. If contact occurs before the slave device becomes stable, the unpredictable motion of the slave device makes the impulse unpredictable for every contact. This results in unpredictable feedback force information, which in turn makes the motion of the master device unpredictable, even when the operational conditions remain unchanged.

If the slave device contacts with the environment with  $\dot{r}_s$  reaches the stable level, the equation of motion for the master device is:

$$F_h + K_h \left( \frac{F_h}{B_m} \cdot t - r_m \right) + B_h \left( \frac{F_h}{B_m} - \dot{r}_m \right) = (M_m + M_h) \cdot \ddot{r}_m + B_m \cdot \dot{r}_m + F_{sc} \cdot K_{en} \cdot r_s \quad (3.9)$$

Equation of motion for the slave device is

$$K_p (r_m - r_s \cdot P_{sc}) + K_v (\dot{r}_m - \dot{r}_s \cdot P_{sc}) = M_s \cdot \ddot{r}_s + K_{en} \cdot r_s \quad (3.10)$$

### 3.3.2 Relationship function derivation

Motion equations (3.9) and (3.10) are more complex in comparison with that of ideal architectures. Additionally, an analytical solution does not exist. Hence, the method used in Section 3.2.2 cannot be used here.

Therefore, in this section, multiple system parameter settings were chosen and implemented in the simulation to obtain the numerical solution of  $\dot{r}_m$  and calculate the corresponding values of index  $C$ . Then, we fit the searching relationship function by one-to-one matching for the value of index  $C$  and the system parameter settings.

The parameters adjusted in this experiment and their value levels are as follows:

Virtual spring gain  $K_v$  (N/mm): 1e-5, 1e-4, 1e-4, 1e-2, 0.1, 1, 10, and 100;

Virtual damping gain  $K_p$  (Ns/mm): 1e-5, 1e-4, 1e-4, 1e-2, 0.1, 1, 10, and 100;

Master damping ratio  $B_m$  (Ns/mm): 0.001 to 0.009 every 0.001;

Feedback stiffness  $K_{en} \cdot F_{sc}$  (N/mm): 0.1 to 1.5 every 0.1.

These four types of parameters were adjusted and combined with each other. Hence, by substituting the parameters settings into simulation, the  $C$  values from 8,640 ( $8 \times 8 \times 9 \times 15$ ) parameter settings were obtained.

In this experiment, the value of the slave device inertia was set to  $5 \times 10^{-5} \text{ kg} \cdot 10^3$  because a master-slave system with low device inertia in the controller was expected [27], [58]. Although the weight of the different slave devices varied from very low to very high, an inertia item of  $5 \times 10^{-5} \text{ kg} \cdot 10^3$  was realized in their controllers. Additionally, the position scaling  $P_{sc}$  was maintained at 1.0.

The  $K_p$  and  $K_v$  gains are related to the stability of the system. In this study, we only investigated their effect on the operator's haptic sensation, and did not consider the stability of the system.

The numerical solution of  $\dot{r}_m$  was obtained using the Runge-Kutta fourth order method. Fig. 3.9 shows the simulation results for the  $C$  values as the  $K_p$  and  $K_v$  parameters changed from  $1e-5$  to 100, respectively. The four subgraphs fall under four  $F_{sc} \cdot K_{en}$  levels.

As can be seen in Fig. 3.9, the  $C$  values remain constant if  $K_p$  or  $K_v$  exceed a certain value ( $K_v \geq 10$  or  $K_p \geq 100$ ), and the constant  $C$  values are equal to those in the cases considering the ideal bilateral control model. Considering the bottom right subgraph of Fig. 3.9 as an example, if  $K_v \geq 10$  or  $K_p \geq 100$ , the  $C$  value is 0.858, which is equal to the  $C$  value in the ideal control model with  $F_{sc} \cdot K_{en} = 1.0 \text{ N/mm}$  and  $B_m = 0.001 \text{ Ns/mm}$  (the same  $C$  value can be obtained from the blue curve Fig. 3.3). This occurs because the virtual spring and damper between the master and slave devices work simply as virtual rigid bodies when the  $K_p$  and  $K_v$  gains are high, and the interaction force within a short amount of time is not sufficiently large to shorten them. Moreover, the motion of the system approximates that of the ideal control model.

If both  $K_p$  and  $K_v$  are less than a certain value ( $K_p \leq 1e-3$  and  $K_v \leq 1e-4$ ), the  $C$  values remain constant and are equal to those in the cases wherein both  $K_p$  and  $K_v$  are equal to zero. When the  $K_p$  and  $K_v$  gains are zero, the left side of (3.10) is also

equal to zero. Hence, the motion of the slave device after contact is simply free contact, and the interaction force is simply determined by the slave controller and the properties of the environment.

The above analysis demonstrates that if the  $F_{sc} \cdot K_{en}$  and  $B_m$  parameters are kept unchanged, the  $C$  values with high  $K_p$  and  $K_v$  gains will be equal to those in the ideal bilateral control model ( $C = 1.0 \times C_{ideal}$ ). Additionally, the  $C$  values with lower  $K_p$  and  $K_v$  gains will be equal to  $C_{ideal}$  multiplied by a coefficient less than 1.0.

Because every subfigure in Fig. 3.9 shows the same tendency, the effect of the  $K_p$  and  $K_v$  parameters can be considered as the coefficient  $\alpha$  multiplied to  $C_{ideal}$ . The objective function calculating the  $C$  values from the system parameters can be formulated as follows:

$$C = \alpha \cdot C_{ideal} \quad (3.11)$$

The function of  $C_{ideal}$  was obtained in Section 3.2; therefore, the formulation of (3.11) can be obtained by deriving how the  $K_p$  and  $K_v$  gains affects coefficient  $\alpha$ .

For the upper left and the bottom right subfigures of Fig. 3.9, the cross sections of the index  $C$  curved surface at four  $K_v$  levels are shown in Fig. 3.10 and Fig. 3.11 respectively, from which it can be observed that the cross sections are sigmoid curves, so the function of coefficient  $\alpha = \frac{C}{C_{ideal}}$  are also a sigmoid function. If  $K_p > 100$  N/mm,

$\alpha \simeq 1$ ; if  $K_p < 1e-3$  N/mm, depends on  $K_v$ . Hence, the objective function of  $\alpha$  to  $K_p$  parameter is supposed to be the following sigmoid function:

$$\alpha = 1 - \frac{1}{f(K_v) + \sigma_1 \cdot e^{f(\log_{10}(K_p))}} \quad (3.12)$$

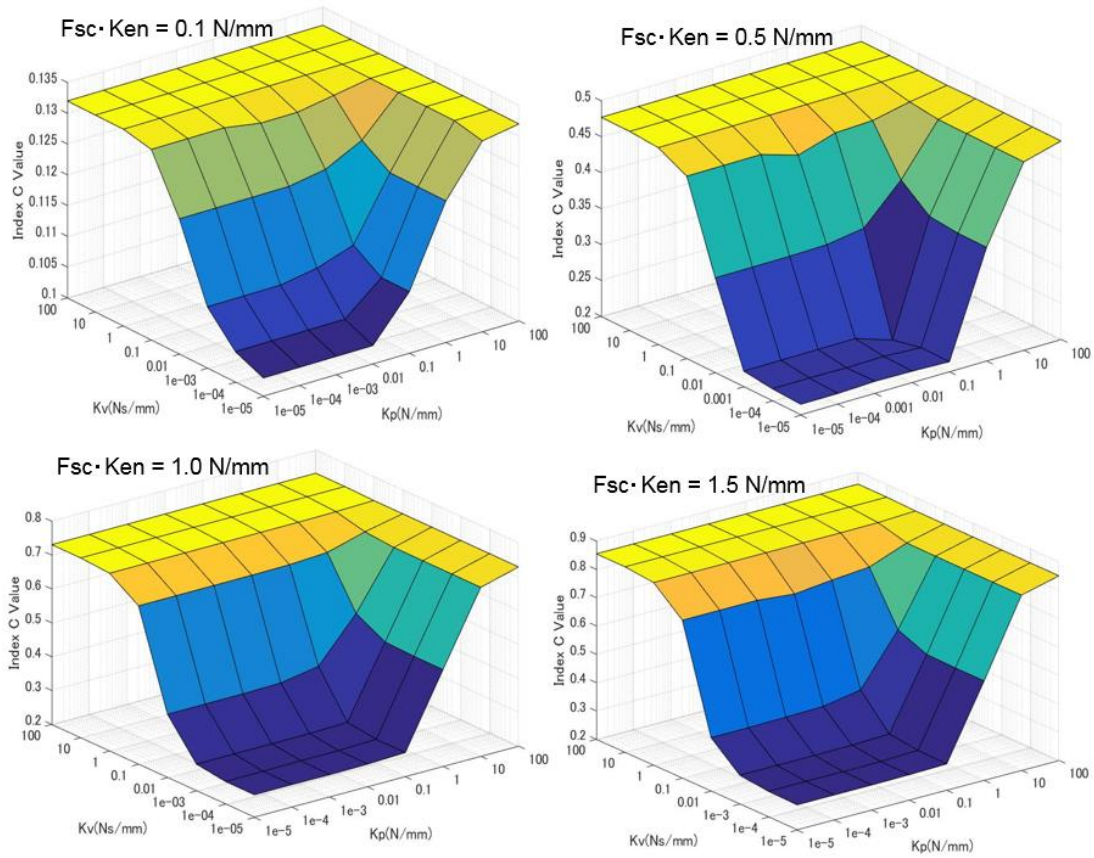


Fig. 3.9 Effect of  $K_p$  and  $K_v$  parameters when  $B_m = 0.001$  Ns/mm.

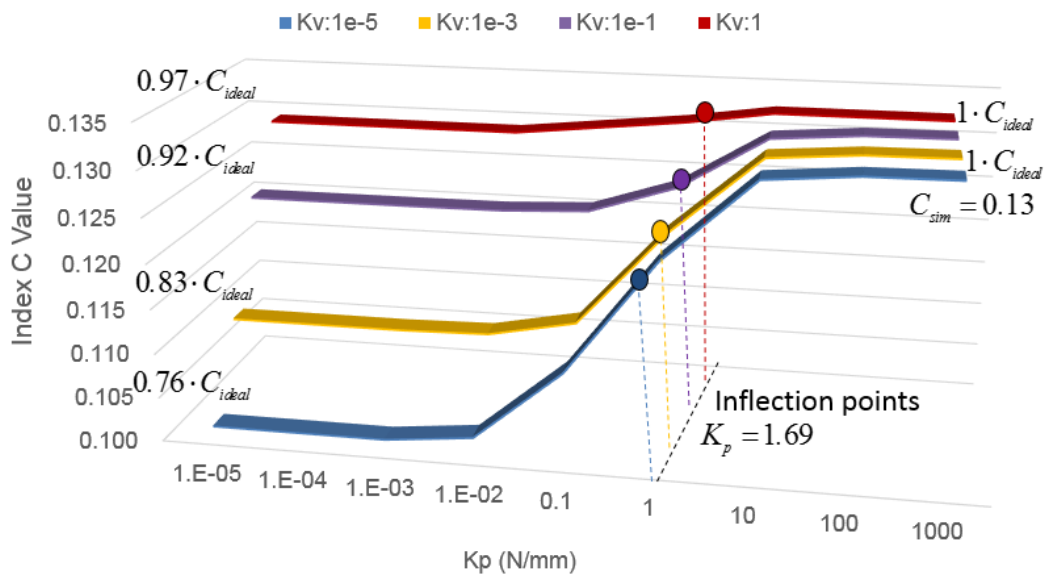


Fig. 3.10 The cross sections of the curved surface in the upper left subfigure of Fig. 3.9 (environment stiffness  $K_{en} = 0.1$  N/mm) at four  $K_v$  levels.

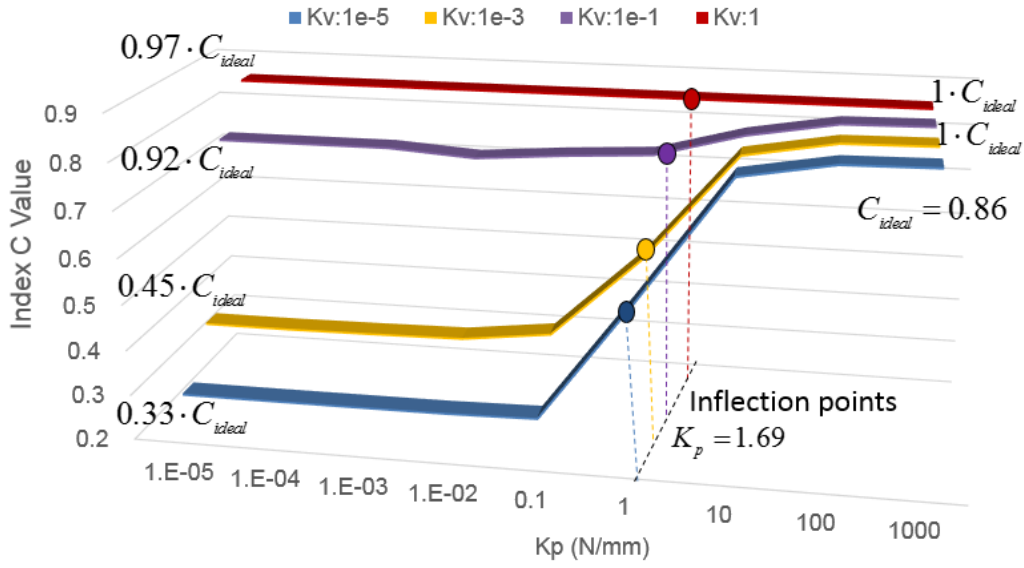


Fig. 3.11 The cross sections of the curved surface in the bottom right subfigure of Fig. 3.9 (environment stiffness  $K_{en} = 1.5 \text{ N/mm}$ ) at four  $K_v$  levels.

Similarly, for the upper left and the bottom right subfigures of Fig. 3.9, the cross sections of the index  $C$  curved surface at four  $K_p$  levels are shown in Fig. 3.12 and Fig. 3.13, respectively. The cross sections are also sigmoid curves. From which it can be observed that if  $K_v > 10 \text{ N/mm}$ ,  $\alpha \simeq 1$ ; if  $K_v < 1e-4 \text{ N/mm}$ ,  $\alpha$  depends on  $K_p$ . Hence, the objective function of  $\alpha$  to  $K_v$  parameter can also be supposed to be the following sigmoid function:

$$\alpha = 1 - \frac{1}{f(K_p) + \sigma_2 \cdot e^{f(\log_{10}(K_v))}} \quad (3.13)$$

Fig. 3.9 shows that the index  $C$  to  $K_p$  and  $K_v$  gains are sigmoid curved surfaces.

Because  $\alpha = \frac{C}{C_{ideal}}$ , the coefficient  $\alpha$  to  $K_p$  and  $K_v$  gains is also a sigmoid curved surface. Combining functions (3.12) and (3.13) together, the objective function of  $\alpha$  to  $K_p$  and  $K_v$  gains is supposed to be:

$$\alpha = 1 - \frac{1}{\beta + \sigma_1 \cdot e^{f_1(\log_{10}(K_p))} + \sigma_2 \cdot e^{f_2(\log_{10}(K_v))}} \quad (3.14)$$

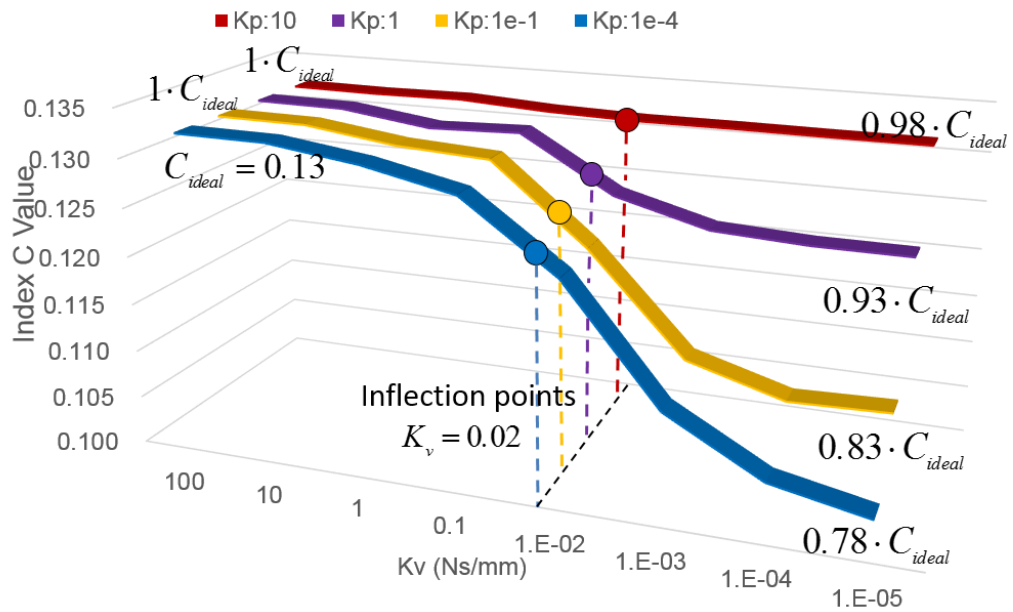


Fig. 3.12 The cross sections of the curved surface in the upper left subfigure of Fig. 3.9 ( $F_{sc} \cdot K_{en} = 0.1$  N/mm) at four  $K_p$  levels.

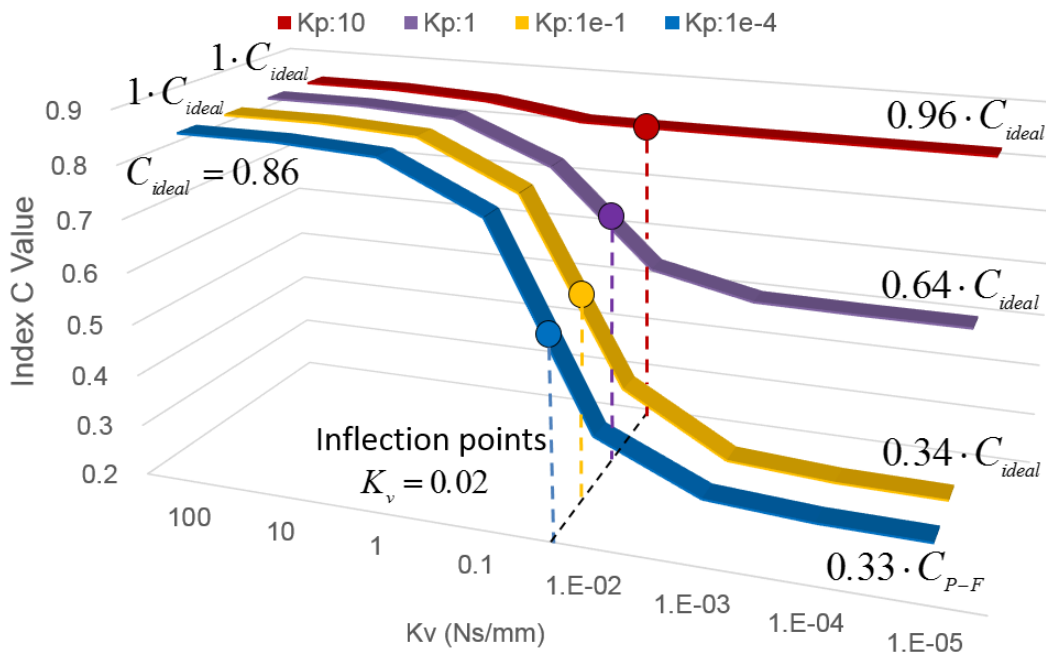


Fig. 3.13 The cross sections of the curved surface in the bottom right subfigure of Fig. 3.9 ( $F_{sc} \cdot K_{en} = 1.5$  N/mm) at four  $K_p$  levels.

When the  $K_p$  and  $K_v$  parameters approach to zero,  $\sigma_1 \cdot e^{f_1(\log_{10}(K_p))} + \sigma_2 \cdot e^{f_2(\log_{10}(K_v))}$  term in function (3.14) should near zero. As discussed above,  $\alpha$  with low  $K_p$  and  $K_v$  parameters is determined by the feedback stiffness and the master damping, so  $\beta$  in function (3.14) is determined by  $F_{sc} \cdot K_{en}$  and  $B_m$ .

From Fig. 3.10 and 3.13, the inflexion points of every sigmoid curve are constant at  $K_p = 1.7$  ( $\log_{10}(K_p) = 0.23$ ), and they are not affected by parameters. Similarly, the inflexion points of every sigmoid curve in Fig. 3.12 and 3.13 are also constant at  $K_v = 0.02$  ( $\log_{10}(K_v) = -0.23$ ). So the terms  $f_1(\log_{10}(K_p))$  and  $f_2(\log_{10}(K_v))$  in function (3.14) can be formulated as  $\varepsilon \cdot (\log_{10}K_p - 0.23)$  and  $\varepsilon \cdot (\log_{10}K_v + 1.69)$ .

Hence, under the objective function of coefficient  $\alpha$  is formulated as

$$\alpha = 1 - \frac{1}{f(F_{sc} \cdot K_{en}, B_m) + \sigma_1 \cdot e^{\varepsilon(\log_{10}K_p - 0.23)} + \sigma_2 \cdot e^{\varepsilon(\log_{10}K_v + 1.69)}} \quad (3.15)$$

Using the proposed objective function and the  $C$  values from the simulation results, the function of coefficient  $\alpha$  is fitted as:

$$\alpha = 1 - \frac{1}{e^{-19.2B_m} \cdot \left(4 + \frac{1}{F_{sc}K_{en}}\right) + \left(1 + \frac{1.62}{F_{sc}K_{en}}\right) \cdot e^{2.64(\log_{10}K_p - 0.23)} + \frac{1.77}{F_{sc}K_{en}} \cdot e^{2.64(\log_{10}K_v + 1.69)}} \quad (3.16)$$

Substituting function (3.16) into (3.11), the searching relationship function for the real bilateral control model that calculates the index  $C$  value from system parameters is as follows:

$$C = C_{ideal} \cdot \left( 1 - \frac{1}{e^{-19.2B_m} \cdot \left(4 + \frac{1}{F_{sc}K_{en}}\right) + \left(1 + \frac{1.62}{F_{sc}K_{en}}\right) \cdot e^{2.64(\log_{10}K_p - 0.23)} + \frac{1.77}{F_{sc}K_{en}} \cdot e^{2.64(\log_{10}K_v + 1.69)}} \right) \quad (3.17)$$

In (3.17), the constant terms are generated from parameters that are not included. For example, in the right side denominator, the power of the natural constants  $2.64 \cdot (\log_{10}K_v + 1.69)$  is determined by the shapes of the sigmoid curves shown in Fig.

3.12 and Fig. 3.13. However, the shapes of those sigmoid curves are affected by the master inertia  $M_m$  and the slave inertia  $M_s$ .

### 3.3.3 Validations of the $C$ calculation function from system parameters

In this section, a psychophysical experiment was conducted to confirm the validation of function (3.17), the method is the same as used in Section 2.4, sensations from two system parameter settings but with the same  $C$  value (the  $C$  values were calculated just from parameters by function (3.17)) were presented to a subject. After presenting the two sensations, the subject was asked to identify in which trial they could more easily sense the contact between the slave and the environment. Subjects could answer “the former one”, “the later one”, or “Same”.

If the function between  $C$  and the system parameters, which is presented in function (3.17), is correct, regardless of how the  $K_v$ ,  $K_p$ ,  $B_m$ , and  $F_{sc} \cdot K_{en}$  parameters were set, the haptic sensations that they provided to the operator should be the same as long as the index  $C$  value calculated by function (3.17) are the same, thus it will be difficult for the operator to distinguish the difference of haptic sensation between the pair elements.

The control model and the experimental apparatus are shown in Fig. 3.14. The designated four pairs of parameter setting with the four types of parameters and their corresponding index  $C$  values are listed in Table 3.1.

Ten subjects were enrolled. For each subject, each parameter setting pair was repeated 10 times. Hence, for every parameter setting pair, 100 answers were obtained. The time interval between every repetition was more than 0.5 hours, thus the subject could not realize that the parameter setting pair was repeated.

For each parameter pair, the proportion of the indistinguishable answers after 100 trials is shown in Table 3.2, from which it can be observed that the proportion of the indistinguishable answers for the parameter setting pairs No.1 to 3 was almost beyond 80 %, the haptic sensations provided by the parameter settings with the same  $C$  values were the same. But for the pairs No.4 and 5, the proportions are less than 40 %.

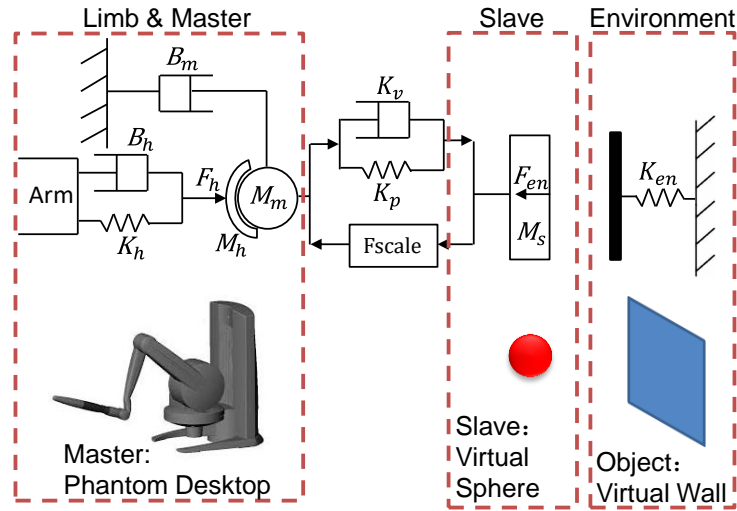


Fig. 3.14 Experimental device and control model.

Table 3.1. Selected parameter settings in validation experiment

No.	Parameter setting of A	C value of setting A	Parameter setting of B	C value of setting B
1	$F_{sc}K_{en} : 0.90$ $B_m : 0.001$ $K_v : 0.1$ $K_p : 0.1$	0.62	$F_{sc}K_{en} : 1.30$ $B_m : 0.007$ $K_v : 0.1$ $K_p : 0.1$	0.62
2	$F_{sc}K_{en} : 0.45$ $B_m : 0.001$ $K_v : 0.01$ $K_p : 1e-5$	0.34	$F_{sc}K_{en} : 0.40$ $B_m : 0.001$ $K_v : 0.1$ $K_p : 0.1$	0.34
3	$F_{sc}K_{en} : 0.80$ $B_m : 0.001$ $K_v : 1e-5$ $K_p : 0.01$	0.47	$F_{sc}K_{en} : 1.10$ $B_m : 0.001$ $K_v : 1e-5$ $K_p : 0.01$	0.47
4	$F_{sc}K_{en} : 0.2$ $B_m : 0.001$ $K_v : 0.1$ $K_p : 0.1$	0.21	$F_{sc}K_{en} : 0.5$ $B_m : 0.004$ $K_v : 1e-5$ $K_p : 1e-5$	0.22
5	$F_{sc}K_{en} : 0.4$ $B_m : 0.002$ $K_v : 1e-5$ $K_p : 1e-5$	0.18	$F_{sc}K_{en} : 1.5$ $B_m : 0.008$ $K_v : 1e-5$ $K_p : 1e-5$	0.16

Table 3.2

In complicate architecture, proportion of indistinguishable answers under the Same  $C$  value, sample size of every pair is 100.

Parameter pair No.	Proportion of indistinguishable answers
$A_1, B_1$	85 %
$A_2, B_2$	81 %
$A_3, B_3$	82 %
$A_4, B_4$	42 %
$A_5, B_5$	27 %

### 3.4 Discussion of this chapter

#### 3.4.1 The results in the experiment in Section 3.3.3.

In the above experiment, the high proportions of indistinguishable answer means the relationship between the system parameters and  $C$  value expressed by function (3.17) is valid.

However, for the parameter setting pair No. 5, the proportion of indistinguishable answers are extremely low (27 %) with a same  $C$  value.

The parameter settings in Table 3.1 can be classified into three types, high  $K_p$  and  $K_v$  gains ( $A_1, B_1, B_2, A_4$ ), medium  $K_p$  and  $K_v$  gains ( $A_2, A_3$  and  $B_3$ ) and low  $K_p$  and  $K_v$  gains ( $B_4, A_5$  and  $B_5$ ). The parameter setting pairs No. 4 and 5 are with low  $K_p$  and  $K_v$  gains. The velocity profiles of the master device for  $A_5$  and  $B_5$  are plotted in Fig. 3.15, from which it can be observed that the largest velocity change for  $A_5$  appears at about 30 ms after contact; while the largest velocity change for  $B_5$  appears at about 15 ms, and then, the master velocity restores back. This is because low  $K_p$  and  $K_v$  gains cannot keep the slave sphere contacting the virtual wall continuously. The slave sphere rebounds back after a short contact with the environment. The force fed back to the master device disappears when the slave device is not in contact with the environment, while the operator's input force is the only input to the master device and is the same as that before contact. So the master device velocity increases again.

As introduced in Section 2.2, the temporal resolution of human's haptic receptor is 20 ms–30 ms, and the objective of using the average velocity over 50 ms after contact is not to measure the mean velocity all over 50ms but to estimate the velocity at about 20 ms–30 ms after contact ( $V_a$  in function (2.1)), then obtaining the velocity change magnitude ( $V_b - V_a$  in function (2.1)) at the moment of 20 ms–30 ms after contact. This objective can be realized when the master velocity profile after contact decreases continuously, just like what appears in Fig. 2.1.

However, when the master velocity profiles approximates the curves in Fig. 3.15, the calculated average velocity over the 50ms cannot represent the true master velocity at the moment of 20 ms–30 ms after contact, resulting that the  $C$  value calculated from it deviates from the real haptic sensation largely.

Therefore, although the calculated  $C$  value for parameter settings A5 and B5 are the same, the true sensation perceived by the subject is different, leading to a remarkably low proportion of the cases that subject cannot tell a difference.

The reason for the low proportion of indistinguishable answers for the parameter setting pair No.4 is the same. The velocity profiles of the master device for parameter setting A4 and B4 are plotted in Fig. 3.16. For the parameter setting B4 (the red curve), the average velocity over 50 ms deviates from the real velocity at the moment of 20 ms–30 ms after contact, and the  $C$  value of B4 cannot represent the true haptic sensation, while for the parameter setting A4 (the blue curve), the average velocity over 50 ms almost equal the real velocity at the moment of 20 ms–30 ms after contact, and the  $C$  value of A4 can represent a true sensation.

Undoubtedly, under the same  $C$  value of A4 and B4, a true sensation is different from a fake one, resulting a low proportion of the cases that subject cannot tell a difference. However, the total deviation between the average velocity over 50 ms and the true velocity at 20 ms–30 ms for parameter setting A4 and B4 (Fig. 3.16) is less than that for parameter setting A5 and B5 (Fig. 3.15), thus the proportion was 42 %, not that low as A5 and B5.

However, in applications of a master-slave system, the velocity profile as parameter settings B4, A5 and B5 is generated from the cases where the motion of slave device after is totally undesirable, which is an unexpected system response. Therefore, the cases that the  $C$  value cannot represent the true haptic sensation do not often appear in real applications.

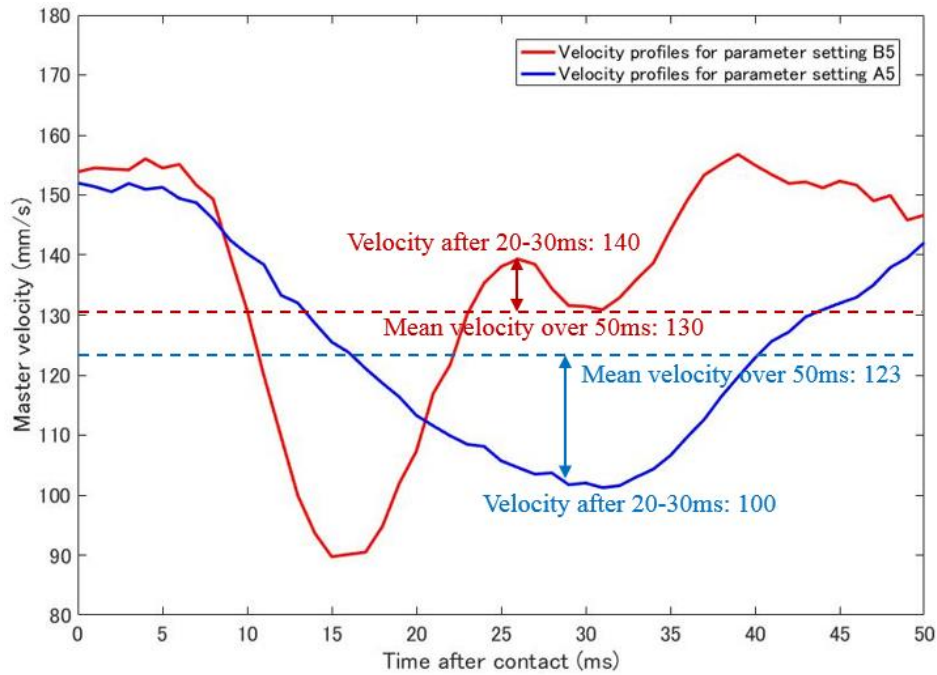


Fig. 3.15 Master velocity profiles for parameter settings A5 and B5 in the experiment of Section 3.3.3

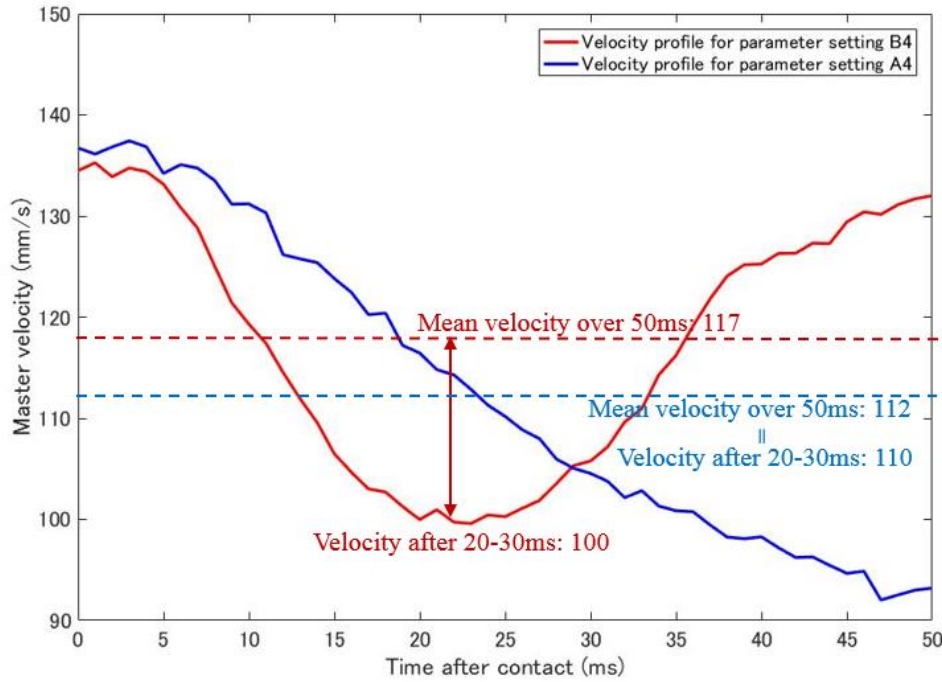


Fig. 3.16 Master velocity profiles for parameter settings A4 and B4 in the experiment of Section 3.3.3

### 3.4.2 Relationship between parameter values and solution of motion equations

For the ideal control model, the motion equation expressed by (3.2) is a second-order differential equation, for which the solution of its characteristic equation may have complex roots and may lead to an oscillation in the solution of (3.2) (the master velocity  $\dot{r}_m$ ).

The characteristic equation of the differential equation (3.2) is expressed as follows:

$$(M_h + M_m)s^2 + (B_h + B_m)s + (F_{sc} \cdot P_{sc} \cdot K_{en} + K_h) = 0 \quad (3.18)$$

where  $s$  is the Laplace operator. According to control theory, the appearance of oscillation is determined by the sign of the following expression:

$$(B_h + B_m)^2 - 4(M_h + M_m)(F_{sc} \cdot P_{sc} \cdot K_{en} + K_h) \quad (3.19)$$

The parameters of the human limb, namely,  $M_h$ ,  $K_h$ , and  $B_h$ , are considered to be fixed values, as mentioned before ( $K_h = 0.5$  N/mm,  $B_h = 0.002$  Ns/mm,  $M_h = 2.0 \times 10^{-4}$  kg  $\cdot 10^3$ ). When the master device controller is perfectly designed

(device inertia is completely eliminated:  $M_m = 0$ ) and the master damping  $B_m = 0.01$  Ns/mm, which gives the operator a very large operational resistance when moving the master device, the sign of (3.19) is positive only if the feedback stiffness  $F_{sc} \cdot P_{sc} \cdot K_{en}$  is less than 0.10 N/mm. The results obtained by our pilot study reveal that the operator will not perceive a haptic sensation when the feedback stiffness is less than 0.07 N/mm. Therefore, the condition of the feedback stiffness  $F_{sc} \cdot P_{sc} \cdot K_{en}$  being less than 0.10 N/mm was not considered in particular because it cannot provide an effective haptic sensation to the operator. Moreover, the master damping  $B_m$  is not expected to have a value larger than 0.01 Ns/mm, and the device inertia cannot be completely eliminated. Hence, in most cases, the master velocity  $\dot{r}_m$  after contact will include oscillations.

However, the oscillation does not affect the operation considerably. First, the oscillation will not increase because the signs of all the characteristic equation coefficients are positive, and the damping of the master device and human limb can attenuate the oscillation. Second, the human's active muscle reaction can naturally restrain the oscillation. The time span a human can input an active muscle reaction after the contact occurrence is approximately 50 ms. The period  $T$  of the oscillation is

determined by  $2\pi \sqrt{\frac{M_h + M_m}{F_{sc} \cdot P_{sc} \cdot K_{en} + K_h}}$ . With normal parameter settings,  $T$  is larger

than 50 ms. This means that the master device cannot even complete one period of oscillation before it is restrained by the operator's active muscle reaction.

Using the parameter setting presented in this paper, the feedback stiffness  $F_{sc} \cdot P_{sc} \cdot K_{en}$  should be more than 3.8 N/mm to make the oscillation period  $T$  less than 50 ms. However, such a high feedback stiffness will make the operator feel uncomfortable without high master damping, whereas the oscillation of the master device will be attenuated quickly if the device damping is high. Therefore, for the most part, the operators will not mind the oscillation.

For the real control model described by the simultaneous differential equations (3.9) and (3.10), by formulating the characteristic equation for the master velocity  $\dot{r}_m$  as  $(s + \alpha_1)(s + \alpha_2)(s^2 + 2\zeta\omega + \omega^2)$ ,  $\zeta$  will be an extremely sophisticated combination of

parameters, and it will thus become difficult to provide a specific parameter range such that  $\zeta > 1$ . Therefore, only a qualitative discussion regarding the oscillation is presented in this paper.

The difference of the real control model compared to the ideal control model is the  $K_p$  and  $K_v$  parameters. If the  $K_p$  and  $K_v$  parameters are high, the motion of the system with the real control model approximates the motion performed with the ideal control model, wherein the oscillation does not have a considerable effect under normal operating conditions. If the  $K_p$  and  $K_v$  parameters are not high, they will affect the master device motion as a dashpot reducing the oscillation. Therefore, it is unnecessary to consider the oscillation in particular.

### 3.4.3 Influence of device inertia on haptic sensation

When the  $K_p$  and  $K_v$  parameters were low, the slave device stopped very shortly after the contact, and only a low interaction force of the contact was fed back to the master device. However, in this study, this situation only occurred when the inertia terms in the master and slave device controllers were low as  $5 \times 10^{-5} \text{ kg} \cdot 10^3$ . In cases of large slave inertia, the abovementioned situation will change dramatically. If the inertia in the slave device controller is large, reducing the  $K_p$  and  $K_v$  gains will not reduce the interaction force but will instead generate a larger one.

This is attributed to the fact that a slave device with large inertia invades deep into the environment after making contact, which results in a large interaction force. Although feedback force information can decelerate the master device and amplifies the error between the motions of the master and slave, because the  $K_p$  and  $K_v$  gains are low, the left side of (3.10) is not sufficiently large to stop the slave device. Therefore, the invasion depth and interaction force will keep increasing.

The qualitative affection of the inertia parameter is a matter to be investigated in future work.

### 3.5 Summarization of this chapter

In this chapter, the relationship between the index  $C$  value proposed in Chapter 2 and the system parameters is clarified and written as functions that can calculate the  $C$  value directly from the parameters.

For the ideal position-force bilateral control model, the functions to calculate the index  $C$  value from the parameters were derived by solving the system's equations of motion. For the real position-force bilateral control model, the function that calculates the index value from the parameters were fitted based on simulation results. The results of the confirmation experiment revealed that the function can validly relating the operator's haptic sensations to the system parameters, which means that it can be used for parameter adjustment with consideration to haptic sensation.

## Chapter 4

# Applications as a guideline for system parameter design

The results presented in the previous two chapters can be used as a guideline for the system design in a master-slave system with consideration to the haptic sensations. This chapter introduces some examples of system parameter design.

As introduced in Section 1.4, the system designer often expects to know the maximum value a parameter can be set to keep the operator's haptic sensation unchanged or the minimum value to set to alter haptic sensations; or the value to which a parameter should be to restore the haptic sensation when the operator's haptic sensation decreases inevitably after adjusting parameters for the task requirement. The expectations of the system designer can be satisfied by the mathematical function calculating the quantified haptic sensation directly from the system parameters.

### 4.1 Assuring maximum and minimum values a parameter can be set

#### 4.1.1 Assuring the maximum parameter setting to keep a haptic sensation

The master damping parameter  $B_m$  is often used to stabilize the system or mitigate the operator's hand vibration. But an overly large  $B_m$  will obscure the operator's haptic sensation, and result in a difficulty for the operator to detect a contact occurrence between the slave device and the environment. Thus the system parameter designer should know the maximum value the  $B_m$  parameter can be set while holding the current haptic sensation.

Here is an example: the bilateral control model in Fig. 3.8 is used, with the following current parameter setting: master damping  $B_m = 0.001$  Ns/mm; environment stiffness  $K_{en} = 1.2$  N/mm; virtual stiffness  $K_p = 0.1$  N/mm; virtual damping  $K_v = 0.1$  Ns/mm;

force feedback scaling  $F_{sc} = 1$ .

Now the system designer intends to increase the master damping  $B_m$  to mitigate the hand vibration, but the operator does not want his/her haptic sensation to decrease. The process of calculating the highest reasonable  $B_m$  value is as follows:

First, the designer calculates the index  $C$  value to estimate the operator's haptic sensation with the current system parameter setting, by substituting the values of current system parameters into function (3.17), the current  $C$  value is 0.716, which is labeled as  $C_1$  for convenience.

Second, the designer calculates the necessary change rate ( $R_c$ ) to  $C_1$  to make a new haptic sensation felt by the operator be noticeably different from the current one. By substituting  $C_1$  as the  $C_{ref}$  term into function (2.4), the  $R_c$  is calculated as 1.198, which means the operator cannot feel a noticeable difference until the  $C$  value for a new haptic sensation is within  $[C_1/R_c, C_1 \cdot R_c]$ . Since increasing  $B_m$  parameter reduces the  $C$  value,  $C_1/1.198 = 0.597$  is the lowest  $C$  with which the haptic sensation decrease cannot be noticed different by the operator. For convenience, the index value 0.597 is labeled as  $C_2$ .

Third, the designer calculates the  $B_m$  value that can produce  $C_2$ , substituting  $C_2$  into the left side of function (3.17), and the fixed parameters  $K_{en} = 1.2$  N/mm,  $K_p = 0.1$  N/mm,  $K_v = 0.1$  Ns/mm,  $F_{sc} = 1$  into the right side of function (3.17), the corresponding  $B_m$  that produces  $C_2$  is back-calculated as 0.0056. A higher  $B_m$  will make  $C_2$  be less than 0.597, hence, 0.0056 is the maximum  $B_m$  value that the system designer can set if the operator does not want the contact detecting to become difficult.

The above process is an example of finding the highest parameter value with consideration to the operator's haptic sensation. Next, an experiment is implemented to check whether the maximum  $B_m$  value is correct or not. The experimental apparatus was the same as shown in Fig. 3.14. The experimental method is that used in Sections 2.4 and 3.3, two haptic sensations (labeled as A and B respectively) from the original parameter and the new parameter settings are presented to the subject in a pair, and check the extent

to which the subjects can distinguish the difference between the two sensations.

Table 4.1. Parameter settings and experimental results

Parameter setting A	C value of setting A	Parameter setting B	C value of setting B	Proportion of indistinguishable answers
$F_{sc} \cdot K_{en} : 1.2$ $B_m : 0.001$	0.716	$F_{sc} \cdot K_{en} : 1.2$ $B_m : 0.0064$	0.567	19 %
		$F_{sc} \cdot K_{en} : 1.2$ $B_m : 0.0048$	0.619	65 %

10 subjects were enrolled, for every subject, the presentation of haptic sensations pair A and B were repeated 10 times. At each presentation, the subject was asked whether they noticed a difference between A and B trials, thus 100 answers can be obtained.

According to the psychophysics theory and the analysis in Section 2.4, if two index values differ just by  $R_c$  ( $R_c = 1.198$  in this experiment), the proportion of indistinguishable answers out of the 100 answers is about 45 %. If the calculated maximum  $B_m$  limit (0.0056 Ns/mm) is correct, when the designer set the  $B_m$  value just above the calculated maximum limit, the proportion of indistinguishable will decrease to a level far more than 45 %, when the designer set the  $B_m$  value just below the maximum limit, the proportion of indistinguishable will decrease to a level far less than 45 %.

The parameter settings of A and B trials are listed in columns 2 and 4 of Table 4.1. In row 1 of Table 4.1, the  $B_m$  value in parameter setting A is 0.0064, just above the maximum limit; in row 2, the  $B_m$  value in parameter setting B is 0.0048, just below the maximum limit.

The experimental results are listed in column 6, it can be observed that the proportion of indistinguishable answer when  $B_m$  above the calculated maximum limit is far more than 45 %; the proportion when  $B_m$  below the calculated maximum limit is far less than 45 %. The calculated 0.0056 Ns/mm is the highest  $B_m$  value the operator can increase

while keeping the current haptic sensation.

#### 4.1.2 Assuring the minimum parameter setting to change a haptic sensation

The force feedback scaling  $F_{sc}$  is often used to strengthen the haptic sensation. However, human's haptic sensation is not continuous, an insufficient  $F_{sc}$  cannot let the operator to detect the contact easier. Thus the system parameter designer should know at least how much  $F_{sc}$  parameter should be set.

Here is an example: the bilateral control model in Fig. 3.8 is used, with the following current parameter setting: master damping  $B_m = 0.001$  Ns/mm; environment stiffness  $K_{en} = 0.1$  N/mm; virtual stiffness  $K_p = 0.1$  N/mm; virtual damping  $K_v = 0.1$  Ns/mm; force feedback scaling  $F_{sc} = 1$ .

Now system designer intends to increase the force feedback scaling  $F_{sc}$  to strengthen the haptic sensation, the process of calculating the minimum necessary  $F_{sc}$  value is similar as that in Section 4.1.1.

First, the designer calculates the index  $C$  value to estimate the operator's haptic sensation magnitude with the current system parameter setting. By substituting the values of current system parameters into function (3.17), the current  $C$  value is 0.131, which is labeled as  $C_1$  for convenience.

Second, by substituting  $C_1$  as the  $C_{ref}$  term into function (2.4), the  $R_c$  is calculated as 1.444, which means the operator cannot feel a noticeable stronger sensation until the  $C$  value for the new haptic sensation reaches  $C_1$ .

Third, substituting  $C_2$  into the left side of function (3.17), and the fixed parameters:  $K_{en} = 0.1$  N/mm,  $K_p = 0.1$  N/mm,  $K_v = 0.1$  Ns/mm, and  $B_m = 0.001$  into the right side, the corresponding  $F_{sc}$  that produces  $C_2$  can be back-calculated as 1.55.

After obtaining the necessary lowest  $F_{sc}$  parameter value to set to strengthen the haptic sensation, an experiment is implemented to check whether the result is correct or not.

Table 4.2. Parameter settings and experimental results

Parameter setting A	C value of setting A	Parameter setting B	C value of setting B	Proportion of indistinguishable answers
$K_{en} : 0.1$	0.131	$K_{en} : 0.1$ $F_{sc} : 1.62$	0.201	20 %
$F_{sc} : 1.0$		$K_{en} : 0.1$ $F_{sc} : 1.47$	0.175	62 %

The subject and the experimental method were the same as used in Section 4.1.1, for the same reference parameter setting A, two comparison parameter settings (all labeled as B) are designed. In one comparison parameter setting, the designer set the  $F_{sc}$  value just above the necessary minimum value; in another the designer set the  $F_{sc}$  value just below the necessary minimum value.

The parameter settings and the experimental results are listed in Table 4.2. It can be observed that the proportion when  $F_{sc}$  being just above the necessary minimum value was far less than 45 %, and the operator can easily tell that the sensation of parameter setting B is stronger; the proportion of indistinguishable answer when  $F_{sc}$  being just below the necessary minimum value is far more than 45 %, and the operator cannot feel that the sensation of parameter setting B is stronger. 1.55 is confirmed as the lowest necessary  $F_{sc}$  value if the designer wants to give the operator a stronger haptic sensation.

#### 4.2 Reasonable parameter design with consideration to both task requirement and haptic sensation

Except for assuring the limit value a parameter can be set, the results in Chapters 2 and 3 can also be used to design the system parameters reasonably with consideration to the operator's haptic sensation while meeting the requirement from the task.

Here is an example: the bilateral control model in Fig. 3.8 is used, with the following

original parameter setting: environment stiffness  $K_{en} = 0.4$  N/mm; master damping  $B_m = 0.001$  Ns/mm; virtual stiffness  $K_p = 0.1$  N/mm; virtual damping  $K_v = 0.1$  Ns/mm; force feedback scaling  $F_{sc} = 1$ . The index  $C$  with the current parameter setting is calculated as 0.388 by substituting the parameter values into function (3.17). For convenience, the original index value is labeled as  $C_1$ .

As to the task requirement, the environment is vulnerable, a large impulse or interaction force applied from the slave device is not expected. Reducing the  $K_p$  and  $K_v$  parameters can reduce the impulse on the environment, so the designer reduces this two parameters to  $K_p = 1e-5$  N/mm and  $K_v = 5e-3$  Ns/mm to meet the task requirement. (This study does not focus on how to adjust parameters for task requirements, herein, the process of designing the desirable  $K_p$  and  $K_v$  parameters is omitted).

The interaction force profiles for the original and the new  $K_p$  and  $K_v$  settings, with two contact (operation) velocity levels are plotted in Fig. 4.1 and 4.2. It can be observed that the peak interaction force and impulse to the environment (within 100ms) after reducing  $K_p$  and  $K_v$  parameters all decreases by 70 %. Moreover, if a peak interaction force more than 1.2 N is not expected, the operator has to cautiously constrain his/her operation velocity under about 100 mm/s with the original parameter setting; whereas the operator can freely range his/her operational velocity until more than 250 mm/s with the new parameter setting. The task requirement is satisfied.

However, it is natural to consider that reducing  $K_p$  and  $K_v$  parameters weakens the operator's haptic sensation, the designer must consider the change in haptic sensation. Substituting the parameter setting  $K_{en} = 0.4$  N/mm;  $B_m = 0.001$  Ns/mm;  $K_p = 1e-5$  N/mm and  $K_v = 5e-3$  Ns/mm and  $F_{sc} = 1.0$  into function (3.17), the index  $C$  value after reducing  $K_p$  and  $K_v$  is 0.252. The change rate to the original  $C$  value ( $C_1 = 0.388$ ) is 1.52, which is above the corresponding  $R_c$  to  $C_1$  that makes the haptic sensation different, the operator's haptic sensation is indeed weakened.

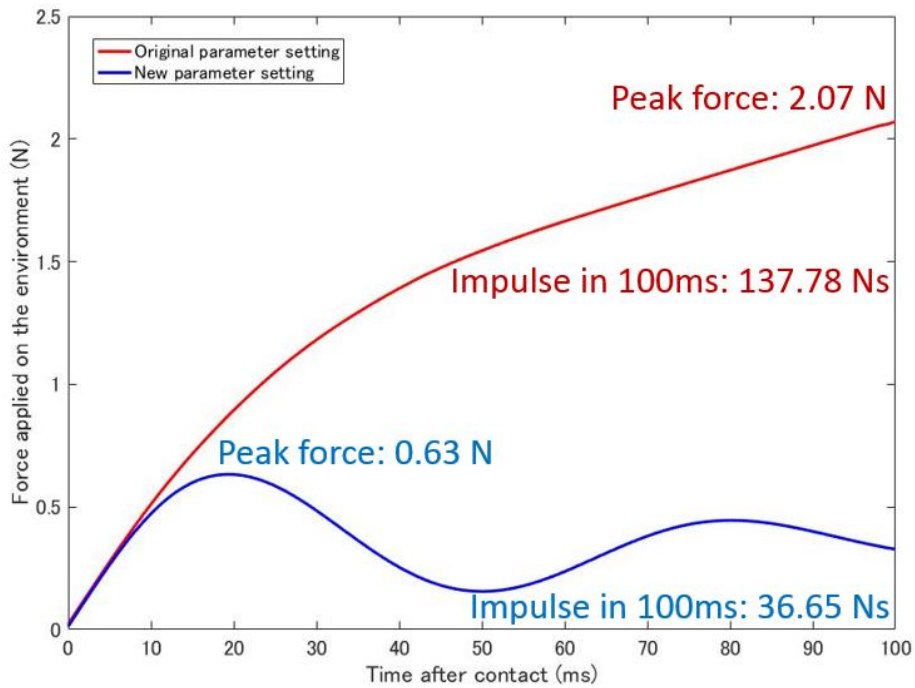


Fig. 4.1 The interaction force profiles for the original and the new  $K_p$  and  $K_v$  settings, with contact (operation) velocity level: 125 mm/s.

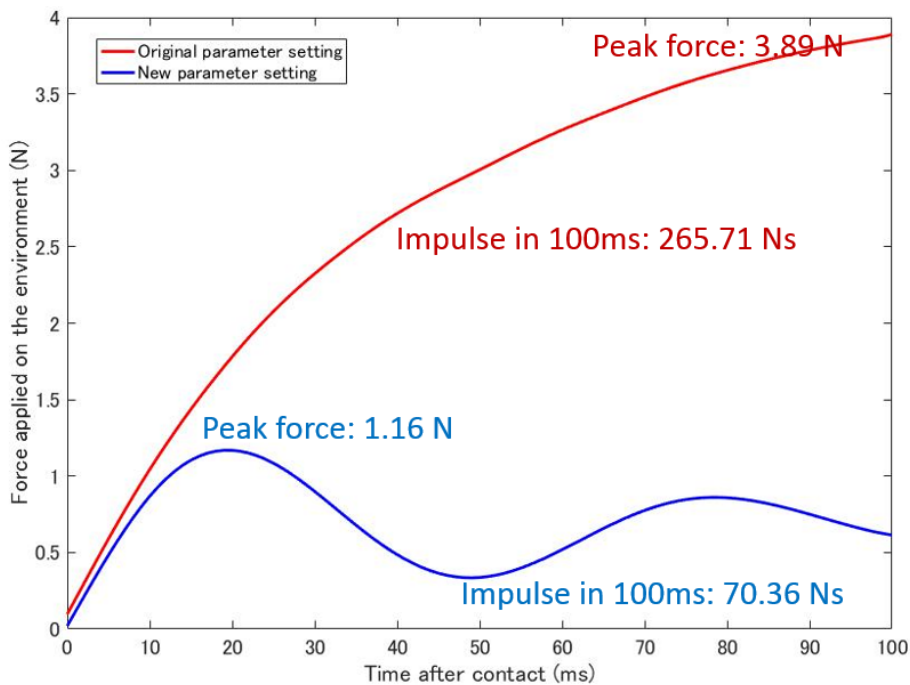


Fig. 4.2 The interaction force profiles for the original and the new  $K_p$  and  $K_v$  settings, with contact (operation) velocity level: 250 mm/s.

Assuming that the operator does not expect the contact detection to become difficult, the designer has to adjust other parameters to restore the haptic sensation, making the index value rise back to  $C_1$  (0.388). One method is increasing the force feedback scaling  $F_{sc}$ .

By substituting  $C = 0.388$  into the left side of function (3.17), and the fixed parameters:  $K_{en} = 0.4$  N/mm;  $B_m = 0.001$  Ns/mm;  $K_p = 1e-5$  N/mm and  $K_v = 5e-3$  Ns/mm into the right side, the corresponding  $F_{sc}$  that produces  $C_2$  can be back-calculated as 3.0.

An experiment is implemented to check whether the result is correct or not. The original and the new parameter settings are listed in Columns 1 and 3 of Table 4.3, their corresponding  $C$  values are in Columns 2 and 4. It can be observed that their  $C$  values are the same. The subject and the experimental method were the same as used in this Chapter, the proportion of difference indistinguishable answers is measured by presenting the haptic sensations with the original and the new parameter settings to 10 subjects.

The experimental result is shown in Column 5 of Table 4.3, the proportion of the indistinguishable answer was high, meaning that the subjects cannot tell a difference between the haptic sensations with the original and the new parameter setting. The requirement for the operator's haptic sensation is also satisfied.

Table 4.3. Selected parameter settings in validation experiment

Original parameter setting	$C$ value of original parameter setting	Parameter setting after adjustment	$C$ value of new parameter setting	Proportion of indistinguishable answers
$K_{en} : 0.4$ $B_m : 0.001$ $K_v : 0.1$ $K_p : 0.1$ $F_{sc} : 1.0$	0.388	$K_{en} : 0.4$ $B_m : 0.001$ $K_v : 1e-5$ $K_p : 5e-3$ $F_{sc} : 3.0$	0.388	78%

### 4.3 Conclusion of this chapter

In this chapter, three application cases of parameter design are introduced. Using the results obtained in this study, the system designer can not only assure the reasonable value range within which a parameter should be set; but also determine the specific value that the parameters should be set to satisfy the both the requirements for the task and operator's haptic sensation.

The experiment results in this chapter shows that, instead of relying on the trial and error method, the parameter design result based on the results of this study is simple but still reliable. The results presented in this study can be used as a guideline for the system design in a master-slave system with consideration to the haptic sensations.

# Chapter 5

## Conclusions and future works

### 5.1 Conclusions of this study

When using the impedance-adjusting bilateral control to provide a force-feedback function to a master-slave system, the system parameters are often adjusted for the requirements of different tasks.

Except for the task requirements, the human factors should also be considered when adjusting system parameters. The operator's haptic sensation, which means "how easily an operator can sense the contact between the slave device and the environment", is an important human factor. However, it is often weakened after an inappropriate system parameters adjustment.

Therefore, a system parameters design requires the consideration to both the task requirements and the haptic sensation. However, the existed related works cannot provide such a method. Thus the system parameters design considering both the two factors are conducted by an unfounded method: the trial and error adjustment.

To address this problem, the objective of this study is to build a method of system parameters design considering both the operator's haptic sensation and the task requirements. Specifically, the main task of this study is to quantify the relationship between the system parameters and the operator's haptic sensation. In this study, the task is accomplished by the following two steps: 1. proposing an index to quantify the haptic sensation; 2. finding relationship between the index and the system parameters.

Chapter 2 summarizes the first step: proposing an index to quantify the haptic sensation. Based on the analysis on operator's sensing mechanism, an index being hypothesized to quantify the operator's haptic sensation is defined, and its value is calculated from the change

magnitude of the master device velocity over 20–30 ms before and after contact. The name of the index is “Dynamic Contrast ( $C$ )”. The experimental results show that the proposed index value is stable to different master velocity before contact; and valid to quantify the operator’s haptic sensation.

Chapter 3 summarizes the second step: finding the relationship between the haptic sensation index and the system parameters and formulate it as a mathematical function for the ideal and the real application models of bilateral control. The relationship was successfully formulated as a function that calculates the index  $C$  just from system parameters without any additional information needed.

Chapter 4 includes three system parameters design cases. These example cases show that, using the results of the previous two chapters, a system designer not only can determine the necessary value for a parameter to realize his/her expectation on the operator’s haptic sensation; but also can realize a reasonable parameter adjustment with consideration to both the task requirement and the operator’s haptic sensation.

In a word, this work can be used as a guideline for system parameter design with consideration to the operator’s haptic sensation. Instead of using trial and error method, system parameter design becomes simple and founded.

## 5.2 Future works

Admittedly, there are still some works and topic to study in future. For example, this study focused on four types of parameters at most, some other parameters such as the device inertia, the time delay between devices etc. should also be involved in the function that calculates the  $C$  value.

Second, this study focused only on the position-force bilateral control architecture, and as introduced in Section 3.1, the position-position and any other bilateral control architectures [49] should also be focused.

Third, the parameters in this study is kept constant after adjustment for one type of task, but the environment and task requirements will vary even within the time span of one task. It is impossible to frequently adjust the parameters by the system designer. System parameter design is expected to be done automatically. In recent years, the adaptive

control method and AI technologies are used to cognize the task situation and moving environment to produce the optimized parameters value [91] – [96].

Forth, other haptic modalities, such as the vibrotactile sensation [97] and texture cognition, are important in operation and also affected by the system parameters. Considering other haptic modalities is necessary.

Finally, this parameter design guideline should be applied to a real master-slave system, where some nonlinear factors such as the gear friction will appear, and these factors should also be considered.

## Appendix

For the ideal position-force bilateral control model, the master velocity after contact can be estimated directly by function (3.5). Its derivation process is as follows.

Within 50 ms after the slave device contacts the environment, motion equation of the master device can be expressed as follows.

$$F_h + K_h \left( \frac{F_h}{B_m} \cdot t - r_m \right) + B_h \left( \frac{F_h}{B_m} - \dot{r}_m \right) = (M_m + M_h) \cdot \ddot{r}_m + B_m \cdot \dot{r}_m + F_{sc} \cdot K_{en} (P_{sc} r_m - r_{en}) \quad (A.1)$$

By applying Laplace transform to function (A.1), it is presented as:

$$\begin{aligned} & \frac{F_h}{s} + K_h \left( \frac{F_h}{B_m} \cdot \frac{1}{s^2} - R_m(s) \right) + B_h \left( \frac{F_h}{B_m} \cdot \frac{1}{s} - (s \cdot R_m(s) - r_{m0}) \right) \\ & = (M_m + M_h) \cdot (s^2 \cdot R_m(s) - s \cdot r_{m0} - V_0) + B_m (s \cdot R_m(s) - r_{m0}) + F_{sc} \cdot K_{en} (P_{sc} R_m(s) - s \cdot r_{en}) \end{aligned} \quad (A.2)$$

Where  $R_m(s)$  is the Laplace transformed form of the master's position ( $r_m$ ).  $r_{m0}$  is the master position when the contact occurred, which equals  $r_{en}$ , for simplicity, both  $r_{m0}$  and  $r_{en}$  are set to zero.  $V_0$  is the master device velocity just before the time point of contact, which is expressed a constant as  $\frac{F_h}{B_m}$  according to function (3.3).

Therefore,  $R_m(s)$  can be expressed as the following formation.

$$R_m(s) = \frac{K_h \cdot \frac{1}{s^2} \frac{F_h}{B_m} + B_m \frac{1}{s} \frac{F_h}{B_m} + B_h \frac{1}{s} \frac{F_h}{B_m} + (M_m + M_h) \cdot \frac{F_h}{B_m}}{(M_m + M_h) \cdot s^2 + B_m \cdot s + B_h \cdot s + F_{sc} \cdot K_{en} P_{sc} + K_h} \quad (A.3)$$

Then, by applying the inverse Laplace transform to function (A.3), the master velocity after the contact can be expressed as follows

$$V_a = \frac{F_h}{B_m} \cdot \frac{e^{-\frac{B_{hm}t}{2M_{hm}}} \left[ K_h \cdot e^{\frac{B_{hm}t}{2M_{hm}}} \cdot A + F_{sc} P_{sc} K_{en} \left( B_{hm} \cdot \sinh\left(\frac{A}{2M_{hm}} t\right) + A \cdot \cosh\left(\frac{A}{2M_{hm}} t\right) \right) \right]}{(K_h + K_{en} \cdot F_{sc} P_{sc}) \cdot A} \quad (\text{A.4})$$

Where,  $M_{hm} = M_m + M_h$  ,  $B_{hm} = B_m + B_h$  ,  $K_{hen} = K_h + F_{sc} P_{sc} K_{en}$  , and  
 $A = \sqrt{B_{hm}^2 - 4(F_{sc} P_{sc} K_{en} + K_h) M_{hm}}$  .

## References

- [1] Jean Vertut and Philippe Coiffet. *Teleoperations and Robotics: Evolution and Development, Robot Technology Volume 3A*. Prentice Hall, 1987.
- [2] TERMEN TAO A new generation Master-Slave Manipulator, GETINGE Group.
- [3] <https://robonaut.jsc.nasa.gov/R2/>
- [4] Geoffrey A. Landis, *Teleoperation from Mars orbit: A proposal for human exploration, Acta Astronautica*, Vol.62, No.1, 59-65, 2008.
- [5] L. Dongjie, R. Weibin, S. Lining, X. Wanzhe, and Z. Yu, *SEM-based Tele-nanomanipulation System with Virtual 3D Visual and Force Interaction, Robot*, vol. 35, pp. 52-59, 2013.
- [6] Zhenjiang Ni, Cécile Pacoret, Ryad Benosman and Stéphane R´egnier, *2D high speed force feedback teleoperation of optical tweezers, Proceedings of ICRA*, 2013.
- [7] G.H Ballantyne, P.F Leahy, and I.M. Modlin, *LAPAROSCOPIC SURGERY*. W.B. Saunders, 1994.
- [8] Rosen et al, *Surgical Robotics: Systems Applications and Visions*, 2011.
- [9] Blake Hannaford, Jacob Rosen, Diana W. Friedman, Hawkeye King, Phillip Roan, Lei Cheng, Daniel Glozman, Ji Ma, Sina Nia Kosari, Lee White, *Raven-II: An Open Platform for Surgical Robotics Research, IEEE Transactions on Biomedical Engineering*, Vol. 60, No. 4, pp. 954-959, 2013.
- [10] Takahiro Kanno, Daisuke Haraguchi, Kotaro Tadano, Kenji Kawashima. *A Pneumatically-Driven Surgical Manipulator with a Flexible Distal Joint Capable of Force Sensing, IEEE/ASME Transactions on Mechatronics*, Vol. 20, No. 6, pp. 2950-2961, 2015.
- [11] <https://www.davincisurgery.com>
- [12] <http://www.k-k.pi.titech.ac.jp/researches/>
- [13] R. Brent Gillespie, Mark R. Cutkosky, *Stable User-specific Haptic Rendering of the Virtual Wall, Proceedings of the ASME International Mechanical Engineering Conference and Exposition, DSC-Vol. 58*, pp. 397-406, 1996.
- [14] Claudio Pacchierotti, Federico Ongaro, Frank van den Brink, ChangKyu Yoon, Domenico Prattichizzo, David H. Gracias, and Sarthak Misra, *Steering and Control of Miniaturized Untethered Soft Magnetic Grippers With Haptic Assistance, IEEE Transactions on Automation Science and Engineering*, Vol. 15, No. 1, JANUARY 2018.
- [15] Blake Hannaford, Laurie Wood, Douglas A. McAfee, *Performance Evaluation of a Six-Axis Generalized Force-Reflecting Teleoperator, IEEE Transactions on Systems, Man and Cybernetics*, Vol. 21, No.3, 1991.
- [16] H.S. Vitense, J.A. Jacko, and V.K. Emery, *Multimodal Feedback: An Assessment of Performance and Mental Workload, Ergonomics*, Vol. 46, No. 1-3, 2003.
- [17] H.S. Vitense, *Multimodal Feedback: An Assessment of Performance and Mental Workload, Ergonomics*, vol. 46, pp. 68-87, 2003.
- [18] Jaesung Yang, Atsushi Konno, Satoko Abiko and Masaru Uchiyama, *Hardware-in-the-loop simulation of massive-payload manipulation on orbit, Robomech Journal*, Vol.5, No.66, 2018.

- 
- [19] A.M. Okamura, Methods for Haptic Feedback in Tele-operated Robot-assisted Surgery, *Industrial Robot: An International Journal*, Vol. 31, Issue 6, 2004.
- [20] Semere, W., Kitagawa, M. and Okamura, A.M. , Teleoperation with sensor/actuator asymmetry: task performance with partial force feedback, *Proceedings of the 12th Symposium on Haptic Interfaces for Virtual Environments and Teleoperator Systems*, pp. 121–127, Chicago, March 2004.
- [21] Ryoken Miyazaki, Takahiro Kanno, Gen Endo, and Kenji Kawashima, Pneumatically Driven Handheld Forceps with Force Display Operated by Motion Sensor, *Proceedings of ICRA*, Seattle, May 26-30, 2015.
- [22] Leonardo Meli, Claudio Pacchierotti, and Domenico Prattichizzo, Sensory Subtraction in Robot-Assisted Surgery: Fingertip Skin Deformation Feedback to Ensure Safety and Improve Transparency in Bimanual Haptic Interaction, *IEEE Transactions on Biomedical Engineering*, Vol. 61, No. 4, 2014.
- [23] Aude Bolopion and Stéphane Régnier, A Review of Haptic Feedback Teleoperation Systems for Micromanipulation and Microassembly, *IEEE Transactions on Automation Science and Engineering*, Vol. 10, No. 3, 2013.
- [24] Henri Boessenkool, David A. Abbink, Cock J.M. Heemskerk, Frans C.T. van der Helm, Haptic Shared Control Improves Tele-Operated Task Performance towards Performance in Direct Control, *Proceedings of IEEE World Haptics Conference*, 2011.
- [25] Henri Boessenkool, David A. Abbink, Cock J.M. Heemskerk, Frans C.T. van der Helm, and Jeroen G.W. Wildenbeest, A Task-Specific Analysis of the Benefit of Haptic Shared Control During Telemanipulation, *IEEE Transactions on Haptics*, Vol. 6, No. 1, 2013.
- [26] E. Beretta, F. Nessi, G. Ferrigno, and E. De Momi. Force Feedback Enhancement for Soft Tissue Interaction Tasks in Cooperative Robotic Surgery. *Proceedings of IROS*, 2015.
- [27] Blake Hannaford, A Design Framework for Teleoperators with Kinesthetic Feedback, *IEEE Transactions on Robotics and Automation*, Vol. 5, No. 4, 1988.
- [28] Angelika Peer and Martin Buss, Robust Stability Analysis of Bilateral Teleoperation Systems Using Admittance-Type Devices, *Proceedings of SICE Annual Conference*, 2008.
- [29] Jeroen G.W. Wildenbeest, David A. Abbink, Cock J.M. Heemskerk, Frans C.T. van der Helm, and Henri Boessenkool, The Impact of Haptic Feedback Quality on the Performance of Teleoperated Assembly Tasks, *IEEE Transactions on Haptics*, Vol. 6, No. 2, 2013.
- [30] Colgate JE, Robust impedance shaping telemanipulation. *IEEE Transactions on Robotics and Automation*, No.9, pp. 374–384, 1993.
- [31] Markus Rank, Thomas Schauß, Angelika Peer, Sandra Hirche, Roberta L. Klatzky, Masking Effects for Damping JND, *Proceedings of Eurohaptics*, 2012.
- [32] Amir Haddadi and Keyvan Hashtrudi-Zaad, Robust Stability of Teleoperation Systems with Time Delay: A New Approach, *IEEE Transactions on Haptics*, Vol. 6, No. 2, 2013.
- [33] Hongbing Li, Kotaro Tadano and Kenji Kawashima, Model-based Passive Bilateral Teleoperation with Time Delay, *Transactions of the Institute of Measurement and Control*, Vol. 38, No. 8, pp. 1010-1023, 2014.
- [34] Robert J. Anderson, Mark W.S pong, Bilateral Control of Teleoperators with Time Delay, *IEEE Transactions on Automatic Control*, Vol. 34, No. 5, 1989.
- [35] Aude Bolopion and Stéphane Régnier, Analysis of stability and transparency for nanoscale force feedback in bilateral coupling, *Journal of Micro-Nano Mech*, No. 4, pp.145–158, 2008.
- [36] Ahmad Mashayekhi, Saeed Behbahani, and Bruno Siciliano, Analytical stability criterion in haptic rendering: The role of damping, *IEEE/ASME Transactions on Mechatronics*, Vol. 23,

- No. 2, 2018.
- [37] Goran A. V. Christiansson, Matthias Mulder, Frans C. T. van der Helm, Slave Device Stiffness and Teleoperator Stability, Proceedings of EuroHaptics, 2006.
- [38] G. Jagannath Raju, Operator adjustable impedance in bilateral remote manipulation, Doctor Thesis, MIT, 1988.
- [39] Blake Hannaford, Stability and Performance tradeoffs in Bi-lateral Telemanipulation, Proceedings of ICRA, 1989.
- [40] Y. Yokokohji, N. Hosotani and T. Yoshikawa, Analysis of maneuverability and stability of Micro-teleoperation systems, Proceedings of the ICRA, 1994.
- [41] Vander Poorten Emmanuel B., Yokokohji Yasuyoshi, Yoshikawa Tsuneo, Stability Analysis and Robust Control for Fixed Scaled Teleoperation, Advanced Robotics; Vol. 20, No. 6, pp. 681 – 706, 2006.
- [42] G. Jagannath Raju, George C. Verghese and Thomas B. Sheridan, Design Issues in 2-port Network Models of Bilateral Remote Manipulation, Proceedings of ICRA, 1989.
- [43] Blake Hannaford and Paolo Fiorini, A Detailed Model of Bi-lateral Teleoperation, Proceedings of the IEEE International Conference on Systems, Man, and Cybernetics, 1988.
- [44] Peter M. Bobgan, H. Kazerooni, Achievable Dynamic Performance in Telerobotic Systems, Proceedings of ICRA, 1991.
- [45] Thomas Hansen, Claus T. Henningsen, Jens J. M. Nielsen, Rasmus Pedersen, et, al, Implementing Force-Feedback in a Telesurgery Environment, Using Parameter Estimation, Proceedings of IEEE International Conference on Control Applications, 2012.
- [46] Chiara Talignani Landi, et.al, Admittance Control Parameter Adaptation for Physical Human-Robot Interaction, Proceedings of ICRA, 2017.
- [47] Angelika Peer and Martin Buss, Robust Stability Analysis of Bilateral Teleoperation Systems Using Admittance-Type Devices, Proceedings of SICE Annual Conference, 2008.
- [48] Hidetaka Morimitsu, Seiichiro Katsura, A Design of Four-Channel Bilateral Control System under Time Delay Based on Hybrid Parameters, Proceedings of ICM, 2013.
- [49] Isura Ranatunga, Frank L. Lewis, Dan O. Popa, and Shaikh M. Tousif, Adaptive Admittance Control for Human–Robot Interaction Using Model Reference Design and Adaptive Inverse Filtering, IEEE Transactions on Control System Technology, Vol. 25, No. 1, 2017.
- [50] Dale A. Lawrence, Stability and Transparency in Bilateral Teleoperation, IEEE Transactions on Robotics and Automation. Vol. 9, No. 5, 1993.
- [51] Hashtrudi-Zaad K, Salcudean SE. Transparency in time-delayed systems and the effect of local force feedback for transparent teleoperation”. IEEE Transactions on Robotics and Automation Vol. 18, No. 1, pp. 108–114, 2002.
- [52] Hirche and Buss, Human perceived transparency with time delay. In: Advances in Telerobotics, Advanced Robotics, vol. 31, pp. 191-209. 2007.
- [53] Kenji Natori, Ryogo Kubo, Kouhei Ohnishi, Effects of Controller Parameters on Transparency of Time Delayed Bilateral Teleoperation Systems with Communication Disturbance Observer, Proceedings of IEEE International Symposium on Industrial Electronics, 2008.
- [54] Thomas Schauß, Angelika Peer, Parameter-Space Transparency Analysis of Teleoperation Systems, Proceedings of the IEEE Haptic Symposium, 2012.

- [55] Abdenbi Mohand Ousaid, Sinan Haliyo, St´ephane R´egnier and Vincent Hayward, A Stable and Transparent Microscale Force Feedback Teleoperation System, *IEEE/ASME Transactions on Mechatronics*, Vol. 20, No. 5, 2015.
- [56] Hyoung II Son, Jang Ho Cho, Tapomayukh Bhattacharjee, Hoeryong Jung, and Doo Yong Lee, Analytical and Psychophysical Comparison of Bilateral Teleoperators for Enhanced Perceptual Performance, *IEEE Transactions on Industrial Electronics*, Vol. 61, No. 11, 2014.
- [57] Sarthak Misra and Allison M. Okamura. Environment Parameter Estimation during Bilateral Telemanipulation. Symposium on Haptic Interfaces for Virtual Environment and Teleoperator Systems, USA, 2006.
- [58] Marcia K., O’Malley and Michael Goldfarb. The Effect of Virtual Surface Stiffness on the Haptic Perception of Detail. *IEEE/ASME Transactions on Mechatronics*, vol. 9, no. 2. 2004.
- [59] Botturi, M. Vicentini, M. Righele, C. Secchi, Perception-centric force scaling in bilateral teleoperation, *Mechatronics* 20, 802–811, 2010.
- [60] Louis B. Rosenberg and Bernard D. Adelstein, Perceptual Decomposition of Virtual Haptic Surfaces, *Proceedings of IEEE Virtual Reality Symposium*, 1993.
- [61] G. A. V. Christiansson, R. Q. van der Linde, and F. C. T. van der Helm, The Influence of Teleoperator Stiffness and Damping on Object Discrimination, *IEEE Transactions on Robotics*, Vol. 24, No. 5, 2008.
- [62] G. De Gerssem, H. Van Brussel, F. Tendick, Reliable and Enhanced Stiffness Perception in Soft-tissue Telemanipulation, *The International Journal of Robotics Research*, Vol. 24, No. 10, 2005.
- [63] Ilana Nisky, Assaf Pressman, Carla M. Pugh, Ferdinando A. Mussa-Ivaldi and Amir Karniel, Perception and Action in Teleoperated Needle Insertion, *IEEE Transactions on Haptics*, Vol. 4, No. 3, 2011.
- [64] Satoko Yamagawa, Kouji Abe, Hideo Fujimoto, Conditions of Force Scaling Methods in Master-Slave Systems Based on Human Perception Abilities for Time-variant Force, *Biomechanisms*, Vol. 18, pp 165-174, 2006.
- [65] Alexandros Kouris, Fotios Dimeas and Nikos Aspragathos, Contact Distinction in Human-Robot Cooperation with Admittance Control, *Proceedings of IEEE International Conference on SMC*, 2016.
- [66] S. Cholewiak, H. Tan, & D. Ebert, Haptic identification of stiffness and force magnitude. *Proceedings of Symposium on Haptic Interfaces for Virtual Environments and Teleoperator Systems*, 2008.
- [67] B. Wu, R. Klatzky, & R. Hollis, Force, torque, and stiffness: Interactions in perceptual discrimination, *IEEE Transactions on Haptics*, vol. 4, no. 3, pp. 221–228, 2011.
- [68] Jae-Bok Song and Woong-Chul Chung, Quantification of Arm Kinesthetic Sense Using an Arm Motion Generator, *IEEE Transactions on System, Man, and Cybernetics-Part A: Systems and Humans*, Vol. 31, No. 2, 2001.
- [69] Dale A. Lawrence, Lucy Y. Pao, Anne M. Dougherty, Mark A. Salada, and Yiannis Pavlou, Rate-Hardness: A New Performance Metric for Haptic Interfaces”, *IEEE Transactions on Robotics and Automation*, vol. 16, no. 4, pp. 357–371, 2000.
- [70] Hyoung II Son, Tapomayukh Bhattacharjee, and Hideki Hashimoto, Effect of Impedance-Shaping on Perception of Soft Tissues in Macro-Micro Teleoperation, *IEEE Transaction on Industrial Electronics*, Vol. 59, No. 8, 2012.
- [71] H. Tan, N. Durlach, G. Beauregard, and M. Srinivasan, Manual discrimination of compliance using active pinch grasp: The roles of force and work cues, *Perception & Psychophysics*, vol.

- 57, no. 4, pp. 495–510, 1995.
- [72] Ravinder S. Dahiya, Giorgio Metta, Maurizio Valle, and Giulio Sandini, Tactile Sensing—From Humans to Humanoids, *IEEE Transactions on Robotics*, vol. 26, no. 1, pp. 1–20, 2010.
- [73] Lynette A. Jones, *Kinesthetic Sensing. Human and Machine Haptics*, MIT Press, 2000.
- [74] Lynette A. Jones and I.W. Hunter, A perceptual analysis of stiffness, *Experimental Brain Research* vol. 79, no. 1, pp. 150–156, 2000.
- [75] Lynette A. Jones and I.W. Hunter, A perceptual analysis of viscosity, *Experimental Brain Research* vol. 94, no. 2, pp. 343–351, 1993.
- [76] C. Pacchierotti, Cutaneous and Kinesthetic Cues to Improve Transparency in Teleoperation, *Cutaneous Haptic Feedback in Robotic Teleoperation*, pp. 93–120, 2015.
- [77] Lei Wei, Hailing Zhou, Saeid Nahavandi, and Dangxiao Wang, Toward a Future with Human Hands-Like Haptics, *IEEE System, Man, and Cybernetics Magazine*, vol. 2, no. 1, pp. 14–25, 2016.
- [78] V. Abraira and D. Ginty, The sensory neurons of touch, *Neuron*, vol. 79, no. 4, pp. 618–39, 2013.
- [79] Amit Bhardwaj and Subhasis Chaudhur, Estimation of Resolvability of User Response in Kinesthetic Perception of Jump Discontinuities, *Proceedings of IEEE World Haptics Conference*, 2015.
- [80] George F. Reed, Freyja Lynn, and Bruce D. Meade, Use of Coefficient of Variation in Assessing Variability of Quantitative Assays, *Clinical and Diagnostic Laboratory Immunology*, Nov, pp. 1235–1239, 2002.
- [81] M. Hirano, T. Maruyama, and Y. Nakahara, Relationship between the recognition of object’s hardness by human finger and contact force under various contact conditions, *Abstract of Dynamic & Design Conference*, vol. 2000, no.00, pp. 370, 2000.
- [82] Gescheider A. George, *Psychophysics: Method, Theory, and Application*, Psychology Press, 1984.
- [83] Lynette A. Jones, Application of psychophysical techniques to haptic research, *IEEE Transactions on Haptics*, vol. 6, no. 3, pp. 268–287, 2013.
- [84] Masaomi Motoji, Hiroaki Nishino, Tsuneo Kagawa, Kouichi Utsumiya, A Haptic Parameter Exploration Method for Force Feedback Devices, *Proceedings of International Conference on Complex, Intelligent and Software Intensive Systems*, 2010.
- [85] Sungmin Seung, Byungjeon Kang, Hongmo Je, Jongoh Park, Kyunghwan Kim and Sukho Park, Tele-Operation Master-Slave System for Minimal Invasive Brain Surgery, *Proceedings of IEEE International Conference on Robotics and Biomimetics*, 2009.
- [86] Mohsen Mahvash and Allison M. Okamura, Friction Compensation for a Force-Feedback Telerobotic System, *Proceedings of the ICRA*, 2006.
- [87] C. R. Wagner and R. D. Howe, Mechanisms of performance enhancement with force feedback, *Proceedings of World Haptics Conference*, 2005.
- [88] Kazuki Into, Yashumichi Aiyama, Intuitive and Direct Teaching System of Multi-Fingered Hand-Arm Robot for Grasping Task, *Proceedings of IEEE/SICE Int. Symposium*, 2010.
- [89] Panadda Marayong, Gregory D. Hager and Allison M. Okamura, Effect of Hand Dynamics on Virtual Fixtures for Compliant Human-Machine Interfaces, *Proceedings of Symposium on Haptic Interfaces for Virtual Environment and Teleoperator Systems*, 2006.
- [90] A. Bolopion and S. Regnier, Analysis of stability and transparency for nanoscale force feedback in bilateral coupling. *Journal of Micro-Nano Mechanics*, Vol. 4, pp. 145–158, 2008.

- 
- [91] Emmanuel Nuno, Ioannis Sarras, Luis Basanez, An Adaptive Controller for Bilateral Teleoperators: Variable Time-Delays Case, Proceedings of the The International Federation of Automatic Control, 2014.
- [92] Yana Yanga, Chao Ge, Hong Wang, Xiaoyi Li, Changchun Hua, Adaptive neural network based prescribed performance control for teleoperation system under input saturation, Journal of the Franklin Institute, Vol. 352, No. 5, 2015.
- [93] Huanqing Wang, Peter Xiaoping Liu, and Shichao Liu, Adaptive Neural Synchronization Control for Bilateral Teleoperation Systems With Time Delay and Backlash-Like Hysteresis, IEEE Transactions on Cybernetics, Vol. 47, No. 10, pp. 3018-3026, 2017.
- [94] Parham M. Kebria, Abbas Khosravi, Saeid Nahavandi, Zoran Najdovski, and Stephen John Hilton, Neural Network Adaptive Control of Teleoperation Systems with Uncertainties and Time-Varying Delay, Proceedins of CASE, 2018.
- [95] Florian Muller, Jan Janetzky, Uwe Behrnd, Jens Jakel and Ulrike Thomas, User Force-Dependent Variable Impedance Control in Human-Robot Interaction, Proceedings of CASE, 2018.
- [96] Hsieh-Yu Li, Ishara Paranawithana, Liangjing Yang, U-Xuan Tan, Physical Human-Robot Interaction Coupled with a Moving Environment or Target: Contact and Track, Proceedings of CASE, 2018.
- [97] Bernhard Weber, Mikel Sagardia, Thomas Hulin, andvi Carsten Preusche, Visual, Vibrotactile, and Force Feedback of Collisions in Virtual Environments: Effects on Performance, Proceedings on VAMR, 2013.

## Acknowledgement

First of all, I want to thank the following three groups. They are my family members, my supervisors and the Rotary Yoneyama Memorial Foundation.

All my family members, my mother, father, grandpa, grandma, and my dear wife, they supported me in financially and spiritually without any complaint. These support are the so important to me that I cannot say I can complete the doctoral course without it. I also want to say thanks to my son, Yuliang Zhou, who arrived in this world in 2018, my life was totally grand new after the day he arrives to the world because of his pure smile.

My supervisor, Prof. Tadano, who leaded me in the way of research. The time and effort he spent in answering my queries, suggesting approaches and solutions, reading all my drafts and making copious comment and enhancement, etc. is so grateful. His wisdom and plentiful knowledge let me always running on the correct path without deviation, his criticism and encouragement motivated me to keep on running.

Prof. Kagawa also gave me a lot of advice in research and inspired me a lot. The parties he/she organized in the lab and his home was so happy.

The Rotary Yoneyama Memorial Foundation and Kawasaki West Rotary Club supported me not only by providing me the scholarship but also introducing many interesting people from various fields of society. I thank their generosity and will cherish their friendship forever.

Second, I would like to thank Prof. Yoshida, Prof. Yoshioka, Prof. Mastumura, and Prof. Kim for spending their precious time on examining my doctor thesis, pointing out the miss and giving useful advices. Your advices helped a lot in progressing this thesis.

Third, I would like to thank all the members of Tadano Lab. The assistant professor Tomohiro Kawase gave me pertinent comment on my paper and my presentation slides. The researcher Dr. Shinji Kawakura revised the miss in my Japanese, both in oral and in documents.

Because my study is somewhat similar with Mr. Yasuyuki Saito's topic. The discussion inspired both of us a lot. Mr. Junpeng Sun comes from the same country with me. The talking appears in dinner table everyday was very delightful. The textbook of Modern Control Theory lent from Mr. Jongha Lim helped me a lot in reading the literatures.

The works of secretaries Mrs. Hiroko Kanai and Ms. Yumiko Yoshida was very helpful and thankworthy, saving a lot of time in the trivial affairs.

The master student Mr. Shintaro Kimura, Mr. Shun Shiozaki and Mr. Solmon Jeong, the years in the same lab was so happy especially the snowboard trip and the summer trip.

I also would like to thank the master students: Mr. Hisami Takeishi, Mr. Koki Aizawa, Mr. Daisuke Mizuno, Mr. Toru Sasajima and Mr. Keita Nakamori, and senior student Mr. Wataru Hayakawa, Mr. Hayato Takeyama, who spend their precious time in the experiments of my research.

Last but not least, all the people that helped me in these years are thankworthy, including all my friends, all the faculties in Tokyo Institute of Technology.

January, 2019